

DURBAN UNIVERSITY OF TECHNOLOGY

**Compactness in superpixel segmentation of digital images using
perceptual colour difference measure**

By

Sadhasivan Govindasamy Moodley

19000958

**A dissertation submitted in fulfilment of the requirement for the
Masters in Information and Communications Technology degree**

**Faculty of Accounting and Informatics, Department of Information
Technology**

Supervisor: Professor O.O. Olugbara

Co-Supervisor: Dr T.T. Adeliyi

2021

DECLARATION

I, *Sadhasivan Govindasamy Moodley*, declare that:

- The research reported in this dissertation, except where otherwise indicated, is my original research.
- This dissertation has not been submitted for any degree or examination at any other university.
- This dissertation does not contain other persons' data, pictures, graphs or other information unless specifically acknowledged as being sourced from other persons.
- This dissertation does not contain other persons' writing unless specifically acknowledged as being sourced from other researchers. Where other written sources have been quoted, then:
 - Their words have been re-written but the general information attributed to them has been referenced.
 - Where their exact words have been used, their writing has been placed inside quotation marks and referenced.
- This dissertation does not contain text, graphics or tables copied and pasted from the Internet, unless specifically acknowledged, and the source is detailed in the dissertation and the Reference Section of this dissertation.

Signature: *S.G. Moodley*

Date: 22 October 2021

Approved for Final Submission

Supervisor: ____
Professor O.O. Olugbara

14 December 2021

Co-Supervisor: ____
Dr T.T. Adeliyi

DEDICATION

In loving memory of my parents Mr Govindasamy and Mrs Parvathy Moodley, whose loving care, upbringing, guidance and understanding brought me to where I am today.

And

my wife Sandra and son Navendran Moodley.

And

daughter Egashnee, son-in-law Nikash and my grandson Kiyaan Bhulaye.

ACKNOWLEDGEMENTS



It is by the grace of God that I am empowered with the knowledge, strength and fortitude during this life cycle, that enabled me to complete this study successfully.

This thesis would not have been possible without the guidance and support of many individuals who contributed and inspired me throughout this journey. I hereby express my gratitude to everyone that had given me encouragement, motivation and moral support throughout this dissertation.

- Firstly, my sincere thanks to my supervisor Professor Oludayo, O. Olugbara, a well-respected and respectful scientist who provided his expertise in the field of ICT that offered his endless support and positive guidance which enabled me to gain intense understanding throughout the process of this thesis.
- Thank you to my co-supervisor Dr Tim T. Adeliyi, an expert in the field of ICT and my research area provided endless support and guidance towards my thesis. His relentless review and immediate constructive feedback helped me enhance my knowledge and improve the quality of my thesis outcomes.
- Thank you to the Department of Information Technology HOD Dr Wing, and my colleagues for all your encouragement, support and guidance throughout my studies.
- My sincere thanks to the Faculty of Accounting and Informatics Executive Dean Professor Oludayo O. Olugbara and staff for your motivation and support.
- My gratitude to my colleagues and friends within the Department of IT/IS especially to Subashnie, Priyalushinee and Esaivanie who motivated and gave me endless support of reassurance that made this journey a memorable one.
- My sincerest gratitude to Ms Sara Mitha, Postgraduate Librarian for her support.
- Last but not least, I would like to express my deepest gratitude and love for my family, especially my wife Sandra, son Navendran, daughter Egashnee, son-in-law Nikash and grandson Kiyaan. Their love, patience, understanding, encouragement, support and continuous prayer towards my success gave me the strength and a source of inspiration towards this journey. I am truly blessed to have all of you in my life. May lord Ganesha bless all of you.

TABLE OF CONTENTS

DECLARATION	ii
DEDICATION	iii
ACKNOWLEDGEMENTS	iv
LIST OF TABLES	viii
LIST OF FIGURES	ix
LIST OF ABBREVIATIONS	xvi
ABSTRACT.....	xvii
CHAPTER ONE INTRODUCTION	1
1.1 Introduction.....	1
1.2 Research Problem Statement	4
1.3 Aim and Objectives	5
1.4 Significance of the study	5
1.5 Thesis Synopsis	6
Chapter One: Introduction to the thesis	6
Chapter Two: Literature Review	6
Chapter Three: Research Methodology	6
Chapter Four: Presentation of Results and Discussion	6
Chapter Five: Summary, Conclusions and Implications of the Study	6
1.6 Chapter summary.....	6
CHAPTER TWO	8
2.1 Introduction.....	8
2.2 Digital Image Segmentation	8
2.3 Non Superpixel Image Segmentation	9
2.3.1 Edge Based Image Segmentation.....	9
2.3.2 Region-Based Image Segmentation.....	10
2.4 Superpixel Segmentation	11
2.5 Meta-Analysis Literature Strategy.....	21
2.5.1 Inclusion and Exclusion Criteria.....	21
2.5.2 Statistical data analysis	22
2.5.3 Meta-Analysis Results	22
2.5.3.1 Overall pooled Estimate.....	23
2.6 Clustering Algorithm	26
2.6.1 K-Means.....	27
2.6.2 Improved K-Means	27

2.6.3 Fuzzy c-mean.....	28
2.6.4 Pixel Intensity Clustering Algorithm.....	28
2.7 Distance measure for image segmentation	29
2.7.1 Euclidean Distance.....	29
2.7.2 Minkowski distance	30
2.7.3 Chebyshev.....	31
2.7.4 Manhattan distance	31
2.7.5 Cosine distance	32
2.7.6 Mahalanobis distance.....	32
2.8 Colour Models	33
2.8.1 RGB	33
2.8.2 CIELAB.....	34
2.8.3 HSV.....	34
2.9 Performance Evaluation Metrics.....	36
2.9.1 Under segmentation Error.....	36
2.9.2 Achievable segmentation accuracy	37
2.9.3 Compactness	37
2.9.4 Boundary recall.....	37
2.9.5 Contour Density	38
2.10 Chapter Summary	38
CHAPTER THREE RESEARCH METHODOLOGY	39
3.1 Introduction	39
3.2 Simple Linear Iterative Clustering (SLIC)	39
3.3 Strong Attribute Influence Distances Distance Measure.....	40
3.4 Perceptual Algorithm - SLIC.....	41
3.5 Dataset	42
3.5.1 Human Images	42
3.5.2 Animal Images	45
3.5.3 Object Images	48
3.6 Evaluation Metrics.....	50
3.7 Chapter summary	50
CHAPTER FOUR.....	51
4.1 Performance Evaluation.....	51
4.2 Qualitative Evaluation for LAB Colour Model	52

4.3 Quantitative Evaluation of LAB Colour Model.....	58
4.4 Quantitative Evaluation for HSV Colour Model	84
4.5 Chapter Summary	110
CHAPTER FIVE SUMMARY AND CONCLUSIONS	111
5.1 Summary.....	111
5.2 Future Work	113
5.3 Conclusion	113
REFERENCES	115

LIST OF TABLES

Table 2.1: Summary of Superpixel image segmentation based on ASA	14
Table 2.2: Summary of Colour image segmentation based on different colour models.....	35
Table 4.1: Result of Superpixel Segmentation (100-1000 pixels) with SAID distance measure	53
Table 4.2: Result of Superpixel Segmentation (100-1000 pixels) with SAID and Euclidean distance measures.....	55

LIST OF FIGURES

Figure: 2.1 Flow diagram of the database searches (Preferred Reporting Items for Systematic Reviews and Meta-Analysis)	23
Figure 2.2: Pooled estimate from the random-effect model... ..	24
Figure 2.3: Pooled estimate from the fixed-effect model... ..	25
Figure 2.4: Subgroup analysis based on the approaches... ..	42
Figure 4.1a: Under-segmentation error against the number of superpixels for overlapping images with regular compactness... ..	58
Figure 4.1b: Under-segmentation error against the number of superpixels for overlapping images with irregular compactness... ..	59
Figure 4.2a: Under-segmentation error against the number of superpixels for overlapping complex images with regular compactness... ..	59
Figure 4.2b: Under-segmentation error against the number of superpixels for complex images with irregular compactness... ..	60
Figure 4.3a: Under-segmentation error against the number of superpixels for multiple object images with regular compactness... ..	60
Figure 4.3b: Under-segmentation error against the number of superpixels for multiple object images with irregular compactness... ..	61
Figure 4.4a: Under-segmentation error against the number of superpixels for Centred object images with regular compactness... ..	61
Figure 4.4b: Under-segmentation error against the number of superpixels for Centred object images with irregular compactness	62
Figure 4.5a: Under-segmentation error against the number of superpixels for low contrast images with regular compactness	63
Figure 4.5b: Under-segmentation error against the number of superpixels for low contrast images with irregular compactness	63
Figure 4.6a: Achievable segmentation accuracy against the number of superpixels for overlapping images with regular compactness	64
Figure 4.6b: Achievable segmentation accuracy against the number of superpixels for overlapping images with irregular compactness	64
Figure 4.7a: Achievable segmentation accuracy against the number of superpixels for complex images with regular compactness.....	65

Figure 4.7b: Achievable segmentation accuracy against the number of superpixels for complex images with irregular compactness	65
Figure 4.8a: Achievable segmentation accuracy against the number of superpixels for multiple object images with regular compactness	66
Figure 4.8b: Achievable segmentation accuracy against the number of superpixels for multiple object images with irregular compactness	66
Figure 4.9a: Achievable segmentation accuracy against the number of superpixels for multiple object images with regular compactness	67
Figure 4.9b: Achievable segmentation accuracy against the number of superpixels for multiple object images with irregular compactness	67
Figure 4.10a: Achievable segmentation accuracy against the number of superpixels for multiple object images with regular compactness	68
Figure 4.10b: Achievable segmentation accuracy against the number of superpixels for multiple object images with regular compactness	68
Figure 4.11a: Compactness against the number of superpixels for overlapping images with regular compactness.....	69
Figure 4.11b: Compactness against the number of superpixels for overlapping images with irregular compactness	69
Figure 4.12a: Compactness against the number of superpixels for complex images with regular compactness.....	70
Figure 4.12b: Compactness against the number of superpixels for complex images with irregular compactness	70
Figure 4.13a: Compactness against the number of superpixels for multiple object images with regular compactness.....	71
Figure 4.13b: Compactness against the number of superpixels for multiple object images with irregular compactness	71
Figure 4.14a: Compactness against the number of superpixels for Centred object images with regular compactness	72
Figure 4.14b: Compactness against the number of superpixels for Centred object images with irregular compactness	72
Figure 4.15a: Compactness against the number of superpixels for low contrast images with regular compactness	73
Figure 4.15b: Compactness against the number of superpixels for low contrast images with irregular compactness	73

Figure 4.16a: Boundary recall against the number of superpixels for overlapping images with regular compactness	74
Figure 4.16b: Boundary recall against the number of superpixels for overlapping images with irregular compactness	74
Figure 4.17a: Boundary recall against the number of superpixels for complex images with regular compactness.....	75
Figure 4.17b: Boundary recall against the number of superpixels for complex images with irregular compactness	75
Figure 4.18a: Boundary recall against the number of superpixels for multiple objects images with regular compactness	76
Figure 4.18b: Boundary recall against the number of superpixels for multiple objects images with irregular compactness	76
Figure 4.19a: Boundary recall against the number of superpixels for Centred object images with regular compactness.....	77
Figure 4.19b: Boundary recall against the number of superpixels for Centred object images with irregular compactness	77
Figure 4.20a: Boundary recall against the number of superpixels for low contrast images with regular compactness.....	78
Figure 4.20b: Boundary recall against the number of superpixels for low contrast images with irregular compactness	78
Figure 4.21a: Contour density against the number of superpixels for overlapping images with regular compactness.....	79
Figure 4.21b: Contour density against the number of superpixels for overlapping images with irregular compactness	79
Figure 4.22a: Contour density against the number of superpixels for complex images with regular compactness.....	80
Figure 4.22b: Contour density against the number of superpixels for complex images with irregular compactness	80
Figure 4.23a: Contour density against the number of superpixels for multiple objects images with regular compactness	81
Figure 4.23b: Contour density against the number of superpixels for multiple objects images with irregular compactness	81
Figure 4.24a: Contour density against the number of superpixels for Centred object images with regular compactness.....	82

Figure 4.24b: Contour density against the number of superpixels for Centred object images with irregular compactness	82
Figure 4.25a: Contour density against the number of superpixels for low contrast images with regular compactness.....	83
Figure 4.25b: Contour density against the number of superpixels for low contrast images with irregular compactness	83
Figure 4.26a: Under-segmentation error against the number of superpixels for overlapping images with regular compactness	84
Figure 4.26b: Under-segmentation error against the number of superpixels for overlapping images with irregular compactness	85
Figure 4.27a: Under-segmentation error against the number of superpixels for complex images with regular compactness	85
Figure 4.27b: Under-segmentation error against the number of superpixels for complex images with irregular compactness	86
Figure 4.28a: Under-segmentation error against the number of superpixels for multiple object images with regular compactness.....	86
Figure 4.28b: Under-segmentation error against the number of superpixels for multiple object images with irregular compactness	87
Figure 4.29a: Under-segmentation error against the number of superpixels for Centred object images with regular compactness.....	87
Figure 4.29b: Under-segmentation error against the number of superpixels for Centred object images with irregular compactness	88
Figure 4.30a: Under-segmentation error against the number of superpixels for low contrast images with regular compactness	89
Figure 4.30b: Under-segmentation error against the number of superpixels for low contrast images with irregular compactness	89
Figure 4.31a: Achievable segmentation accuracy against the number of superpixels for overlapping images with regular compactness	90
Figure 4.31b: Achievable segmentation accuracy against the number of superpixels for overlapping images with irregular compactness	90
Figure 4.32a: Achievable segmentation accuracy against the number of superpixels for complex images with regular compactness.....	91
Figure 4.32b: Achievable segmentation accuracy against the number of superpixels for multiple object images with irregular compactness	91

Figure 4.33a: Achievable segmentation accuracy against the number of superpixels for multiple object images with regular compactness	92
Figure 4.33b: Achievable segmentation accuracy against the number of superpixels for multiple object images with irregular compactness	92
Figure 4.34a: Achievable segmentation accuracy against the number of superpixels for Centred object images with regular compactness.....	93
Figure 4.34b: Achievable segmentation accuracy against the number of superpixels for Centred object images with irregular compactness.....	93
Figure 4.35a: Achievable segmentation accuracy against the number of superpixels for low contrast images with regular compactness.....	94
Figure 4.35b: Achievable segmentation accuracy against the number of superpixels for low contrast images with regular compactness.....	94
Figure 4.36a: Compactness against the number of superpixels for overlapping images with regular compactness.....	95
Figure 4.36b: Compactness against the number of superpixels for overlapping images with irregular compactness.....	95
Figure 4.37a: Compactness against the number of superpixels for complex images with regular compactness.....	96
Figure 4.37b: Compactness against the number of superpixels for complex images with irregular compactness.....	96
Figure 4.38a: Compactness against the number of superpixels for multiple object images with regular compactness.....	97
Figure 4.38b: Compactness against the number of superpixels for multiple object images with irregular compactness.....	97
Figure 4.39a: Compactness against the number of superpixels for Centred object images with regular compactness.....	98
Figure 4.39b: Compactness against the number of superpixels for Centred object images with irregular compactness.....	98
Figure 4.40a: Compactness against the number of superpixels for low contrast images with regular compactness.....	99
Figure 4.40b: Compactness against the number of superpixels for low contrast images with irregular compactness	99

Figure 4.41a: Boundary recall against the number of superpixels for overlapping images with regular compactness.....	100
Figure 4.41b: Boundary recall against the number of superpixels for overlapping images with irregular compactness	100
Figure 4.42a: Boundary recall against the number of superpixels for complex images with regular compactness.....	101
Figure 4.42b: Boundary recall against the number of superpixels for complex images with irregular compactness	101
Figure 4.43a: Boundary recall against the number of superpixels for multiple object images with regular compactness.....	102
Figure 4.43b: Boundary recall against the number of superpixels for multiple object images with irregular compactness	102
Figure 4.44a: Boundary recall against the number of superpixels for Centred object images with regular compactness.....	103
Figure 4.44b: Boundary recall against the number of superpixels for Centred object images with irregular compactness	103
Figure 4.45a: Boundary recall against the number of superpixels for low contrast images with regular compactness.....	104
Figure 4.45b: Boundary recall against the number of superpixels for low contrast images with irregular compactness	104
Figure 4.46a: Contour density against the number of superpixels for overlapping images with regular compactness.....	105
Figure 4.46b: Contour density against the number of superpixels for overlapping images with irregular compactness	105
Figure 4.47a: Contour density against the number of superpixels for complex images with regular compactness.....	106
Figure 4.47b: Contour density against the number of superpixels for complex images with irregular compactness	106
Figure 4.48a: Contour density against the number of superpixels for multiple object images with regular compactness.....	107
Figure 4.48b: Contour density against the number of superpixels for multiple object images with irregular compactness	107
Figure 4.49a: Contour density against the number of superpixels for Centred object images with regular compactness.....	108

Figure 4.49b: Contour density against the number of superpixels for Centred object images with irregular compactness	108
Figure 4.50a: Contour density against the number of superpixels for low contrast images with regular compactness.....	109
Figure 4.50b: Contour density against the number of superpixels for low contrast images with irregular compactness.....	109

LIST OF ABBREVIATIONS

AFI	<u>A</u> rea fit Index
AID	<u>A</u> tttribute Concurrence Influence Distances
ASA	<u>A</u> chievable Segmentation Accuracy
BR	<u>B</u> oundary Recall
CAS	Content Adaptive Superpixel
CD	<u>C</u> ontour Density
CI	<u>C</u> onfidence Interval
CMYK	<u>C</u> yan, Magenta, Yellow, Key/Black
CO	<u>C</u> ompactness
DES	Differential Evolutionary Superpixels
EUC	<u>E</u> uclidean Distance
ESFs	<u>E</u> dge Stop Functions
FCM	<u>F</u> uzzy C-Means
HSV	<u>H</u> ue, Saturation, Value
KNN	<u>K</u> -Nearest Neighbour
LSC	<u>L</u> inear Spectral Clustering
LRW	<u>L</u> azy Random Walks
MCL	<u>M</u> arkov Clustering
RGB	Tristimuli Red, Green and Blue
RISA	Region-Based image segmentation Algorithm
ROI	<u>R</u> egion of Interest
SAID	<u>S</u> trong Attribute Influence Distances
SLIC	<u>S</u> imple Linear Iterative Clustering
SVM	<u>S</u> upport Vector Machine
UE	<u>U</u> nder Segmentation Error

ABSTRACT

Digital image segmentation is a thrilling but challenging open problem that has been well-researched in the fields of computer vision, and image processing. It has many practical applications like biometric identification, ship detection, building extraction, road marking recognition, deoxyribonucleic acid matching, welding inspection, pedestrian re-identification, object tracking, image editing, pest monitoring, and shopping items recommendation. In recent years, image segmentation has come to rely heavily on superpixel methods to circumvent the computational complexity inherent in pixel processing. The superpixel approach is generally used to group similar pixels into a semantic cluster of fewer pixels to increase the processing speed and simplify computational intricacy. However, the reliance on the existing superpixel based segmentation methods on the Euclidean distance metric as a measure of similarity between two pixels in an image presents an inherent challenge. The Euclidean distance has a real-world advantage because of its assumption of non-uniformity that most image colour distributions generally follow. This assumption states that real data will occupy a small clustered subset of the entire space, but not necessarily distributed evenly in a higher-dimensional space. However, since it cannot deal with illumination change in images, it is limited in compactly measuring similarity in the context of an application that complies with the human perception of similarity. The human eyes can recognise similar or irrelevant image colours under the illumination change for which the Euclidean distance does not perform well. This study aimed to investigate the performance of an attribute concurrence influence distance metric on image compactness in a superpixel segmentation algorithm. It is hypothesized that superpixel segmentation based on attribute co-occurrence similarity measure is likely to achieve better results than Euclidean distance in terms of the performance metrics of under segmentation error, achievable segmentation accuracy, compactness, boundary recall, and contour density. Superpixel segmentation experiments were performed using two widely used colour models which are hue, saturation, value (HSV), and lightness, redness, yellowness (LAB) with the strong attribute concurrence influence distance (SAID) and Euclidean distance in a superpixel segmentation algorithm. The results presented for the LAB colour model showed that SAID outperformed the Euclidean distance for images reflecting overlapping and complex objects with regular compactness. However, the Euclidean distance performed better than the SAID for images with multiple, centre, and low contrast objects with regular compactness across the under segmentation error, achievable segmentation accuracy, boundary recall and contour density performance evaluation metrics. Consequently, for irregular compactness, SAID further outperformed the Euclidean distance for images with overlapping, complex, multiple, Centred and low contrast objects for boundary recall. However, the Euclidean distance performed better than SAID for under segmentation error, achievable segmentation accuracy, and contour density. Furthermore, the compactness performance for SAID and Euclidean distance gave the same compactness value for both regular and irregular compactness. Consequently, based on the analysis of the results for the HSV colour model, it was observed that performances of SAID and Euclidean with regular compactness were at par across all the performance metrics used for images with overlapping, complex, multiple, centre, and low contrast objects. However, the Euclidean distance outperformed SAID with irregular compactness for images with overlapping, complex, multiple, centre, and low contrast objects.

CHAPTER ONE

INTRODUCTION

1.1 Introduction

As human awakens their eyes and other senses a wealth of information signals about the environment is provided. Usually, human vision can or may want to process only a minute amount of this information signals that reach our awareness and memory. Human vision's cognitive system, on the other hand, can focus on important things in a busy visual scene with a variety of backgrounds without any training. As a result, humans are proficient in quickly detecting a vast variety of objects (Lou et al., 2016; Zhang et al., 2018a). Superpixels are a vital component of image processing in automatically distinguishing prominent objects because they split a digital image into clusters or groups of pixels. The purpose of superpixel is to simplify and change an image's depiction to make it more relevant and understandable.

Image segmentation is crucial for a range of applications in image analysis, including object recognition, video, and computer vision. To select the appropriate segmentation, critical information such as colour, borders, or texture information is gathered from the object (Khattab et al., 2016; Bukola., 2017). Image segmentation has grown in popularity for usage in computer vision applications which is seen as a perceptual grouping within an image that gains more human attention. The initial step of image processing is image segmentation and is crucial to obtaining analytical results from objects within an image. It relates to the process of classifying each pixel belonging to a particular label or dividing an image into several liberal clusters that are eloquent and semantically related including multiple object categories eg: human, animal and objects (Minaee et al., 2021; Zheng et al., 2018). Despite being a fundamental problem in computer vision since early days, image segmentation has improved considerably in recent years.

Image segmentation is one of the hotspots in image processing and computer vision, according to the literature (Gu. 2017). Image segmentation is a technique for converting an image into evocative qualities based on image areas. It is also a crucial foundation for image segmentation, as it is based on certain metrics to segment an input image into several similar pixels to excerpt the area of concentration as captured by the human eye, which serves as the basis for the analysis of the segmented images and further helps with separating the image foreground from the

background (Zheng et al., 2018). Image segmentation can be divided into two types: non-superpixel and superpixel. Non-superpixel segmentation employs a region comparison function to make simple greedy decisions that result in segmentations that are neither too coarse nor too fine (Felzenszwalb and Huttenlocher, 2004). Ren and Malik (2003) introduced the concept of superpixels with the aim of grouping pixels with a similar colour together and other lower-level properties. Superpixel segmentation made it possible to compute image attributes quickly and easily, removing the challenge of image processing through segmenting images into smaller regions of uniform colour or texture (Alexe et al., 2010; Neubert et al., 2013; Wang et al., 2017).

In the field of computer vision, superpixel segmentation has recently received much interest since it gives a rapid and easy way to calculate images based on regions rather than pixels. Pixels were grouped into perceptually homogeneous regions providing compressed representation of images which helped trim down the number of different image primitives for consequent processing (Yang et al., 2020; Zhang et al., 2017). Superpixel segmentation algorithms have been adopted for many computer vision problems to improve their performance, detecting saliency and decreasing redundancy (Liu et al., 2013), object detection (Yan et al., 2015), tracking (Yang et al., 2015), semantic segmentation (Mi and Chen, 2020), classification (Xiang et al., 2013), object recognition (Lu et al., 2013). According to the literature, many algorithms are used to ensure the success of this pre-processing step using the following desired performance metrics:

1. Accuracy - Superpixel adherence to image borders is measured. Superpixel segmentation should be precise to preserve as much information as possible for further processing on superpixels. (Siva and Wong., 2014).
2. Regularity - The regularity of a superpixel influences how close it is to be square. Superpixels are used to represent the information in pixels. The standard qualities of pixels, including topology, structure, homogeneity, and isometric information, can be preserved in regular superpixels (Wang et al., 2017).
3. Efficiency - In computer vision, the superpixel is employed as a pre-processing technique to minimize computing complexity. It should be simple to operate and calculate quickly and accurately (Wei et al., 2018).

Superpixel segmentation further provides a precise image illustration that improves performance and increases efficiency for both memory usage and processing time as fewer frames are required

in memory during processing hence guaranteeing the overall quality of segmented image objects (Papazoglou et al., 2013; Lim et al., 2014; Giordano et al., 2015; Li et al., 2015). Superpixel has risen in popularity in literature and has turned into an emerging research subject area with a diverse set of applications:

1. Face detection and recognition (Ranjan et al., 2017; Jiang and Learned-Miller, 2017)
2. Fingerprint recognition system (Krishna and Aithal, 2017; Cao and Jain, 2017)
3. Video fire detection (Kanwal et al., 2017; Zhang et al., 2018b)
4. Geographic imaging (Kaiser et al., 2017; Chen et al., 2018)
5. Smart agriculture (Roopaei et al., 2017; Shapero et al., 2017)
6. Lung cancer classification (Adetiba and Olugbara, 2015a; Adetiba and Olugbara, 2015b; Soufi et al., 2017; Lavanya and Kannan, 2017)

In computer vision, a perceptually uniform colour model is preferred for image processing, which is represented in three distinctive autonomous attributes (lightness, chroma and hue) colour pixels (Safdar et al., 2017). This colour model is frequently utilized in computer vision applications because it serves as the basis for the RGB and CIELAB colour models, which are defined by their linear or nonlinear conversions. Therefore, the RGB colour model needs to be first converted to the CIE XYZ colour model before transformation to perceptual colour models for use. According to the literature, CIELAB is regarded as a perceptual colour model that improves the performance of expression recognition (Wang et al., 2015). Since it is constructed from the perceptual colour model LMS, the non-linear connotations of LAB resemble the eye's logarithmic reaction (Long, Medium, Short). Furthermore, LAB is a colour model centred on the cone response functions in the eye's retina (Bianco et al., 2015).

However, enormous benefits exist from using superpixels for image processing. The current problems of computer vision applications and processing require instant turnaround time with incredible precision which can be satisfied using superpixels for segmentation. Superpixel based representation speeds up the colourization method and increases spatial coherency compared to using non-superpixels (Gupta et al., 2012). In the age of digital technology, digital images have rapidly increased and become popular within digital content. As a result, research in superpixel segmentation has received enormous attention in literature from cognitive neuroscience to computer vision and image processing (Ahn et al., 2017). According to the literature, algorithms

that does not take into account spatial compactness result in under segmentation error due to complicated image background and foreground, especially in digital images with foreground close to the edges (Van den Bergh et al., 2012; Chen et al, 2017). Furthermore, retrieving high-level information from low contrast images with a high level of noise and inhomogeneity intensity in digital images also becomes a daunting challenge. To resolve this gap, the variants of the selected superpixel segmentation algorithm was used by amalgamating the SLIC (simple linear iterative clustering) algorithm efficiently generates compact, nearly homogeneous superpixels by clustering pixels in a combined five-dimensional colour and image plane space with the strong attribute concurrence influence distances (SAID) while strikingly simple, it addresses the aforementioned gap and produces high quality, compact superpixels.

1.2 Research Problem Statement

The superpixel segmentation algorithms documented in the literature compute pixels based on the difference between the colour feature and the global mean of the feature. The research identified the challenge of differentiating comparable colour elements in the background and foreground parts of a digital input image in the existing superpixel segmentation algorithms. To address this challenge, the perceptual colour difference method was used in the research. The perceptual colour difference method was introduced to extend the single global mean computation to computation of background and foreground means to seamlessly incorporate the background and object information that would help improve the pixel clusters. This latest approach is highly desirable under the fundamental assumption of homogeneous background which most digital images follow. However, when the input image possesses a complex background and the foreground image is close to the edge that is the background, the digital image pixels could be wrongly segmented, leading to segmentation errors.

Superpixel-based image segmentation is commonly used, although it has limits when the focus is on precision and boundary adherence, resulting in poor picture segmentation precision. (Xie et al., 2019). Compactness refers to each superpixel's consistent shape and size, as well as its seamless boundaries. Compact superpixels are superior at capturing spatially coherent information and retrieving data from their boundaries. Overfitting in machine learning can be compared to non-compact superpixels with irregular shapes: too much data (i.e. boundary pixels) is used to represent the key information (i.e. object boundaries).

However, there is a gap in the literature failing to incorporate spatial compactness, which results in under segmentation. Therefore, there is a growing need for research on distance measures in superpixel segmentation. Subjective and objective approaches are two subcategories of the methodologies accessible for this purpose. The subjective evaluation depends on the human evaluation of the segmentation quality and objective evaluation relies on a perfect segmentation reference which is often called the ground truth (Tiburzi et al. 2008).

1.3 Aim and Objectives

This study aimed to investigate the performance of an attribute concurrence influence distance metric on image compactness in a superpixel segmentation algorithm. The following study objectives were set to accurately attain this aim:

1. To comprehensively review the relevant primary studies based on the existing superpixel image segmentation algorithms.
2. To experiment with the variants of a selected superpixel image segmentation algorithm realised by utilising the strong attribute concurrence influence distance and Euclidean distance in two colour models.
3. To compare the performances of variants of the selected superpixel segmentation algorithm based on the standard superpixel evaluation measures.

1.4 Significance of the study

Due to the rising need for an improved and effective result for image segmentation in the domains of computer vision and image processing, digital image segmentation is a popular area of research. Superpixels, which are considered as a perceptual grouping within an image that attracts greater human attention, is becoming more common in image processing applications. In trying to improve efficiency for image segmentation, a comparison of commonly used algorithms to perform an extraction of images from their background using incredible precision. According to literature Euclidean distance measure is very popular and frequently used however it has limitations when used for complex images. This study aims to reduce this limitation by using the SAID algorithm that captures the background and foreground much better focusing on the region of interest as well as the dimensions of boundaries with complex images.

1.5 Thesis Synopsis

The thesis is succinctly divided into five comprehensive chapters, which are arranged as follows.

Chapter One: Introduction to the thesis

Chapter one introduces a brief background to the study including the need for superpixel segmentation with the use of perceptual colour difference measures for digital images. The chapter identifies the research problem which led to the aim and objectives as well as the contribution of this study.

Chapter Two: Literature Review

The second chapter contains a thorough evaluation of important and useful publications on superpixel segmentation methods for digital images. Furthermore, a systematic review and meta-analysis were carried out to substantiate the advantage of superpixel segmentation over non-superpixel segmentation.

Chapter Three: Research Methodology

Chapter three presents a well-described step-by-step approach carried to achieve the set aim and objectives proposed in this study. The variants of the selected superpixel segmentation algorithm amalgamated the SLIC algorithm with the strong attribute concurrence influence distances (SAID) which addresses the aforementioned gap and produces high-quality compact superpixels.

Chapter Four: Presentation of Results and Discussion

This chapter presents the qualitative and quantitative analysis of the variants of the selected superpixel segmentation algorithm results of the strong attribute concurrence influence distance and Euclidean distance in two colour models. The selected superpixel segmentation algorithm was compared based on the standard superpixel evaluation measures.

Chapter Five: Summary, Conclusions and Implications of the Study

This chapter wraps up the dissertation while reiterating the research contribution and offering suggestions for further work.

1.6 Chapter Summary

The first chapter begins with a brief overview of the study's background, followed by the problem statement, aim, and objectives. After that, it moved on to a summary of the study's relevance.

Finally, the thesis' structure was discussed. The next chapter contains reviews of key publications that serve as a foundation for the study's background.

CHAPTER TWO

LITERATURE REVIEW

2.1 Introduction

This chapter provided a thorough overview of the literature, which served as the foundation for this research. The second chapter is sub-divided into eight sections, with the first presenting the digital image segmentation setting the building blocks of this study. The second section presents the non-superpixel image segmentation which includes edge-based and region-based image segmentation while the third section emphasized superpixel segmentation. The fourth section includes a statistical data analysis using meta-analysis to assist us in determining the best image segmentation approach grounded on the literature. The fifth and sixth section discusses the clustering algorithms and distance measure for image segmentation respectively, they are building blocks for the variants of the selected superpixel segmentation algorithm. In the seventh section, colour models will be described, and in the eighth section, performance evaluation will be used to evaluate the variants of the selected superpixel segmentation algorithm method to the state-of-the-art algorithm.

2.2 Digital Image Segmentation

Image segmentation is a complex problem in image processing that can be addressed using a repertoire of techniques (Pathegama and Özdemir Göl.,2004). The importance of image segmentation is extensively emphasized in literature for image processing and computer vision (Vidal and Amigo, 2012; Cong et al., 2018; Minaee et al., 2021). Image segmentation is the process of splitting a digital image into multiple regions (sets of pixels, also known as super-pixels) based on homogenous criteria to extract relevant information from the segmented images (Cao and Wu, 2017). Image segmentation seeks to transform an object's representation into relevant attributes based on image areas; a process of locating salient objects and boundaries in an image. Every pixel that shares a common visual attribute is given a label in image segmentation.

Furthermore, image segmentation partitions a natural image into meaningful regions characterized by homogenous extents like colour, intensity and texture, grayscale (Haralick., 1983; Liu and Yang., 1994; Chehikian., 1999). These regions reveal salient information about the images such

as colour, motion, position, texture, intensity and spectrum which is used for easy analysis (Bora and Gupta., 2014). The image pixels are labelled so that each pixel in the image has a common set of properties that can be shared.

Furthermore, the technique of segmenting an image into multiple different sections that are expected to be semantically connected and meaningful is known as image segmentation (Wang et al., 2013). Practical applications of image segmentation include the following: trace tumours and additional pathologies (Wu et al., 2014; George and Karnan, 2012), machine vision, object detection (Delmerico et al., 2011), face detection, medical imaging (Pham et al., 2000; Forouzanfar et al., 2010) and diagnosis of anatomical construction (Kamalakaran et al., 2010), fingerprint recognition and video surveillance. The technique of segmenting an image into multiple different sections that are expected to be semantically connected and significant can be grouped into superpixel and non-superpixel image segmentation.

2.3 Non Superpixel Image Segmentation

Image segmentation that is not reliant on superpixels is known as non-superpixel image segmentation. According to the literature, the most often used non-superpixel image segmentation techniques are divided into two categories: edge-based and region-based. (Saini and Arora., 2014; Zheng et al., 2018).

2.3.1 Edge Based Image Segmentation

Edge-based image segmentation is used in the literature to avoid the over-segmentation problem by avoiding the selection of incorrect pixels during the marker selection step. (Kakhani et al., 2019). Edge detection is the classification and identification of discontinuities in images. An edge is defined as a border between two uniform regions (Al-Amri et al., 2010). Boundary detection and image segmentation play an important pre-processing role for object identification and scene interpretation for most computer vision applications (Ma and Manjunath., 1997; Ganguly et al., 2009).

Edge-based segmentation methods aim to detect discontinuities in an image by drawing edges on the region by detecting pixel values that match those of neighbouring pixels (Zuva et al., 2011; Yogamangalam and Karthikeyan., 2013). Edges were modelled as intensity discontinuities for grey-level digital images with a variety of brightness on pixels between boundaries as an edge

signifies a physical boundary between dissimilar regions within an image with the aim of feature detection and extraction (Thanammal and Sudha., 2014). The traditional edge-based method detects salient objects by using a range of techniques such as colour gradient computation followed by non-maximal suppression (Dollár and Zitnick, 2014). Unfortunately, many visually salient edges, such as texture edges and illusory contours, do not match colour gradients. Finding a consistent approach for edge detection is difficult since visually prominent edges correspond to a range of visual phenomena. (Deng et al., 2017).

Many edge detector operators have been traditionally used for edge detection and boundary extraction of images over the years which are intended for different edges. There are two types of image segmentation based on edges: the first-order differential image edge detection which includes Sobel operator, Prewitt operator, Kirsch operator, and Roberts operator, and second-order differential edges detection operator, like Laplacian operator, LOG operator, and others such as Canny operator and SUSAN operator (Acharjya et al., 2012; Thanammal and Sudha., 2014; Kaur and Garg., 2011). These operators are modest yet influential in many applications used and have been modified for colour images (Wesolkowski., 1999).

2.3.2 Region-Based Image Segmentation

Image segmentation is extremely important for image recognition and image analysis, according to decades of research (Chen et al., 2009). The main goal is to partition an image into homogenous regions which entail image exploration, object illustration and overall image analysis (Kaur and Goyal., 2015). Therefore, the need to explore different segmentation methods. In region-based segmentation, image pixels are grouped into homogenous regions based on spatially localised features such as intensity, colour and texture (Leung and Malik., 1998; Kang et al., 2009; Zuva et al., 2011). These techniques aim to separate objects from the background and focus on the areas of interest (Lalaoui and Mohammadi., 2013).

According to literature region growing is a commonly used algorithm for region-based segmentation (Kaur and Goyal., 2015; Saini and Arora., 2014; Peng et al., 2012). The region growing segmentation algorithm partitions an image into equivalent primitive regions based on similarities such as grey level intensity or colour if the pixel belongs to the same class it is fused to form larger regions (Yogamangalam and Karthikeyan., 2013). This process continues until no pixel can be added to the region (Chang and Li., 1994; Hojjatoleslami and Kittler., 1998; Saini and

Arora., 2015). Performance is substantially improved with region-based models compared to edge-based models reducing sensitivity levels to noise, added robustness and improved detection of poor boundaries (Niu et al., 2017; Meher et al., 2019).

In 1998, Felzenszwalb and Huttenlocher introduced a pairwise region comparison-based picture segmentation method. They established a function that quantifies the evidence for a boundary between two regions as too coarse or too fine segmentation. Their suggested region-based segmentation method uses a specific region comparison function to execute straightforward greedy assessments while providing segmentations that conforms with the global features of not being overly abrasive or fine. However, the same author enhanced the proposed technique in 2004 by introducing an efficient graph-based image segmentation method (Felzenszwalb and Huttenlocher., 2004). To solve the difficulty of image segmentation, their proposed solution used a predicate to measure the boundary between two sections using a graph-based depiction of the image. Thereafter the predicate is used to create an effective segmentation algorithm. Image segmentation is performed using the algorithm, which constructs the graph using two different types of local neighbourhoods and illustrates the results with actual and simulated images. According to literature numerous region-based segmentation approaches were recommended for improved segmentation including split and merge (Haralick and Shapiro., 1985; Kaur and Goyal 2015). The efficiency of region-based algorithms is application dependant.

2.4 Superpixel Segmentation

Ren and Malik (2003) pioneered the idea of superpixel as a pre-processing stage for segmentation. Superpixels is simply the grouping of pixels into meaningful regions. Having compared several superpixel segmentation algorithms it is found that that most of the performance of the algorithm is exceptional with benefits ranging from memory efficiency, reduced computational cost, higher accuracy, increased speed and incredible precision.

There are a few reasons why superpixel is preferred to pixels in image processing. An image with a moderate resolution has several pixels, which is very inefficient to process whereas if the same image is processed using superpixels will lead to reduced computational costs and minimal loss of image information. Superpixels contains more information than pixels. The pixels belong to a group of superpixels that share similar visual properties giving superpixel meaningful regions. Superpixels allow for easy and compact image segmentation, resulting in significant

improvements in image processing. Grouping pixels into meaningful regions reduces image primitives and redundancy (Zhang et al., 2017).

There are enormous benefits from using superpixels for image processing. The current problems of computer vision applications and processing require instant turnaround time with incredible precision which can be satisfied using superpixels for segmentation. Superpixel based representation speeds up the colourization method and increases spatial coherency compared to using individual pixels (Gupta et al., 2012). According to the literature decreases the number of image primitives and enhances representational efficiency. Properties for good superpixels include coherence, compactness and regularity. (Wang et al., 2017)

Linear Spectral Superpixel (LSC) Segmentation Clustering extracts perceptually significant image features and runs them in linear complexity with optimal memory performance (Li and Chen., 2015). Every image pixel is linked to a position in a ten-dimensional feature space that is segmented using weighted K-means, resulting in superpixels that are compact and uniform in shape, with increased memory efficiency and linear time complexity. Experiments show that LSC performs well when compared to other algorithms. The distance function, which has two items, the seed distance and neighbour distance item, was used in Real-Time Superpixel Segmentation by DBSCAN Clustering Algorithm (Shen et al., 2016). A DBSCAN density-based clustering algorithm produced superpixel results with similar colours and geometric restrictions. Colour and spatial information are measured and used to merge the small initial superpixel and their closest neighbour superpixels. According to the author, this algorithm reduces the computational cost and produces exceptional results. On the contrary, the suggested DBSCAN superpixel algorithm has certain drawbacks. Because DBSCAN is a local optimum technique in both the clustering and merging stages, the existing DBSCAN superpixel algorithm cannot completely meet the compactness constraint.

The image segmentation is based on a superpixel's optimal spatial feature (Tian et al., 2015). It divides an image into several sections with uniform and similar characteristics. Two experiments are used to evaluate the method: (1) synthetic and actual SAR image segmentation, and (2) the suggested method's application extension. The wavelet feature F is used to segment SAR images. For natural image segmentation, the application extension for texture images is based on texture

feature, i.e. grey level co-occurrence matrix (GLCM), and the feature of 3-D CIE Lab colour are extracted. The proposed approach achieves improved segmentation accuracy of SAR images, according to experimental data.

A simple superpixel segmentation technique with a border constraint (Zhang et al., 2016) presented a superpixel segmentation model based on a distance measure that is developed to equalize boundary adherence by combining texture features and compactness parameters of the ensuing superpixels to assess the similarity of pixels and superpixel seeds. The algorithm is simple, effective, and precise, ensuring object boundary compliance. For colour image segmentation, Superpixel-Based Fast Fuzzy C-Means Clustering for Colour Image Segmentation (Lei et al., 2019) used a superpixel-based fast FCM (SFFCM). The technique achieves colour image segmentation with good segmentation accuracy at a minimal computing cost. The first contribution is a multiscale morphological gradient reconstruction (MMGR) operation to generate superpixel images with precision segmentation, and the second is a basic colour histogram to obtain a fast FCM for colour image segmentation using a simple colour histogram. The experiments yielded the best segmentation results, which are fast, however practical applications are limited because the number of clusters must be pre-determined.

Homogeneous Superpixels from Random Walks (Perbet and Maki., 2011), presented an approach to compute a superpixel image using the Markov random walks over graph representation of an image. Their approach was using the Markov clustering methodology however when used in its original form has limitations whereby it produces non-homogenous superpixels and it does not scale well for large images as it fails to compute the square of the stochastic matrix in a reasonable time. These limitations were addressed with a combination of both MCL and a compact pruning strategy, which enforced the flow circulation to be local which ultimately led to producing more homogenous superpixels faster and making the flow computation tractable at the same time.

Superpixels via Pseudo-Boolean Optimization (Zhang et al., 2011) introduced two new Pseudo-Boolean optimization-based formulas for creating superpixels. Smaller sizes or irregular forms are inhibited by the smoothing cost, therefore superpixels created by this method are regular in size and shape. Most superpixels formed have a regular lattice configuration, with their boundary adjusted to the image content's curves. The Elimination algorithm was used to compare four algorithms, and it developed the pseudo-Boolean optimization step for this algorithm. The number

of superpixels does not influence the efficiency of their method. The experiment shows that their approach can produce superpixels with the accuracy of Expansion Moves at the speed of Super Lattices. The proposed method is substantially faster and more accurate than conventional algorithms.

Shen et al. (2014) used Lazy Random Walks (LRW) to insert initial seeds of allotted superpixels before using the LRW approach to acquire initial superpixels and bounds to make borders more consistent. As a result, this approach assists in the optimization of seed positions and the splitting of huge superpixels into smaller ones, resulting in improved superpixel segmentation performance. Several superpixel segmentation algorithms have been created, according to the literature, with outstanding performance rates and enhanced accuracy levels. (Minaee et al., 2021; Sultana et al., 2020).

Table 2.1: Summary of Superpixel image segmentation based on ASA

Title	Author/Year	Method	Approach	Achievable Segmentation Accuracy	Dataset
“Superpixel Segmentation using Linear Spectral Clustering”	Li and Chen, 2015	Linear Spectral Clustering	Super Pixel	0.962	1
“Real-Time Superpixel Segmentation by DBSCAN Clustering Algorithm”	Shen et al., 2016	DBSCAN Clustering	Super Pixel	0.964	1
Content-Adaptive Superpixel Segmentation	Xiao et al., 2018	Content-adaptive superpixel (CAS) segmentation algorithm	Super Pixel	0.9624	4

		Uses the CIELAB colour model			
Differential Evolutionary Superpixel Segmentation	Gong et al., 2017	Differential Evolutionary Superpixels (DES)	Super Pixel	0.962	2
“Use of Spectral Clustering Combined with Normalized Cuts (N-Cuts) in an Iterative k-Means Clustering Framework (NKSC) for Superpixel Segmentation with Contour Adherence”	Ghosh et al., 2018	“Superpixel segmentation algorithm, NKSC, which is of linear computational complexity and high memory efficiency”	Super Pixel	0.961	1
“SLIC Superpixels Compared to State-of-the-Art Superpixel Methods”	Achanta et al., 2012	“Adapts k-means clustering to generate superpixels with Euclidean distance measure”	Super Pixel	0.769	2

“VCells: Simple and Efficient Superpixels Using Edge-Weighted Centroidal Voronoi Tessellations”	Wang et al., 2012	Voronoi-Cells.	Super Pixel	0.9570	1
“Manifold SLIC: A Fast Method to Compute Content-Sensitive Superpixels”	Liu et al., 2016	“Manifold SLIC is an extension of SLIC to compute content-sensitive superpixels”	Super Pixel	0.9763	1
“Entropy Rate Superpixel Segmentation”	Liu et al., 2011		Super Pixel	0.9593	1
“Superpixels and Supervoxels in an Energy Optimization Framework”	Veksler et al., 2010		Super Pixel	0.9501	1
“Real-Time Coarse-to-fine Topologically Preserving Segmentation”	Yao et al., 2015		Super Pixel	0.9584	1

“An improved region-based model with local statistical features for image segmentation”	Ge et al., 2012		Region-based	0.966	2
“Multi-Class Support Vector Machine”	Wang et al., 2014	Support Vector Machine (SVM)	Region-based	0.9274	1
“Mass Classification in Mammograms Using Selected Geometry and Texture Features, and a New SVM-Based Feature Selection Method”	Liu and Tang, 2013	SVM	Region-based	0.930	1
“Fast opposite weight learning rules with application in breast cancer diagnosis”	Saki et al., 2013	“Opposite Weight Back Propagation per Epoch (OWBPE)”	Region-based	0.8928	1
“Learning-based alpha matting using support vector regression”	Zhang et al., 2012	SVM	Region-based	0.7300	1

“Classification of benign and malignant masses based on Zernike moments”	Tahmasbi et al., 2011	Multi-layer Perceptron (MLP)	Region-based	0.9643	1
“Directional features for automatic tumour classification of mammogram images”	Buciu and Gacsadi., 2011	Proximal Support Vector Machines (PSVM)	Region-based	0.8230	1
“Morphological region-based initial contour algorithm for level set methods in image segmentation”	Rad et al., 2017	Morphological Region-Based Initial Contour (MRBIC)	Region-based	0.9744	1
“Region-Based Convolutional Networks for Accurate Object Detection and Segmentation”	Girshick et al., 2015	Region-based Convolutional Network (R-CNN)	Region-based	0.842	1
“An automatic region-based image segmentation algorithm for remote sensing applications”	Wang et al., 2010	“Region-based Image Segmentation Algorithm based on k means clustering (RISA)”	Region-based	0.864	1
“Integrating machine-learning with	Pratondo et al., 2017	k-NN and SVM	Region-based	0.930	1

region-based active contour models in medical image segmentation”					
“A hybrid edge-based segmentation approach for ultrasound medical images”	Gupta et al., 2017	“Active contour method using distance regularized level set (DRLS) function”	Edge-based	0.930	1
“A Level Set Method for Infrared Image Segmentation Using Global and Local Information Image Segmentation: Automated Learning from Examples”	Wan et al., 2018	“Constructs a hybrid SPF made up of a global term and a local term”	Edge-based	0.980	1
“Robust Edge-Stop Functions for Edge-Based Active Contour Models in Medical Image Segmentation”	Pratondo et al., 2015	“Edge-stop functions Developed new ESFs for edge-based active contour models”	Edge-based	0.910	1
“Weighted Level Set Evolution Based on Local Edge Features for Medical Image Segmentation”	Khadidos et al., 2017	“active contours implemented using level set methods for segmentation”	Edge-based	0.9549	1

“A hybrid edge-based technique for segmentation of renal lesions in CT images”	Kaur et al., 2019	Spatial IFCM clustering (SIFCM)	Edge-based	85.57	1
“A Comparative Study of Segmentation Quality for Multi-resolution Segmentation and Watershed Transform”	Kavzoglu, T. and Tonbul, H., 2017	Area Fit Index (AFI and Quality Rate (Qr)	Edge-based	80.83	1
“Fully automatic ROI extraction and edge-based segmentation of radius and ulna bones from the hand radiographs”	Simu et al.,2017	“automatic extraction of radius and ulna bones from a left-hand radiograph (RUROI)”	Edge-based	98	1
“Classification of very high-resolution remote sensing images by applying a new edge-based marker-controlled watershed segmentation method”	Kakhani et al., 2019	watershed strategy	Edge-based	94.67	1
“An Efficient and Robust Iris Segmentation	Li et al., 2019	Iris segmentation	Edge-based	95.49	1

Algorithm Using Deep Learning”					
--------------------------------------	--	--	--	--	--

2.5 Meta-Analysis Literature strategy

A literature search was undertaken for the meta-analysis to find all published publications on superpixel and non-superpixel kinds of segmentation. The research was conducted using scholarly resources such as the Web of Science and Google Scholar to find relevant published publications. The literature search was conducted using the recommended reporting items for systematic reviews and meta-analysis (PRISMA) technique (Panic et al., 2013; Hutton et al., 2016; Toews., 2017). The following keywords were used to search these databases for English publications published between 2010 and 2021. Image segmentation and text words in Web of Science: image segmentation [All Fields]: ('superpixel image segmentation' [All Fields] AND 'edge-based image segmentation [All Fields]) OR 'region-based image segmentation'[All Fields]. Boolean operators like "OR" and "AND" were used to separate or combine the search terms. The studies retrieved using the search strategies were imported into EndNote X9. Between 2010 and 2021, a total of 50,243 published papers were discovered, as shown in Figure 2.1. In addition, the reference lists of the relevant papers were manually reviewed for any citations that were overlooked during the electronic database search.

2.5.1 Inclusion and Exclusion Criteria

The studies conducted for image segmentation served as the papers' inclusion criteria. Superpixel segmentation approach was included while non-superpixel segmentation such as edge-based and region-based segmentation approach was also considered. Performance metrics such as achievable segmentation accuracy was also included in the study. Books, book chapters, brief reports, and theses authored in languages other than English and published before January 2010 were eliminated. Articles that did not match the criteria for inclusion were also omitted.

2.5.2 Statistical data analysis

The data were extracted and entered into an excel spreadsheet. Stata 15.0 was used to conduct the statistical analysis. The data from image segmentation approaches were analyzed in a meta-analysis, and the estimates and 95% confidence intervals were pooled. An inverse-variance model was used to quantify heterogeneity using both fixed and random effects meta-analysis (DerSimonian and Laird, 1986).

2.5.3 Meta-Analysis Results

The results of this investigation were obtained using the PRISMA criteria, as indicated in Figure 2.1. A total of 50,243 articles were found in two databases after the initial search. After EndNote X9 deleted duplicates, only 14,933 documents remained in the sample. 10,000 articles were crossed out after reading the abstracts. After the documents were examined, a total of 4,000 were discarded for a variety of reasons. Finally, based on the inclusion and exclusion criteria, thirty-one relevant published papers between 2010 and 2021 were selected for final review.

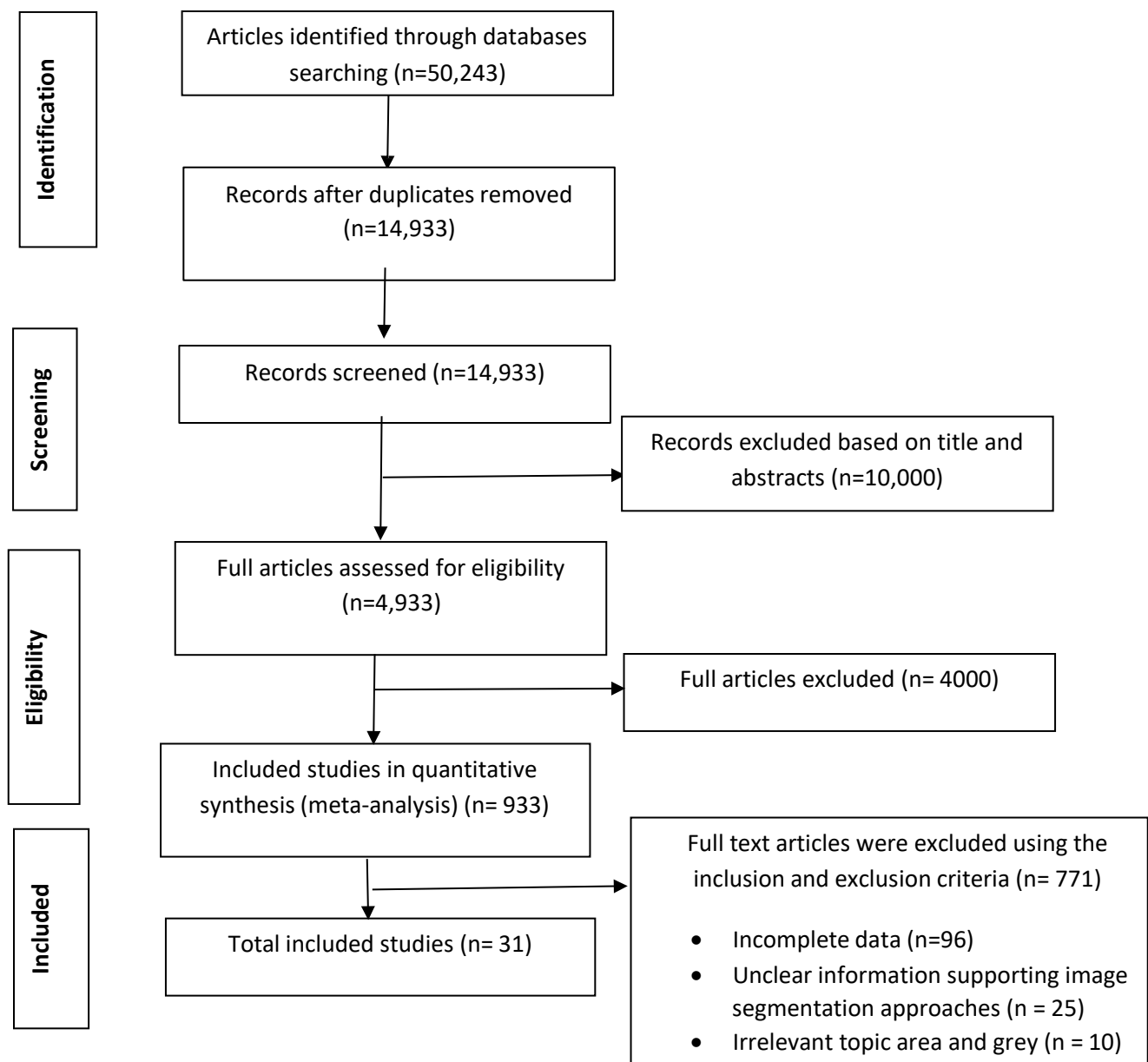


Figure: 2.1 Flow diagram of the database searches (Preferred Reporting Items for Systematic Reviews and Meta-Analysis)

2.5.3.1 Overall pooled Estimate

Figure 2.2 shows the forest plot resulting from the meta-analysis, which shows the studies, effect sizes, confidence intervals, and weight. The overall estimates of image segmentation approaches were 90.0% (95% CI: 82.0, 98.0) using a random-effects model. According to the data of $\tau^2 = 1.69$, chi-square = 16.78, degree of freedom = 30 and $P = >0.01$, between-study variability

(residual amount of heterogeneity) was substantial. The quantity of residual heterogeneity reflects the degree of variability. The I^2 statistic (95.0%, $P > 0.01$) indicated significant heterogeneity among the included studies

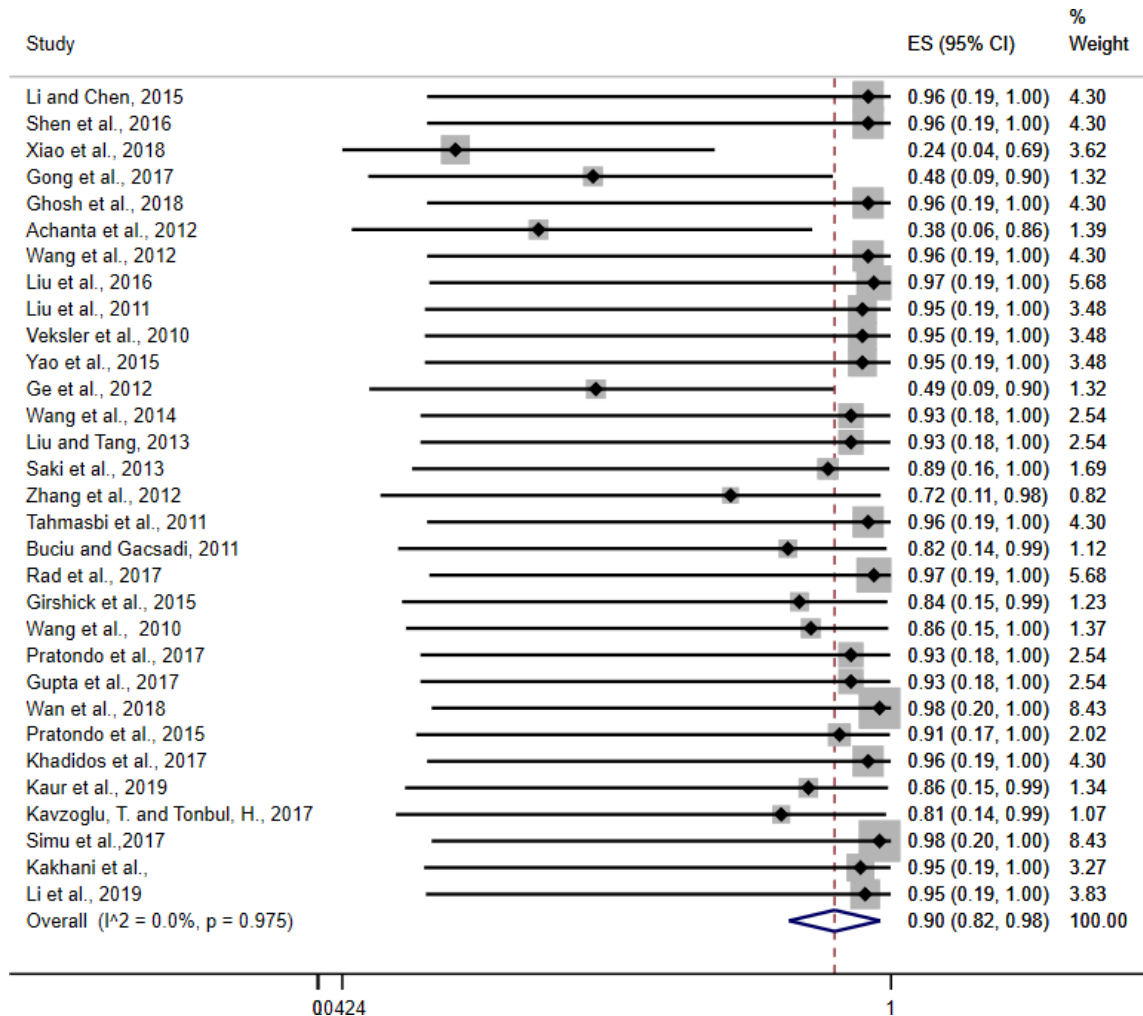


Figure 2.2: Pooled estimate from the random-effect model

The heterogeneity chi-square test result obtained in this study affirmed the statistical significance of heterogeneity (Figure. 2.3). The diamond indicates the pooled estimate, and each line represents the confidence interval around the estimate.

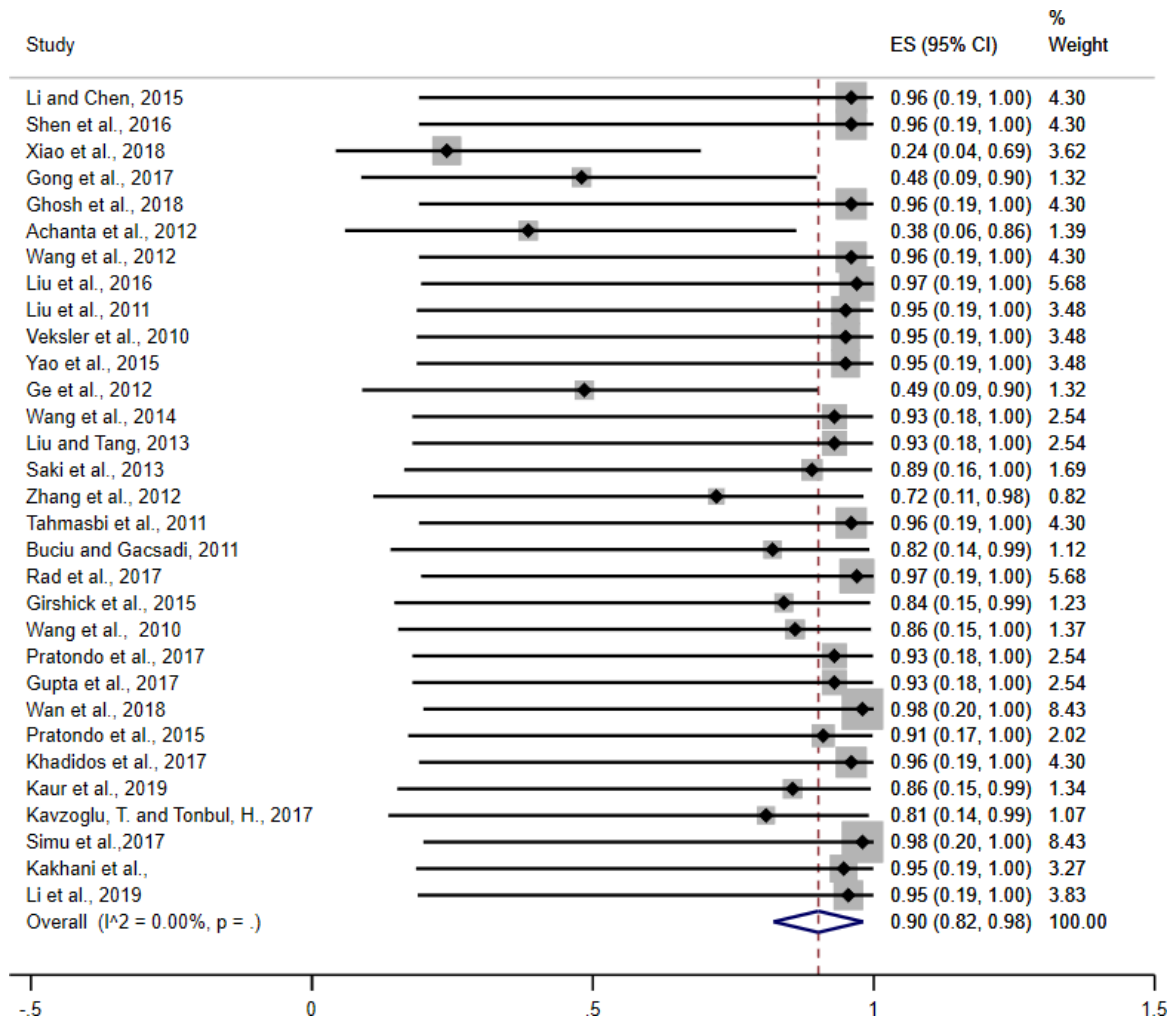


Figure 2.3: Pooled estimate from the fixed-effect model

Although, the pooled estimate indicated that there is no heterogeneity but this study went further to examine the subgroup analysis to ascertain the findings of this paper. To investigate the origins of heterogeneity, a subgroup analysis was performed for the selected grouping. The main flaw of heterogeneity measurements is that they only provide global measures with no information on the origins of heterogeneity. Due to the extreme gap, subgroup analysis is required to uncover sources of heterogeneity. Subgroup analysis is the process of dividing participant data into subgroups to make comparisons between them. Subgroup meta-analytic interpretation can provide useful insights into moral implications that would not be acquired from a non-subgroup study. In subgroup analyses, the method with the highest approach was estimated to be 95% (95% CI: 79.0%- 1.11%; $I^2 = 0.0\%$), followed by Region-based with 90% (95% CI: 74.0%; 1.05%; $I^2 = 0.0\%$), and superpixel 85% (95% CI: 70.0%- 1.0%; $I^2 = 25.70\%$) and edge-based approach to be

(Figure 2.4). The advantage of a superpixel over the other approaches is that it possesses a high heterogeneity.

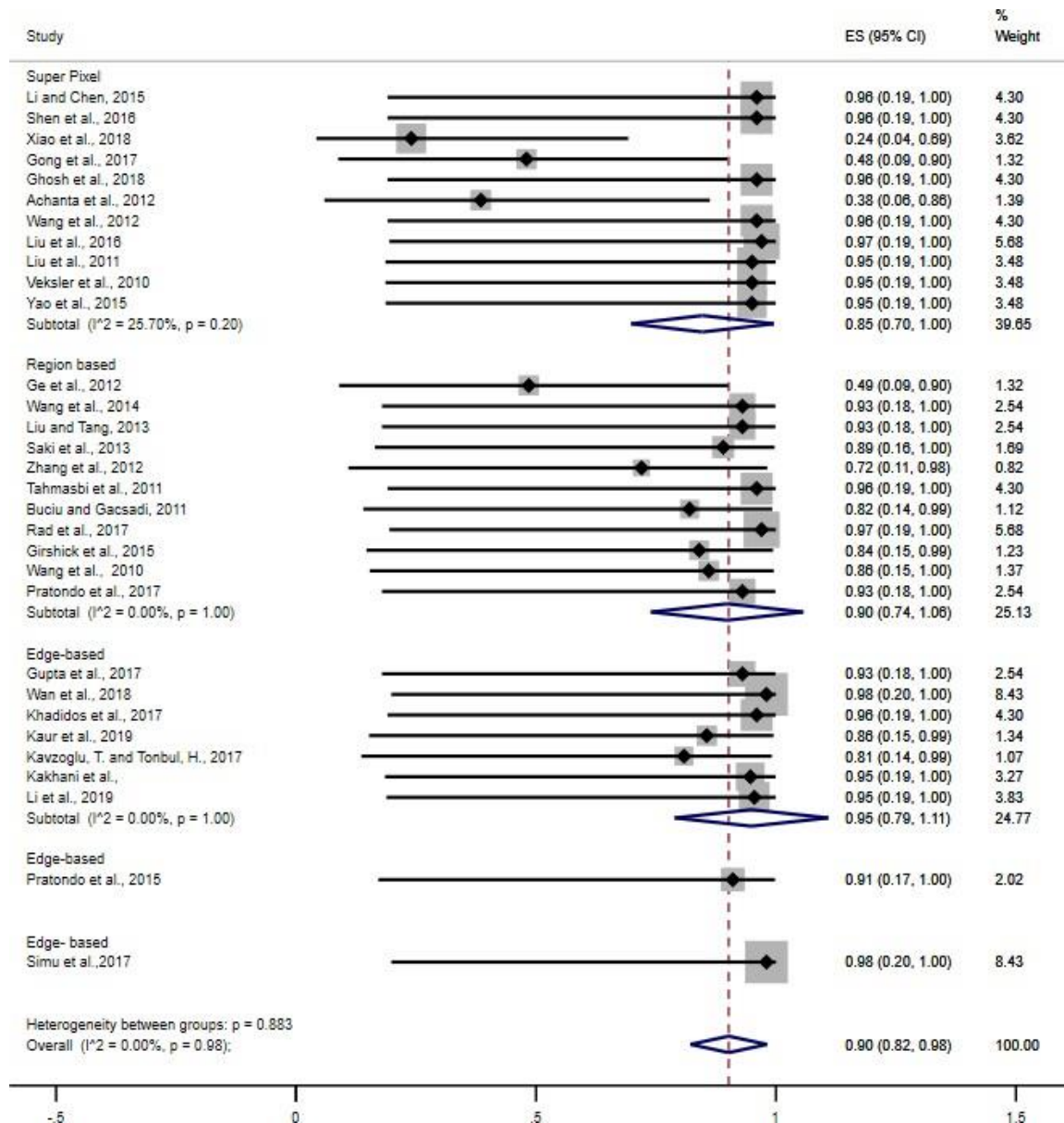


Figure 2.4: Subgroup analysis based on the approaches

2.6 Clustering Algorithm

Clustering is the process of dividing a collection of unlabeled objects into subgroups called clusters so that objects in the same group are more related than objects in other groups. Clustering has many application areas which include: Machine learning, data mining, pattern recognition, image

analysis, and bioinformatics all use clustering as a statistical data processing procedure. (Ajala et al., 2012). Even though clustering algorithms and classifier methodologies are likely to work together, clustering algorithms may not necessitate training data; instead, they repeat through segmenting the image and identifying the attributes of the individual classes. As a result, they are often known as unsupervised approaches. Clustering algorithms are often based on a similarity or dissimilarity index between pairs of data points (Isa et al., 2009). Clustering is one of the most efficient strategies among the various techniques. Clustering can be divided into several types: K-means clustering, improved K-means and Fuzzy C-means clustering.

2.6.1 K-Means

K-means is an unsupervised and one of the key fundamental algorithms for handling clustering issues, according to the literature. (Dehariya et al., 2010; Lala et al., 2013). The K-means approach is used to assign each point to a cluster, whose Centred is known as the closest centroid. The cluster centred is the average of all of its points, and its parameters are the mean value of each measure over all of the cluster's points (Madhulatha., 2012). There are two aspects to the K-means algorithm. In the first phase, it calculates the k centroid, and then in the second phase, it shifts each point to the cluster with the closest centroid to the data point. K-means clustering is beneficial for biomedical image segmentation since the number of clusters is usually known for images of certain regions of the human anatomy (Wu et al., 2007; Lala et al., 2013). The K-mean clustering approach, according to (Rauf et al., 2012), is where the clusters are completely dependent on the centroids of the initial clusters. The distances between all data components are determined using the Euclidean distance formula once K data elements are chosen as initial centres.

Although the K-means algorithm has the advantage of its simplicity and eases of implementation. K-means algorithm can be used for grouping large information sets (Nazeer et al., 2009). It has drawbacks, one of which is that the quality of the final clustering results is dependent on the initial centroid selection which could vary for different initial centres which need to be carefully chosen for the desired result (Dhanachandra et al., 2015). Another drawback of K-means is that the user needs have prior knowledge of the number of clusters that are searched for (Napoleon et al., 2010).

2.6.2 Improved K-Means

Any type of integer data can be used in an upgraded K-mean clustering algorithm. During each iteration, the method saves the cluster labels and the distance of all data objects to the nearest

cluster using two basic data structures so that they can be reused in the next iteration. After then, the distance between the current data object and the new cluster Centred is determined (Na et al., 2010).

2.6.3 Fuzzy c-mean

Fuzzy clustering is the method for pre-structuring and analyzing fuzzy data to classify it and make inferences. It is possible to create homogeneous data pools for the same cluster and heterogeneous data pools for distinct clusters (Kavitha and Prabakaran, 2019). Within the group, distances are kept to a minimum, but distances between groups are increased. Although there are additional alternative categorizations, fuzzy clustering can be classified into hierarchical and non-hierarchical techniques. Agglomerative (grouping) and divisive (dividing) approaches fall under the first category. Single-pass methods, relocation methods, nearest neighbour methods, and so on are all subcategories of the non-hierarchical category. Even with memory constraints, fuzzy C-means has proven to be efficient without affecting clustering accuracy. In terms of the amount of the dataset, the approach is also ideal.

2.6.4 Pixel Intensity Clustering Algorithm

While clustering-based algorithms have shown to be effective for a limited number of criteria, the computation complexity for a significant number of thresholds poses a problem. Pixel Intensity Clustering Algorithm (PICA) is an innovative multilevel clustering approach developed by Olugbara et al. (2015) to alleviate the problem of the computational cost faced by clustering algorithms. Their innovative approach starts with a linear partitioning approach that uses a group of image pixels, the amount of chosen clusters, and a set of image pixel intensities to establish cluster centroids. This initialization technique differs significantly from traditional clustering-based segmentation algorithms, which randomly hand-pick the primary cluster centroids. Furthermore, the initialization technique in the first phase achieves the critical goal of preventing dead centres, a typical delinquent in traditional clustering algorithms. The second step is the apportionment of image pixels into groups and the computation of final images is the last phase of their innovative algorithm.

2.7 Distance measure for image segmentation

In the age of digital technology, digital images have rapidly increased and become popular within digital content. As a result, research in superpixel segmentation has received enormous attention in literature from cognitive neuroscience to computer vision and image processing (Ahn et al., 2017). A cluster is a set of objects that are similar within one group but different from those in other groups. To determine how similar two objects are, a distance measure is utilized. Clustering produces groupings that can be used as a pre-processing step in classification algorithms. Grouping data into classes of similar entities (related) is known as clustering a method of grouping homogeneous regions of objects with a high level of similarity into a cluster when compared to one another and dissimilar data (not related) within other clusters (Bora and Gupta., 2014). Dissimilarities are assessed on features related to the objects requiring further investigation on how to compute dissimilarities between objects represented by interval scaled variables. Various distance measures can be used to compute dissimilarity matrix interval-scaled variables using Euclidean, Manhattan, Minkowski (Thant and Aye., 2020; Faisal et al., 2020).

2.7.1 Euclidean Distance

According to Kokare et al., (2003), the Euclidean distance (EUC) metric is the distance between two points that can be measured with a yardstick or the diagonal-line distance between two points. It requires preprocessing before implementation which compromises the image quality. Although it is easy to implement and test hence, it is ineffective for image data and document categorization (Pandit and Gupta., 2011; Wu et al., 2013). Euclidean distance is a commonly used distance measure to extract similarities between two vectors (Hanoun and Hashim., 2019; Alias et al., 2019). Which is used to find the square root of the sum of absolute differences between two vector elements (Wady and Ahmed., 2019; Kavitha and Rao., 2019). It is considered to be a straight-line distance between two points and can assess any dissimilarity between two objects (Ricotta., 2021).

Presently a preferred distance measure and is also known as a Ruler Distance and L2 Distance (Elen and Avuclu., 2021; Patel and Ghosh., 2020; Varma and Choudhary., 2019). Euclidean Distance is suited for cluster boundaries that are linear but has limitations when these group boundaries are non-linear or complex as the distance measure is insufficient to discover them (Sharma and Seal., 2020). Exceptional outcomes are achieved with compact datasets that have the same metrics however when two objects do not have uniform metrics could lead to a variation of

distance when compared with other pairs of objects that have similar features (Patel and Upadhyay., 2020). According to the literature, there are numerous advantages to employing the EUC distance measure, including the fact that the distance between two items is unaffected by the addition of new objects to the study and that it is spontaneous (Mercioni and Holban., 2019; Vélez-Falconía et al., 2020).

However, scale discrepancies between the dimensions from which the distances are generated can alter the distances, increasing the computing cost (Mercioni and Holban., 2019). Euclidean distance is represented by Patel and Upadhyay., (2020):

$$d(x_i, x_j) = \sqrt{\sum_{k=0}^n (x_{ik} - x_{jk})^2} \quad (2.1)$$

2.7.2 Minkowski distance

The Minkowski distance measure generally evaluates the similarity among objects. It combines three methods to compute similarity, these include the nearest neighbour similarity, Minkowski distance and Euclidean distance methods. Minkowski distance aims to calculate similarity based on geometric distance (Salmin et al. 2020). It is a metric on the Euclidean space which is considered a generalization of the Euclidean and Manhattan distance defining two points in the vector space (Al-Sbou., 2020; Kavitha and Rao., 2019; Wady and Ahmed., 2019). Provides the finest results when the dataset is dissimilar from each other producing fast, robust, and easier to comprehend however the algorithm does not work well for categorical data and fails for non-linear datasets (Vélez-Falconía et al., 2020). An added weakness of the Minkowski distance function is that if one element in the vectors has a larger range than the other elements, this value takes over the other elements (Al-Sbou., 2020). Minkowski norm is defined by Gueorguieva et al., 2017:

$$d_m(x_i, x_j) = m\sqrt[m]{\sum_{k=1}^n |x_{ik} - x_{jk}|^m} \quad (2.2)$$

2.7.3 Chebyshev

The Chebyshev distance metric is also known as a chessboard or maximum value distance is acquired if the regulating value is boundless (Patel and Ghosh., 2020) also referred to as an exceptional case of the Minkowski distance with $\lambda = \infty$ (Wady and Ahmed., 2019). The Chebyshev Distance between point's p and q is given whereby p_i and q_i are the standard coordinates (Varma, N.M. and Choudhary., 2019). Chebyshev distance provides the benefit of taking less time to decide on the distances between datasets however a weakness if the middle position is adjacent may not perform optimally (Vélez-Falconía et al., 2020).

Chebyshev distance or infinity norm between two vectors is the highest of their absolute magnitude alongside the vector dimension. Chebyshev distance can be an alternative for systems that require fast calculation when compared to other distance measures. It's also referred to as the greatest value distance and calculated as the absolute magnitude of a pair of data points' coordinate differences. The following is the distance. (Gultom et al., 2018):

$$d(x_i, x_j) = \max |x_{ik} - x_{jk}| \quad (2.3)$$

2.7.4 Manhattan distance

Manhattan Distance also known as City Block or L1 distance evaluates space among two points x and y with k measurements which is the sum of distances from all the attributes (Varma and Choudhary., 2019; Wady and Ahmed., 2019; Suwanda et al., 2020; Abdulrahman et al., 2020). Manhattan distance is fairly limited as its effectiveness is dependent on the coordinates used (Sharma and Seal., 2020). It calculates the grid distance using diagonal movements and pixels (Patel and Ghosh., 2020), which is illustrated as computing the sum of two sides of a right triangle except for the longest side (Motwani and Sharma., 2020). An advantage of this measure is that it is less sensitive to noise as the distance measure is not squared and can salvage images at a faster rate (Patel, B. and Ghosh), however, it is dependent on the variation of the coordinates (Vélez-Falconía et al., 2020).

The Manhattan distance is a measurement of two points along axes at right angles, which is commonly employed in integrated circuits using parallel wires. It can be generalized to higher dimensions, but it is ineffective for image data and document categorization. (Tolentino and Gerardo.,2019). Manhattan distance measures between two points along the axes at right angles.

In a plane with p1 at (x1, y1) and p2 at (x2, y2), it is $|x1 - x2| + |y1 - y2|$. This distance measure is frequently used in integrated circuits where the wires run parallel to the X or Y axis only:

$$d(x_i, x_j) = \sum_{k=0}^n |x_{ik} - x_{jk}| \quad (2.4)$$

2.7.5 Cosine distance

The cosine distance is a measure of similarity between two vectors of n dimensions that are calculated by determining the angle between them, and it is frequently used in data mining to compare documents. Cosine angle distance describes the vector similarity using the angle that separates two vectors (Wady and Ahmed.,2019), which discovers a regularized dot product of two feature points (Kavitha and Rao., 2019). The cosine angle distance metric efficiently discovers the angle of cosine between the Eigen standards of vectors (Patel and Gosh., 2020). It initiates a measure that can differentiate amongst similar texts, ranking them in similar order but has a weakness of its inability to deliver data on the scale of differences (Vélez-Falconía.,2019). Cosine distance expression is (Wang et al., 2018):

$$COSINE(X_K, X_L) = 1 - \frac{\sum_j^p x_{Kj} x_{Lj}}{\sqrt{\sum_{j=1}^p x_{Kj}^2} * \sqrt{\sum_{j=1}^p x_{Lj}^2}} \quad (2.5)$$

2.7.6 Mahalanobis distance

Mahalanobis distance metric was named after an Indian statistician during 1893 and the concept was implemented in 1936. It is a well-known tool in multivariate analysis with multiple applications (Ghorbani., 2019). Prevalent applications included supervised classification, outlier detection, multivariate depth measures and hypothesis testing (Berrendero et al.,2020). It is also known as the quadratic distance which computes the differences amid two groups (Patel and Ghosh., 2020; Varma and Choudhary., 2019). Mahalanobis distance metric is a correlation-based statistical-based distance metric that evaluates the dissimilarity between two multivariate sets of data (Sarmadi et al., 2021). It's a metric for comparing a feature vector to a multivariate normal

distribution with a specified mean feature vector and covariance matrix. (Wady and Ahmed., 2019).

The Mahalanobis distance is used to calculate the distance between two points in a space defined by relevant structures. It accounts for imbalanced variances and relationships between features, therefore, evaluating the distance by allocating varying weights to data points. When the features are dissimilar the distance measure using Mahalanobis is similar to the Euclidean distance metric. The Mahalanobis distance is well-known for its ability to cluster data, but it has drawbacks in terms of processing time and the need for large samples for training. It further has difficulty in determining the covariance matrices accurately and requires huge amounts of memory and time for processing (Kokare et al., 2003). The Mahalanobis distance is indicated by (Leys et al., 2018):

$$d = \sqrt{(x - \mu)^T \Sigma (x - \mu)} \quad (2.6)$$

2.8 Colour Models

The variety of colour models developed for colour image segmentation is significantly greater than one may expect at first glance. There are dozens of colour models, most of which are related to their intended usage. A survey of previous studies in this area reveals that choosing the best colour model for colour image segmentation remains a difficult topic in image processing and computer vision. To date, no colour model has proven to be superior to the others in terms of suitability for all types of images.

2.8.1 RGB

Human perception of colour is the way it is recognised and visualized based on common characteristics such as hue and intensity (Ibraheem et al., 2012). Many mathematical colour models were used to quantify colours and segment images based on their colour content (Chikando and Kinser 2005). According to literature choosing a suitable colour model for computer vision algorithms is extremely important for feature detection, object recognition, and tracking enforcing similarities of colour properties within a class of image pixels that have similar colours (Stokman and Gevers., 2007; Khattab et al., 2014). The RGB model represents colours that are tristimuli red (R), green (G) and blue (B) as its primary colours (Cheng et al., 2001; AlQadi et al., 2017).

RGB is an additive model in which the main colours are added together to form a comprehensive array of colours, therefore is considered as the base colour model for various applications which include procurement, storage and display (Basilio et al., 2011). The lack of separation between the luminance and chrominance components is a shortcoming of this model, making it an unsuitable choice for colour analysis and colour-based recognition, as well as robotic vision applications (Bruce et al., 2000; Chikando and Kinser 2005; Al-Tairi et al., 2014).

2.8.2 CIELAB

CIELAB is a perceptually homogenous colour model that has been authorized by the Commission Internationale de l'Eclairage and is used for image analysis (Weatherall and Coombs., 1992). The international standard was established in the early 1970s to assist with quantifying colour reproduction errors focusing on enormous identical coloured areas (Zhang and Wandell., 1996). Colour combinations such as red and yellow, blue and red, green and yellow, and blue and green-blue make up the CIELAB colour model.

An object's brightness is measured on a scale of 0 to 100, with 0 being black and 100 representing white. The a^* coordinate represents the position of an object's colour on a pure green and pure red scale, where -127 represents pure green and +127 represents pure red. The b^* coordinate represents the position of the object's colour on a pure blue background (Ganesan et al., 2010). Unlike the RGB and CMYK colour models, CIELAB has the advantage of being built to resemble human vision. Its L component closely reflects how individuals sense lightness, and it seeks perceptual homogeneity. It can thus be used to fine-tune the colour balance by modifying the output curves in the a and b components, as well as the lightness contrast by adjusting the L component.

2.8.3 HSV

HSV is one of the colour models that has been employed in an attempt to use ones that are more similar to how people see colour. HSV is made up of three elements: hue (H), saturation (S), and value (V). H stands for "colour," S stands for "colour dominance," which ranges from unsaturated (grey areas) to saturated (no white element), and V stands for "brightness." HSV colour model has earned the potential to assist applications in noisy colour image segmentation in recent years (Bora et al, 2015). HSV colour model, as stated by (Sural et al, 2002), can perceive colour with high intensities, making it easier to discern salient objects from the backdrop. As a result, their study

of HSV-based characteristics is utilized to investigate segmentation clustering techniques such as FCM and K-means.

Table 2.2: Summary of Colour image segmentation based on different colour models

Title Author	Year	Type of image used	Colour model	Segmentation algorithm
“Automatic seeded region growing for colour image segmentation”	Shih et al., 2005	Nature scene images	RGB	Seeded region growing
“Colour image segmentation using fuzzy clustering techniques and competitive neural network”	Sowmya et al., 2011		RGB	FCM, PFCM,CNN
“LS-SVM based image segmentation using colour and texture information”	Yang et al., 2012	BSD, MSRC, SED	HSV	FCM
“Determination of Number of Clusters in K-Means Clustering and Application in Colour Image Segmentation”	Ray et al., 1999	Synthetic and natural	RGB	K-Means
“A Study of Efficiency and Accuracy in the The transformation from RGB to CIELAB Colour model”	Connolly and Fliess, 1997	Captured image	CIELAB	
“Comparison between YCbCr Colour model and CIELab Colour model for Skin Colour Segmentation”	Kaur and Kranthi, 2012	Skin colour	YCbCr CIELAB	
“Colour Image Segmentation for Medical Images using L*a*b* Colour model”	Baldevbhai and Anand, 2012	Medical images	CMYK	
“White Blood Cell Segmentation by Colour-	Zhang et al., 2014	White blood cell	RGB CMYK	K-Means

Space-Based K-Means Clustering”				
“Skin Segmentation Using YUV and RGB Colour models”	Al-Tairi et al., 2014	Skin detection	YUV and RGB	
“Intra-prediction for colour image coding using YUV correlation”	Lucas et al., 2010		YUV and RGB	Multidimensional Multiscale Parser
“An accurate algorithm for head detection based on XYZ and HSV hair and skin colour models”	Zhang et al., 2008b	Hair and skin colours	XYZ and HSV	expectation-maximization algorithm

2.9 Performance Evaluation Metrics

In the literature, boundary recall, under-segmentation error, compactness, boundary recall and contour density have all been proposed as measures for analyzing the variants of the selected superpixel segmentation algorithm. These metrics are meant to highlight segmentation precision, superpixel compactness, regularity, coherence, and efficiency (Wang et al., 2017). It is just as crucial to choose the right evaluation metric for evaluating the quality of segmentation for ground truth segmentations as it is to evaluate the quality of segmentation for ground truth segmentations. Which will invariably save time and work when it comes to achieving ideal systems. (Taha et al., 2015).

2.9.1 Under segmentation Error

The amount of overlap between superpixels and a ground-truth segmentation boundary is measured by under segmentation error (UE). Hence, the quality is being evaluated by penalizing superpixels overlapping with multiple objects. Inaccuracies in image segmentation occur when over-segmentation or under-segmentation of an image takes place that is when too many or too few segments are generated (Möller et al., 2007). Equation 2.7 is used to compute the under segmentation error (Hahm et al., 2015):

$$UE = \frac{\sum_{j=1}^n \sum_{i=1}^m 1(s_i \cap g_j \triangleright k \cdot |s_i|) - \sum_{j=1}^n |g_j|}{\sum_{j=1}^n |g_j|} \quad (2.7)$$

2.9.2 Achievable segmentation accuracy

The highest achievable segmentation accuracy (ASA) is calculated by labelling each superpixel with the ground truth label with the largest overlap area. (Liu et al., 2011). ASA refers to the degree to which the segmentation output matches the real object, as well as efficiency, which refers to the amount of computer and human time required to complete an activity. A high ASA indicates that the superpixels interact well with the image's objects. Equation 2.8 depicts the ASA (Xiao et al., 2018):

$$ASA = \frac{\sum_{i=1}^n \max_j |s_i \cap g_j|}{\sum_{j=1}^n |g_j|} \quad (2.8)$$

2.9.3 Compactness

Each superpixel has a regular shape and size with smooth boundaries, which is referred to as compactness. Compact superpixels capture spatially coherent information better and retrieve data from their boundaries more easily. Superpixel compactness (CO) is computed using the isoperimetric quotient as shown in equation 2.9 (Xiao et al., 2018; Dolz et al., 2017):

$$CO = \sum_{S \in \Xi} Q \cdot \frac{|S|}{|I|} \quad (2.9)$$

2.9.4 Boundary recall

Boundary recall (BR) is a common metric for boundary adherence that estimates the percentage of ground truth edges that fall inside two pixels of a superpixel boundary. With a strong border recall, only a few real edges are missed (Liu et al., 2011; Li et al., 2021; Xiao et al., 2018):

$$BR = \frac{\sum_{p \in B(g_j)} \frac{1(\min_{q \in B(s_i)} \|p - q\| \leq \epsilon)}{n}}{\sum_{j=1} |B(g_j)|} \quad (2.10)$$

2.9.5 Contour Density

The number of pixels utilized to represent the edges of superpixels, normalized by the total number of pixels in an image, is known as contour density (CD). The smaller the CD, the better the outcome (Zhang et al., 2016). Hence, the CD is mathematically represented as shown in the equation ... as the proportion between the number of contour pixels of superpixel and the total number $|D|$ of pixels in the image (Machairas et al., 2014; Machairas et al., 2015):

$$CD = \frac{|C|}{|D|} \quad (2.11)$$

2.10 Chapter Summary

A complete survey of literature papers based on superpixel segmentation algorithms for digital images is presented in Chapter 2. The chapter is divided into eight sections, with the first presenting the digital image segmentation setting the foundation of this study. The second section presents the non-superpixel image segmentation which includes edge-based and region-based image segmentation while the third section emphasized superpixel segmentation. The fourth section includes a statistical data analysis through meta-analysis to guide us in choosing the optimum strategy for image segmentation based on the literature. The fifth and sixth section discusses the clustering algorithms and distance measure for image segmentation respectively, they are building blocks for the variants of the selected superpixel segmentation algorithm. The seventh section discusses colour models and finally, the eighth section presents the performance evaluation that will be used in measuring the suggested algorithm with the state-of-the-art algorithm.

CHAPTER THREE

RESEARCH METHODOLOGY

3.1 Introduction

This chapter outlines the methods that were used in this study to achieve the research aim and objective 2 specified in Chapter 1. Firstly, the basic procedures are taken to construct the suggested image segmentation algorithm, which is based on four sequential phases: the SLIC algorithm, the SAID distance measure, and the perceptual algorithm that incorporates SLIC and SAID. The dataset used and performance evaluation was further discussed.

3.2 Simple Linear Iterative Clustering (SLIC)

The SLIC superpixel technique uses k-means-based local group pixels to efficiently generate extremely uniform and compact superpixels in a combined five-dimensional colour and picture plane space to detect important regions or the focus of attention in digital images. (Ren and Reid., 2011). For grouping digital images in constructing a background template, a 5-D spectral clustering and boundary-focused region merging are utilized.

The CIELAB colour model was chosen because it is perceptually homogeneous over a wide range of colour distances. The clustering process for colour images in the CIE L*A*B colour model begins with an initial part in which k circular seeds are arranged in a lattice formation and the distance between lattice neighbours of initial cluster centres $C_i = [L^*a^*b^*x^*y]$ is validated on a regular grid spaced S pixels apart to generate nearly equal superpixel sizes, which represent the saliency detection performance of each segment. The space grid $S = \sqrt{N/k}$. Where N is the nth amount of pixels in the image to verify that the superpixel of the digital image is distributed evenly (Ranjan et al., 2017; Archanta et al., 2012; Ahn et al., 2015). Instead of using the Euclidean distance directly in this 5-D context, SLIC proposes a novel distance measure that considers superpixel size. D_s is a distance measurement that is defined as follows:

$$d_s = \sqrt{(x_j - x_i)^2 + (y_i - y_j)^2} \quad (3.1)$$

We start by sampling K cluster centres that are evenly distributed and shifting them to seed positions that correspond to the lowest gradient position in a 3 x 3 neighbourhood. This is done to

prevent them from being placed on the edge of the screen and limit the odds of picking a noisy pixel. Image gradients are calculated as follows (Liu et al., 2016):

SLIC saves you time by avoiding hundreds of point-to-point calculations. In practice, a pixel is found within a cluster of less than eight cluster centres, implying that SLIC is complicated. Algorithm 1 contains three main steps: initialization, local k-means clustering and postprocessing. Simple linear iterative clustering (SLIC) uses a five-dimensional CIELAB colour and coordinate space defined by (L, a,b,x,y) for its local clustering of pixels (Achanta et al., 2010). It is implemented as a basic K-means-based local clustering of pixels in the 5-D [labxy] space, which is determined by the CIELAB colour model L, a,b values and the pixel coordinates. When utilizing SLIC, the CIELAB colour model is chosen since it is perceptually homogeneous over tiny colour distances.

3.3 Strong Attribute Influence Distances Distance Measure

The difficulties with content-based image retrieval led to the development of a distance function that assesses image similarity in a way that is consistent with human perception. The Attribute concurrence influence distances (AID) is a new distant function that seeks to load images based on their similarity. This allows the user to set settings and sway attribute concurrence's influence. Variations of attribute concurrence lead to either strong (high) or weak (low) levels of perceptual effects of dissimilarity. (SAID) Strong Attribute Influence Distances algorithm compares objects where the attribute concurrence influence is strong (Felipe et al., 2009). When compared to the L_p class, SAID generated the best results in literature experiments on medical images using the qualities (uniformity, homogeneity, variance, and entropy).

The minimum background and foreground colour difference with SAID similarity measure similarity will be used to get the salient pixel instead of Euclidian. Therefore, the SAID similarity measure d_s is defined as follow: (Felipe et al., 2009)

$$d_s = \frac{y(n-1)^2 - 2x + (n-1)\sqrt{4x^2 - 4xy + y^2(n-1)^2}}{2(n-2)} \text{ for } n > 2 \quad (3.2)$$

Based on the result analysis it was concluded that Euclidean distance performed better than SAID in general images, however, SAID outclassed Euclidean distance when segmenting complex images. The compactness of SAID and Euclidean distance gave the same value for compactness. Hence it was concluded that neither Euclidean nor SAID is the best distance measure. Therefore an alternative distance measure that works well especially when segmenting complex images with difficult foreground and background colour complexity was introduced.

3.4 Perceptual Algorithm - SLIC

The literature presents the SLIC algorithm as a popular choice because superpixels are produced rapidly without compromising on segmentation accuracy, however, it has several limitations like boundary adherence with larger superpixels and relies on local features like colour and coordinates of pixels with high computational costs (Li et al., 2015; Shen et al., 2016; Ren and Reid., 2011). Therefore, alternative superpixel segmentation algorithms in this thesis that better balance crucial complexity trade-offs were introduced. The variants of the selected superpixel segmentation algorithm were adapted and summarized in Algorithm 2 to reduce the spatial compactness gap in superpixels. Which give a better perceptual outcome hence reducing the under-segmentation error when compared to the Euclidean distance measure. The original image is inputted into the variants of the selected superpixel segmentation algorithm which performs a local colour mean that partitions the original image into clusters that is, superpixels, which will be used in capturing structural information; by segmenting the digital images into N segments.

Algorithm 1: Perceptual Colour Superpixel Algorithm

- 1: Initialize cluster centres $C_k = [l_k; a_k; b_k; x_k; y_k]^T$ by sampling pixels at regular grid steps S .
 - 2: Perturb cluster centres in an $n \times n$ neighbourhood, to the lowest gradient position.
 - 3: repeat
 - 4: for each cluster Centred C_k do
 - 5: Assign the best matching pixels from a $2S \times 2S$ square neighbourhood around the cluster Centred according to the SAID distance measure (Eq. 1).
 - 6: end for
 - 7: Compute new cluster centres and residual error E {L1 distance between previous centres and recomputed centres}
 - 8: until the $E \leq \text{threshold}$
 - 9: Enforce connectivity.
-

3.5 Dataset

It is crucial to have ground truths when comparing image segmentation techniques to obtain any measure of objectivity. The Berkley Segmentation 500 dataset was used for this study which includes three digital image categories with 500 colour images that include humans, animals and objects which are designed to be challenging consisting of both complex and homogenous foreground and background colour similarity. This benchmark has become a standard for image segmentation, over-segmentation and edge detection within the field of computer vision (Wang et al., 2020). A boundary is defined as a change in pixel ownership from one object or surface to another, which is referred to as an image contour (Martin et al., 2004).

The publicly available BSDS500 dataset (Shen et al., 2014; Arbelaez et al., 2010) as shown in Table 1 is the most extensively used dataset for superpixel image segmentation. This dataset includes three digital image categories with 500 images which include humans, animals, objects outdoor scenes and landscapes. These images are designed to be challenging consisting of both complex and homogenous foreground and background colour similarity. The dataset was grouped into three subsections namely; overlapping, multiple, and complex images. The challenge of showing that segmentation algorithms work to a sufficient level of performance is a fundamental problem in the design of image processing algorithms. Algorithm testing has a dual purpose. For starters, it allows you to evaluate an algorithm using either a qualitative or quantitative way. Second, it provides a comparison of the method to other algorithms, providing that the same criteria are applied (Wirth et al., 2006).

3.5.1 Human Images

The following human images were extracted from the Berkeley 500 segmentation dataset with composite backgrounds. It's easy to identify some objects within an image but difficult on others due to the number of humans captured on the image and variations in the background making the image blur.



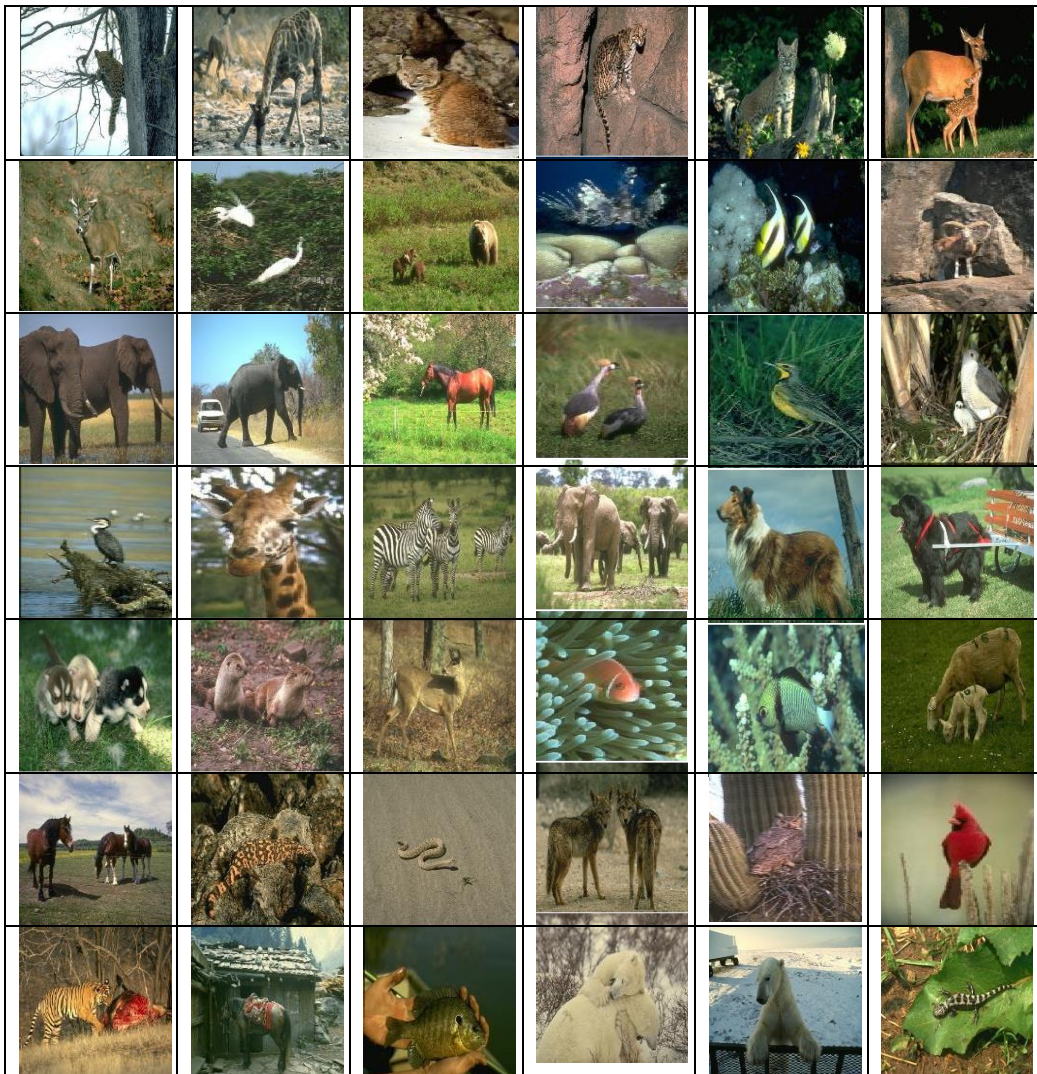


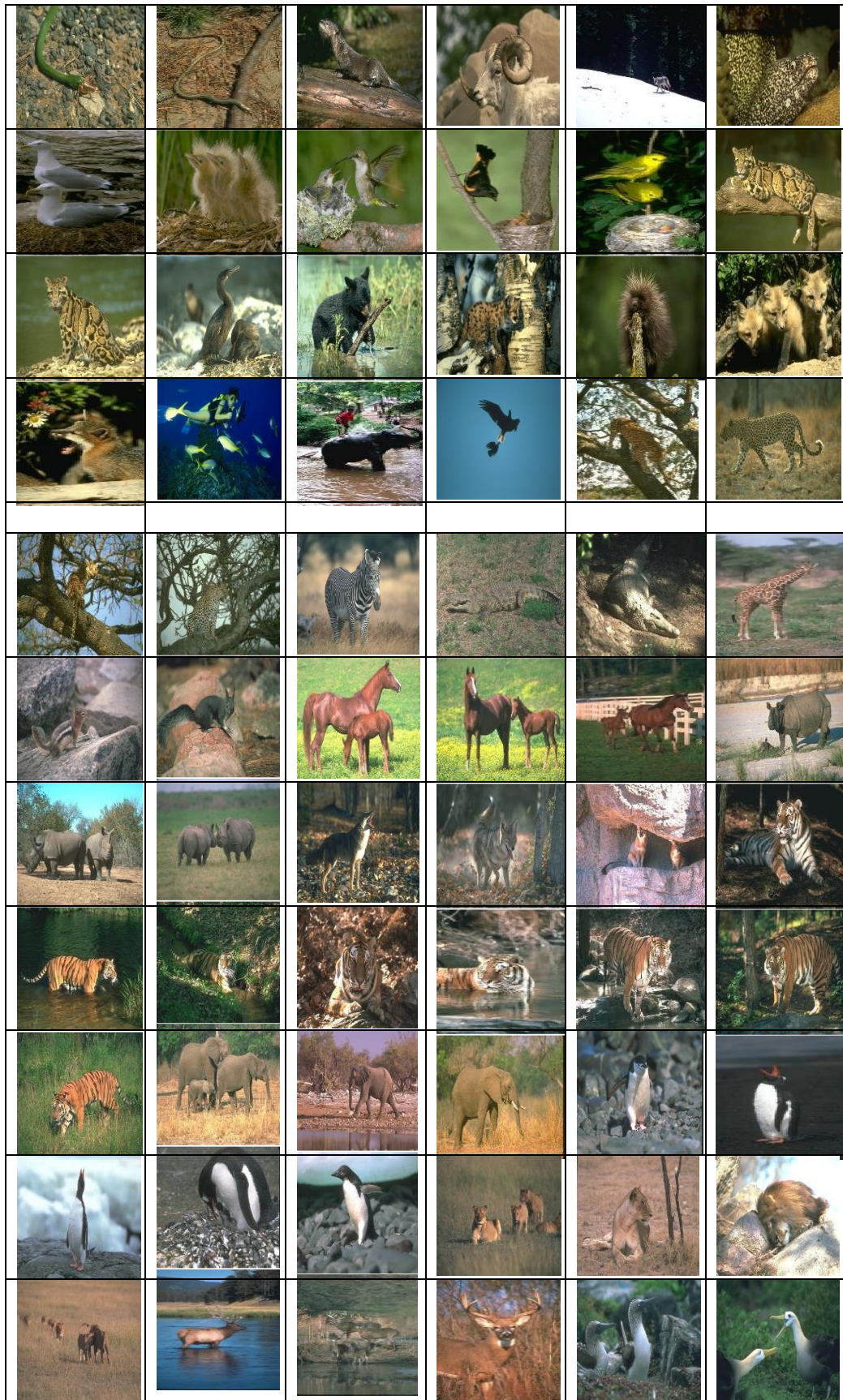


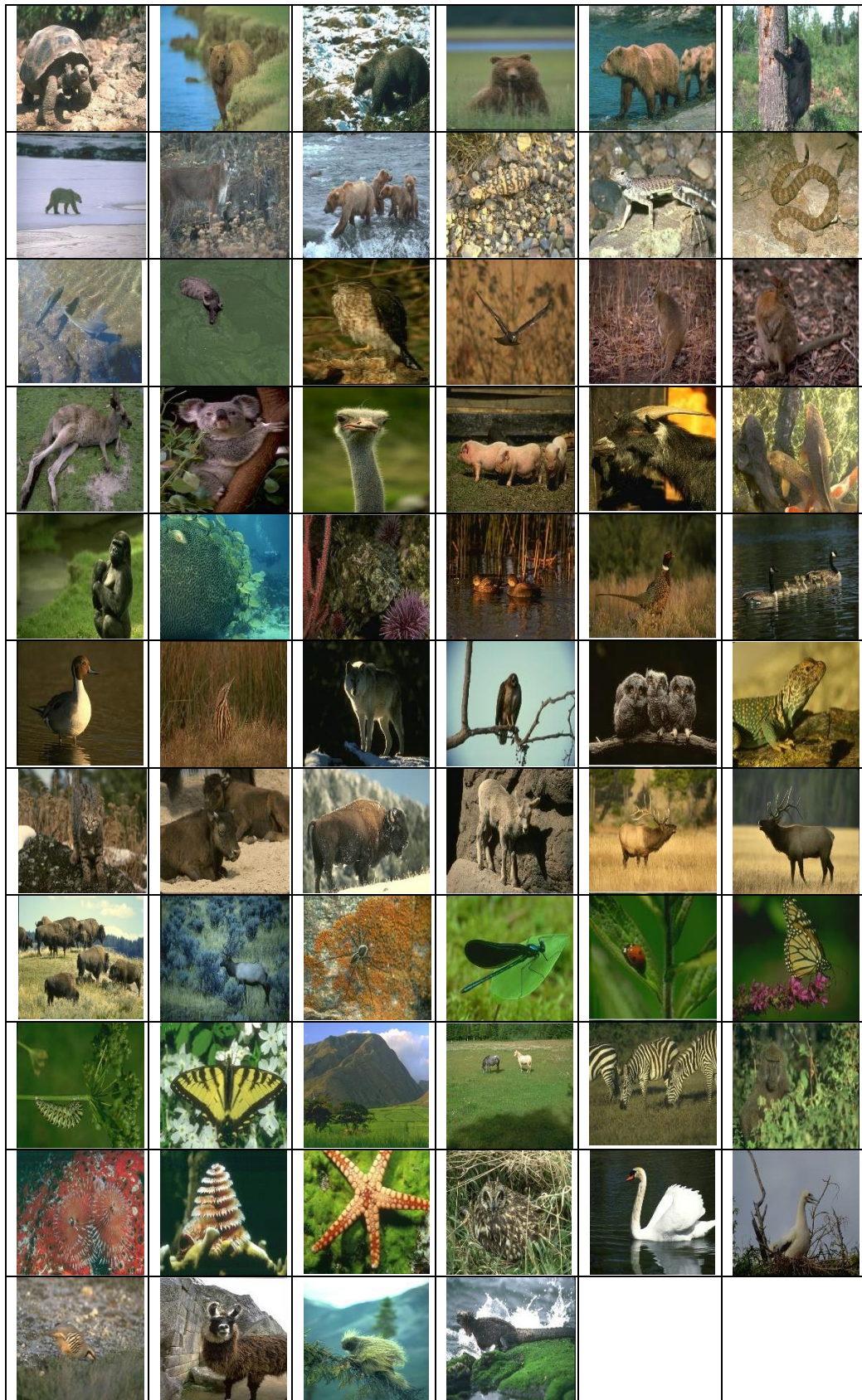


3.5.2 Animal Images

The following animal images were extracted from the Berkeley 500 segmentation dataset with multifaceted backgrounds. It's easy to establish the ground truth of some images but difficult with others due to the variations in the background making it difficult to determine the type of animal.





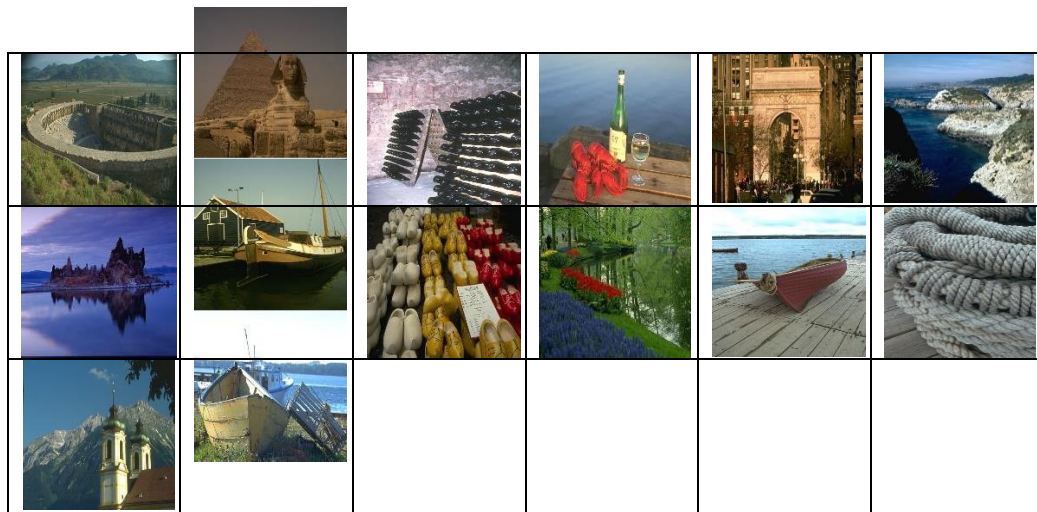


3.5.3 Object Images

The following object images are extracted from the Berkeley 500 segmentation dataset with complex backgrounds some of which are easily identifiable from the background whilst others are unclear and contain multiple objects.







3.6 Evaluation Metrics

In a variety of ways, the congruence between the final binary segmentation result and the ground truth image can be evaluated. A segmentation algorithm's main purpose is to capture the object of features in an image as precisely as possible. The efficacy of the given methodology must be demonstrated for quality utilizing appropriate assessment criteria. The following measures were used to assess the performance of the Perceptual Colour Superpixel Algorithm: segmentationerror (UE), boundary recall (BR), achievable segmentation accuracy (ASA), compactness, and contour density.

3.7 Chapter summary

The chapter presents a well-described step-by-step approach to achieve the set aim and objectives proposed in this study. The variants of the selected superpixel segmentation algorithm amalgamated the simple linear iterative clustering (SLIC) that performs a local clustering of pixels in the 5-D space defined by the L, a, b values of the CIELAB colour model with the strong attribute concurrence influence distances (SAID) while strikingly simple, it addresses the aforementioned gap and produces high quality, compact superpixels.

CHAPTER FOUR

RESULTS AND DISCUSSION

To achieve the third objective of this thesis, this chapter describes the analysis of experiments, their outcomes, and their accompanying interpretations. The chapter begins with a discussion of performance evaluation. Furthermore, the qualitative analysis of the superpixel image result is presented for the animal, human, object categories. The suggested algorithm's performance is then evaluated via quantitative analysis using well-known performance evaluation indicators.

4.1 Performance Evaluation

Image segmentation problems persist despite various solutions that have been proposed over the years. The quality of dataset images is an issue that includes image blurring, additive noise, image contrast, and lossy compression (Borel-Donohue and Young, 2019). Due to this challenge, performance evaluation becomes a mandatory step in evaluating the performance for the variants of the selected superpixel segmentation algorithm. As a result, the performance of the suggested algorithm was evaluated qualitatively and quantitatively in this thesis.

Qualitative evaluation is performed to perceptually analyse the quality of the superpixel image segmentation results based on the capacity to accurately segment the foreground object in an image. While quantitative analysis uses evaluation metrics to assess the success of the image segmentation algorithm, the qualitative analysis does not. Under-segmentation error, achievable segmentation accuracy, compactness, boundary recall, and contour density were the five assessment measures used in this thesis. These quantitative evaluation metrics have been explained in detail in section 2.8 of this thesis.

According to the literature, substantial progress has been made towards resolving problems with image processing in determining the distance between images. The most popular distance measure used is Euclidean distance due to its simplicity and ease of use (Wang et al., 2005; Xia et al., 2007). The SAID distance measure was compared to the extensively used Euclidean distance measure. Despite its popularity and the range of applications it has been implemented on Euclidean distance measure does not consider the spatial connection of pixels. The images processed using Euclidean are distorted. According to Wesolkowski (1999), the Euclidean distance between two

colours in RGB does not always match their perceptual separation therefore choosing a distance measure that needs to quantify hue and saturation is preferred for processing colour images.

Although the cost of Euclidean distance is popular in literature it compromises the quality of clustering which makes it a weak metric to apply for maximizing both the homogeneity within each cluster and the heterogeneity between different clusters. SAID captures the background and foreground much better than Euclidean using attributes uniformity, variance and entropy. Subjective and objective approaches are two subcategories of the methodologies accessible for this goal. Subjective evaluation is based on a human assessment of segmentation quality, while objective evaluation is based on a perfect segmentation reference, also known as the ground truth. Hence, the objective evaluation approach was adopted to prevent subjectivity.

4.2 Qualitative Evaluation for LAB Colour Model

An experiment using a sample of images from three categories namely animals, humans and objects from the Berkley Segmentation 500 dataset were executed with Matlab and a comparison of perceptual colour difference measure algorithm with the SAID distance measure and the SLIC segmentation algorithm with the Euclidean distance measure of images between led to the following results.

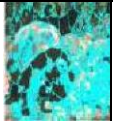


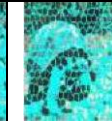






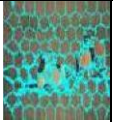
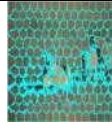
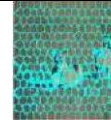
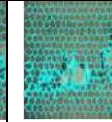
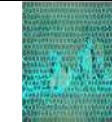

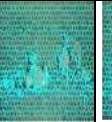
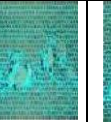
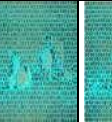




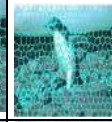







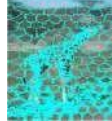

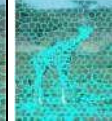



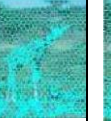


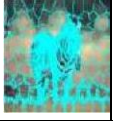


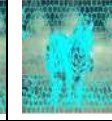






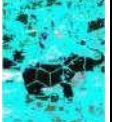
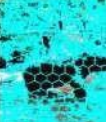
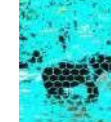
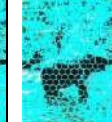
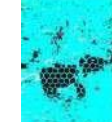


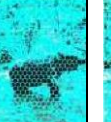
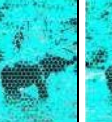




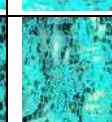

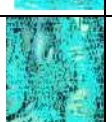

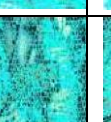
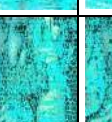
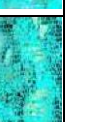
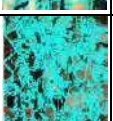
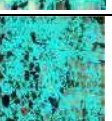
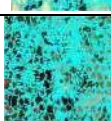
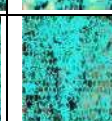
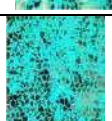
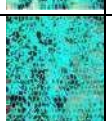

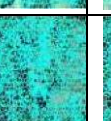
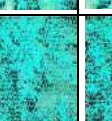
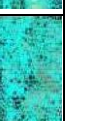
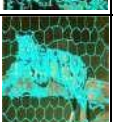
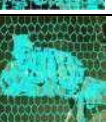
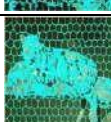


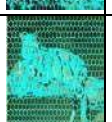

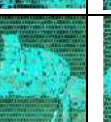


Table 4.1 shows the result of Superpixel Segmentation for 100 to 1000 pixels using SAID and Euclidean distance measure. Perceptually SAID clusters are of evenly regular shapes and have better boundary adherence when compared to Euclidean distance which also shows regular size and shapes. SAID further shows better compactness avoiding over-smoothing hence preserving object boundaries. The qualitative analysis of images in Table 4.1 shows that perceptually, the SAID distance measure achieved three key features:


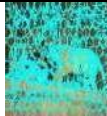

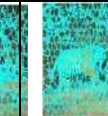
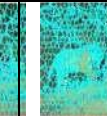
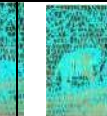
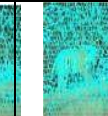
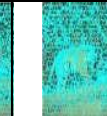
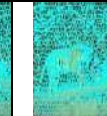
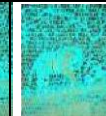



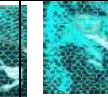



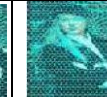




















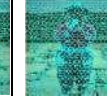














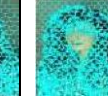

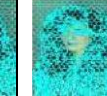
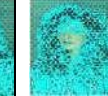
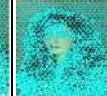





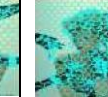
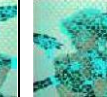
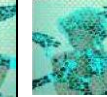
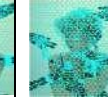






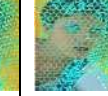
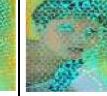








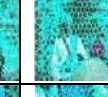







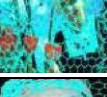

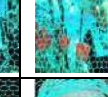





























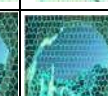









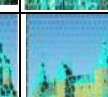
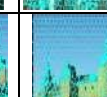
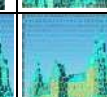
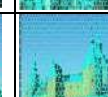






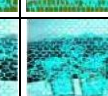





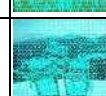
- a. Uniform superpixel size: As shown in Table 1 it can be seen that SAID partitioned the images into a uniform pixel in size and shape hence, ensuring compactness in contrast to the irregular pixel shape of Euclidean distance.
- b. Smooth superpixel edge flow: The SAID distance measure, shows that the superpixel boundaries correspond with image edges hence the superpixel displays straight smooth

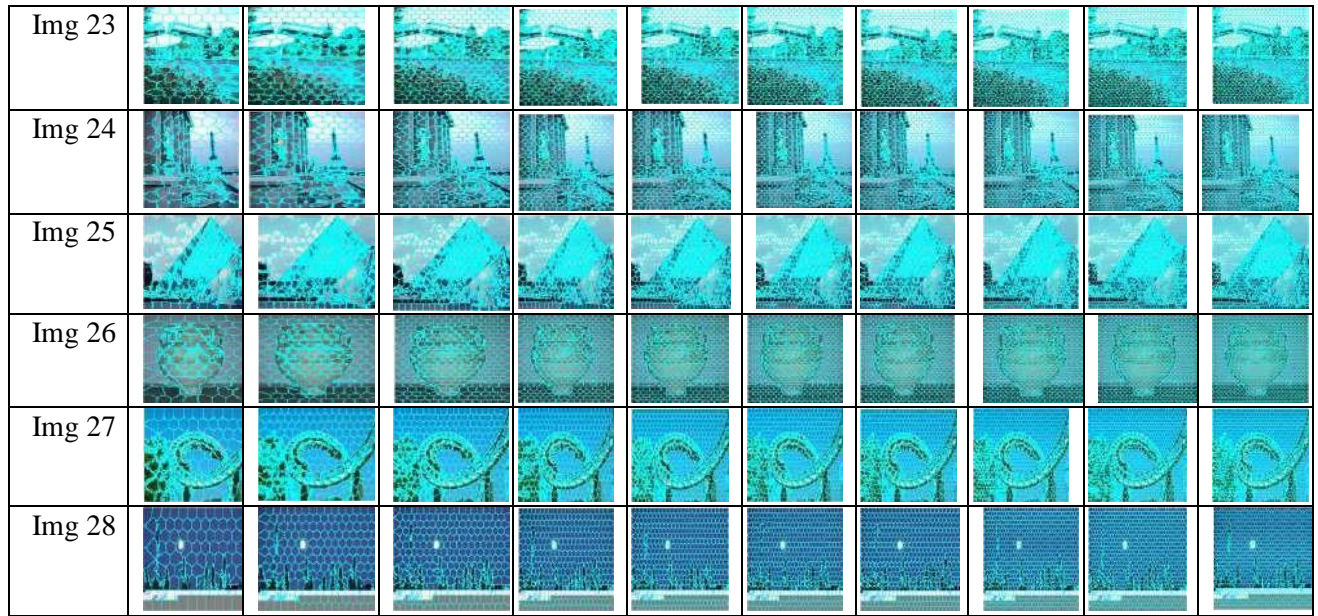
superpixel boundaries. However, the Euclidean distance measure did not give a smooth boundary.

c. Superpixel connectivity The SAID distance measure, perceptually shows that each superpixel represents a simply connected set of pixels while the Euclidean distance measure produces some unconnected set of the pixel.

Table 4.1: Result of Superpixel Segmentation (100-1000 pixels) with SAID distance measure

SAID	100	200	300	400	500	600	700	800	900	1000
Animal										
Img 1										
Img 2										
Img 3										
Img 4										
Img 5										
Img 6										
Img 7										
Img 8										
Img 9										




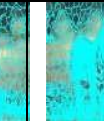
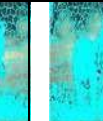
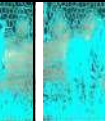
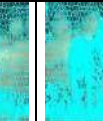
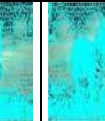

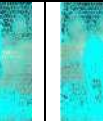
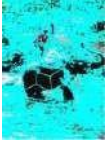

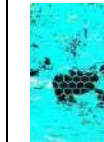
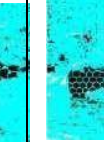
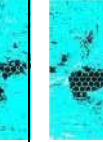
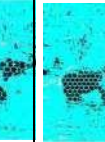
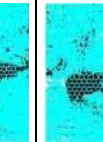
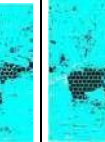
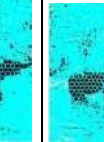
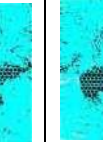


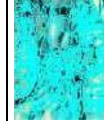
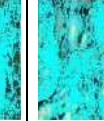
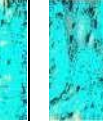
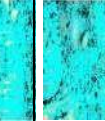
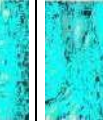
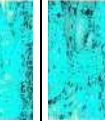
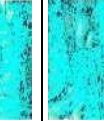
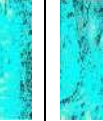
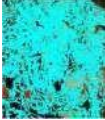
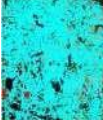
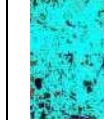
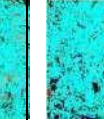
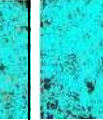
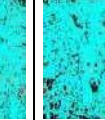
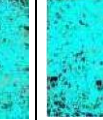
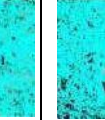
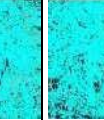
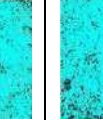

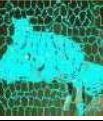
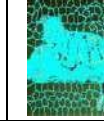
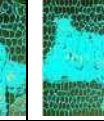
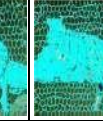
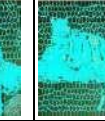

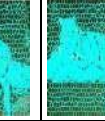
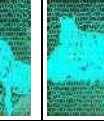
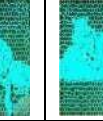


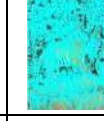
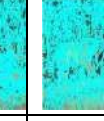
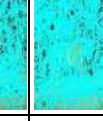
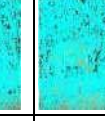
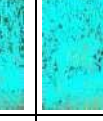
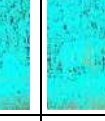
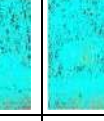
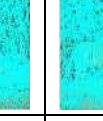


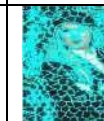
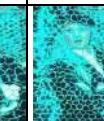

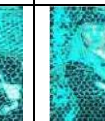

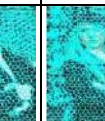
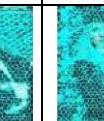
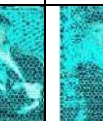




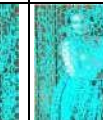

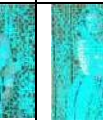
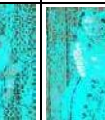
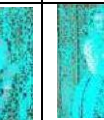
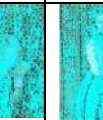


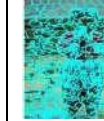
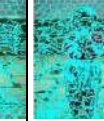
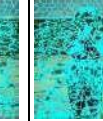
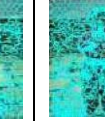
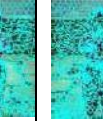
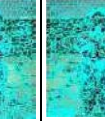
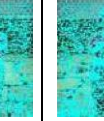
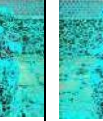




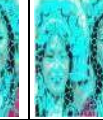
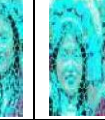

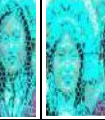
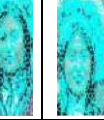




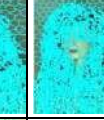

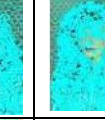
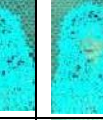
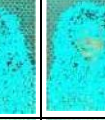
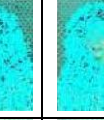
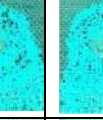


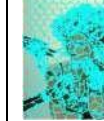
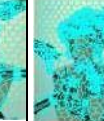
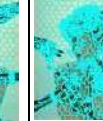
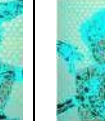
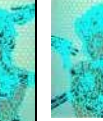
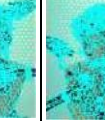
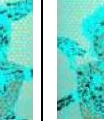
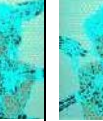


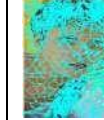

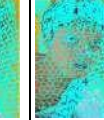
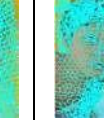
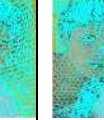
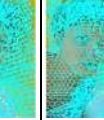
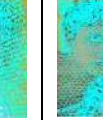
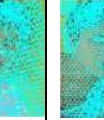
Img 10										
SAID	100	200	300	400	500	600	700	800	900	1000
Human										
Img 11										
Img 12										
Img 13										
Img 14										
Img 15										
Img 16										
Img 17										
Img 18										
Img 19										
SAID	100	200	300	400	500	600	700	800	900	1000
Objects										
Img 20										
Img 21										
Img 22										



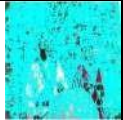
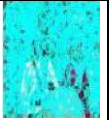
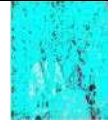


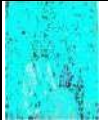
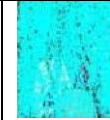
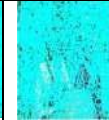

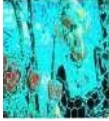
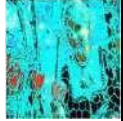
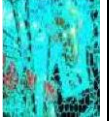
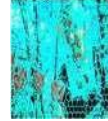



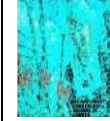





















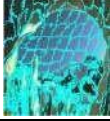






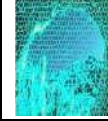




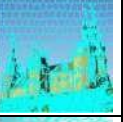


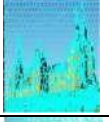

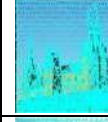

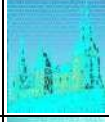


















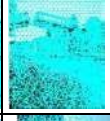













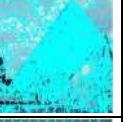













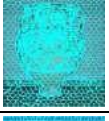






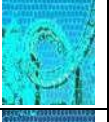



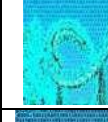






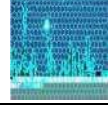


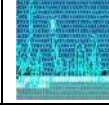




In Table 4.2 the Euclidean distance measure presented fluctuating compactness for images 1, 2,9,16,19,25 with irregular boundary adherence for the other images. Furthermore, as it can be seen in Table 4.2 it can be perceptually evaluated that there is the inaccuracy of superpixel segmentation which leads to inconsistency of superpixel blocks for the Euclidean distance measure.

Table 4.2: Result of Superpixel Segmentation (100-1000 pixels) with SAID and Euclidean distance measure

EUC	100	200	300	400	500	600	700	800	900	1000
Animal										
Img 1										
Img 2										
Img 3										
Img 4										

Img 5										
Img 6										
Img 7										
Img 9										
Img 10										
Img 11										
EUC	100	200	300	400	500	600	700	800	900	1000
Human										
Img 12										
Img 13										
Img 14										
Img 15										
Img 16										
Img 17										
Img 18										

Img 19										
Img 20										
Img 21										
EUC	100	200	300	400	500	600	700	800	900	1000
Objects										
Img 22										
Img 23										
Img 24										
Img 25										
Img 26										
Img 27										
Img 28										
Img 29										
Img 30										
Img 31										

4.3 Quantitative Evaluation for LAB Colour Model

The objective assessment of image quality utilizing well-known performance metrics to evaluate segmented images with the ground truth is referred to as quantitative performance evaluation. The purpose of a quantitative evaluation is to guarantee that a segmentation algorithm's overall performance is significant. This study considered five quantitative performance evaluation metrics namely: Under-segmentation error, achievable segmentation accuracy, compactness, boundary recall and contour density.

Figure 4.1 present an under-segmentation error, an essential metric that reveals errors made by an algorithm while segmenting. Figure 4.1a depicts the under-segmentation error for overlapping images with regular compactness; the result shows that the SAID distance measure performed better than Euclidean (EUC) distance when segmenting.

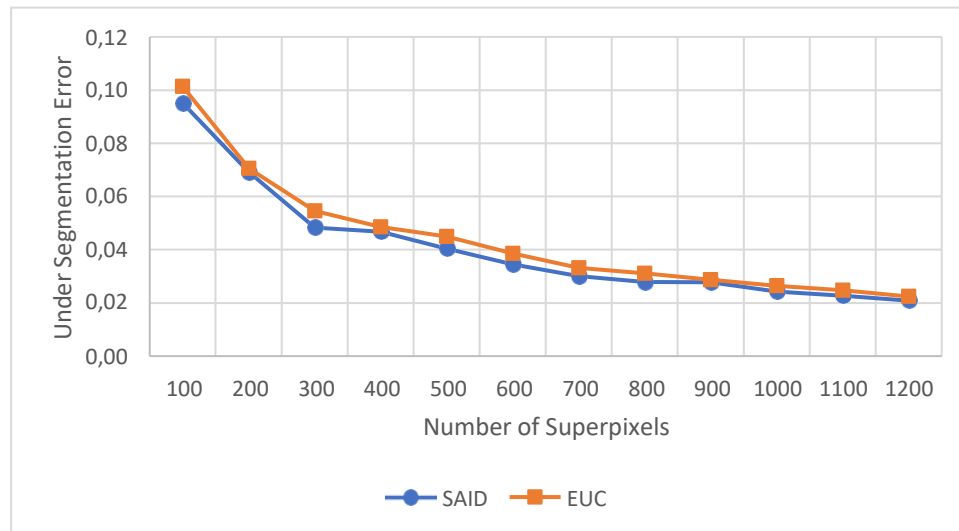


Figure 4.1a: Under-segmentation error against the number of superpixels for overlapping images with regular compactness

However, Figure 4.1b depicts that SAID failed to capture salient image structure accurately for overlapping images with irregular compactness. This could be as a result that the region is ambiguous due to the irregularity of compactness. Hence EUC gave a better performance when segmenting overlapping images with irregular compactness.

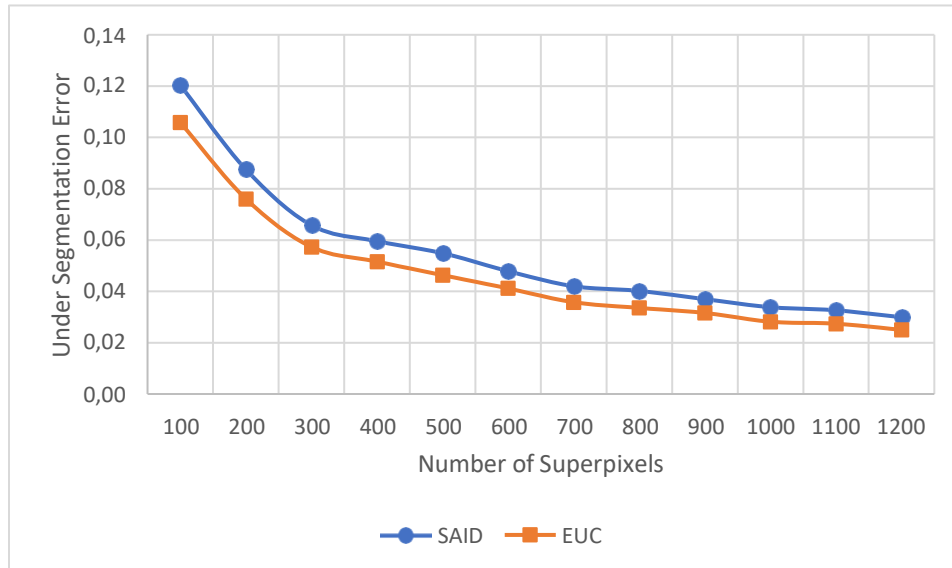


Figure 4.1b: Under-segmentation error against the number of superpixels for overlapping images with irregular compactness

Furthermore, Figure 4.2a corroborate the effectiveness of SAID as the presented result depicts SAID outperforming Euclidean when segmenting complex images with regular compactness. Complex images are with attributes such as images with irregularly shaped objects, complex foreground and background colour complexity.

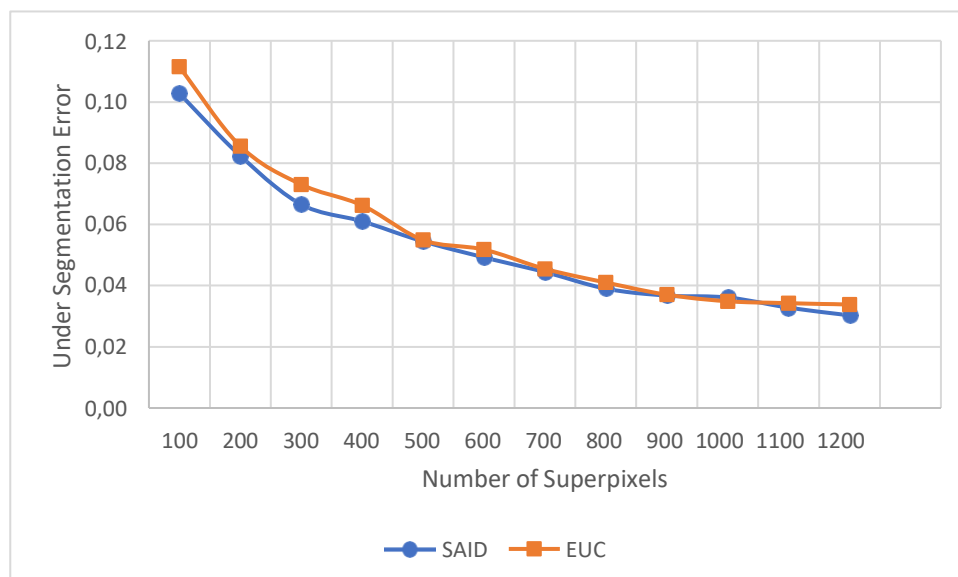


Figure 4.2a: Under-segmentation error against the number of superpixels for complex images with regular compactness

However, Euclidean distance outperformed SAID for complex images with irregular compactness as shown in Figure 4.2b.

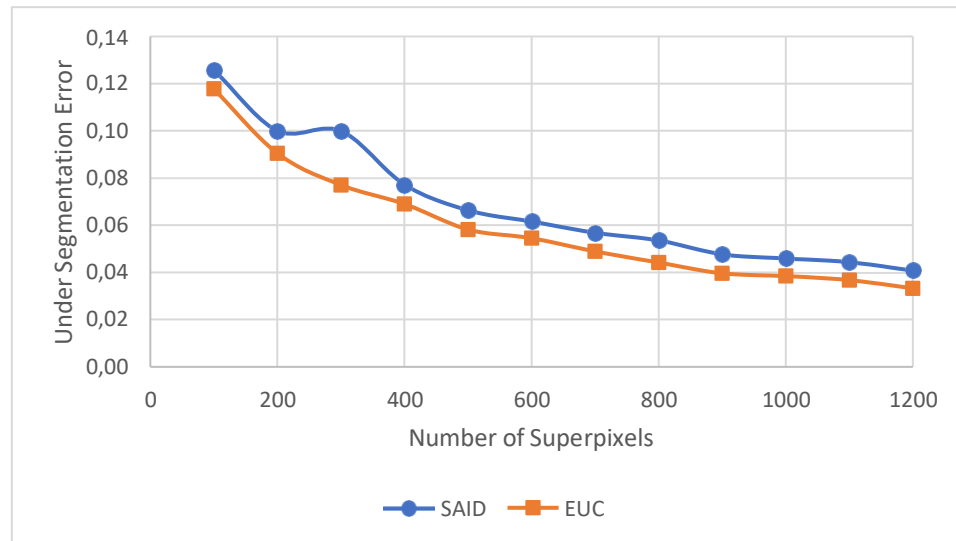


Figure 4.2b: Under-segmentation error against the number of superpixels for complex images with irregular compactness

Contrary to Figures 4.1a and 4.2a, Figure 4.3a shows a different result which depicts Euclidean outperforming SAID when segmenting multiple images with regular compactness. However, Figure 4.3a corroborate Figure 4.3b as it further depicts that Euclidean distance captures the salient object better than SAID while segmenting complex images with irregular compactness.

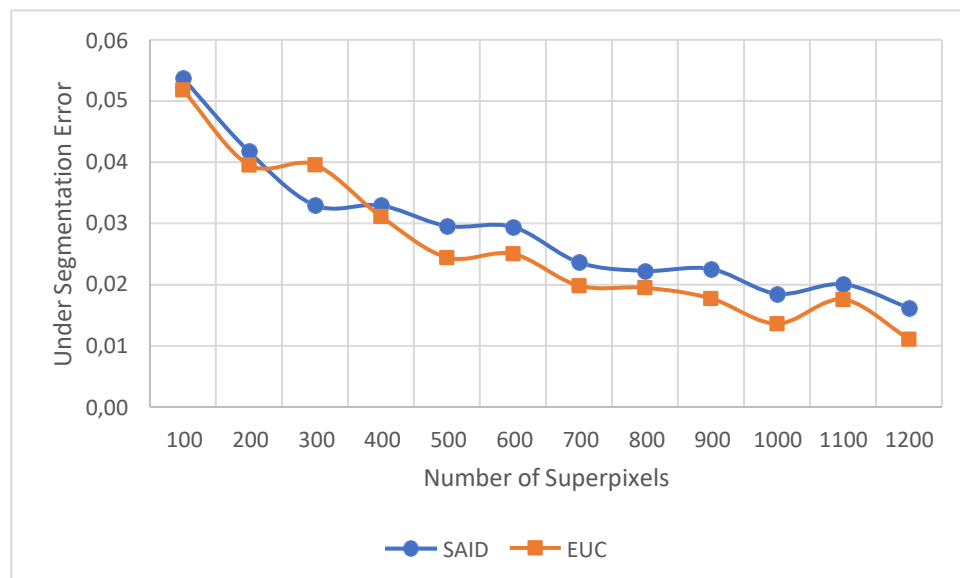


Figure 4.3a: Under-segmentation error against the number of superpixels for multiple objects images with regular compactness

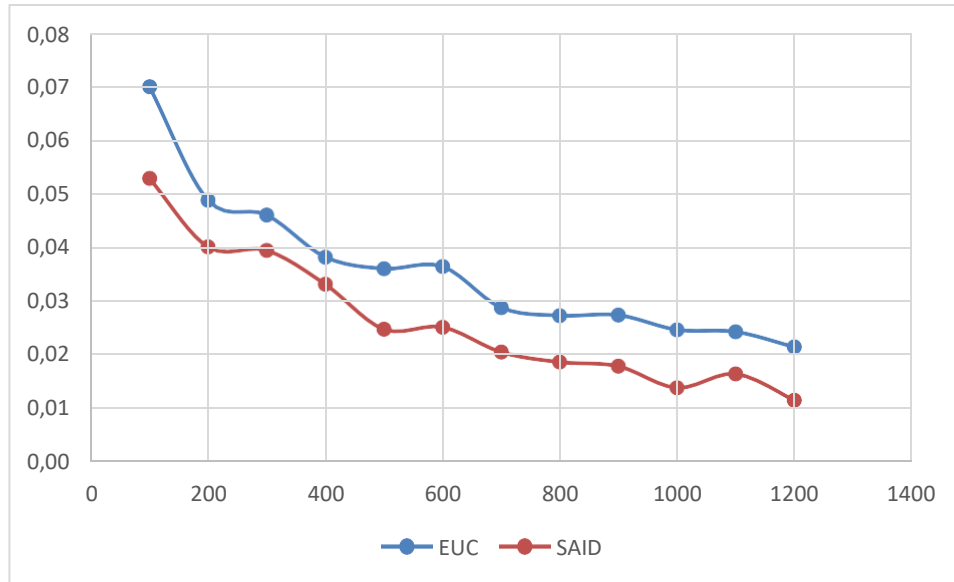


Figure 4.3b: Under-segmentation error against the number of superpixels for multiple objects images with irregular compactness

Figure 4.4a presents the under-segmentation error metric when the object is at the Centred of the image with irregular compactness superpixel, the experimental result shows that Euclidean distance outperforms SAID.

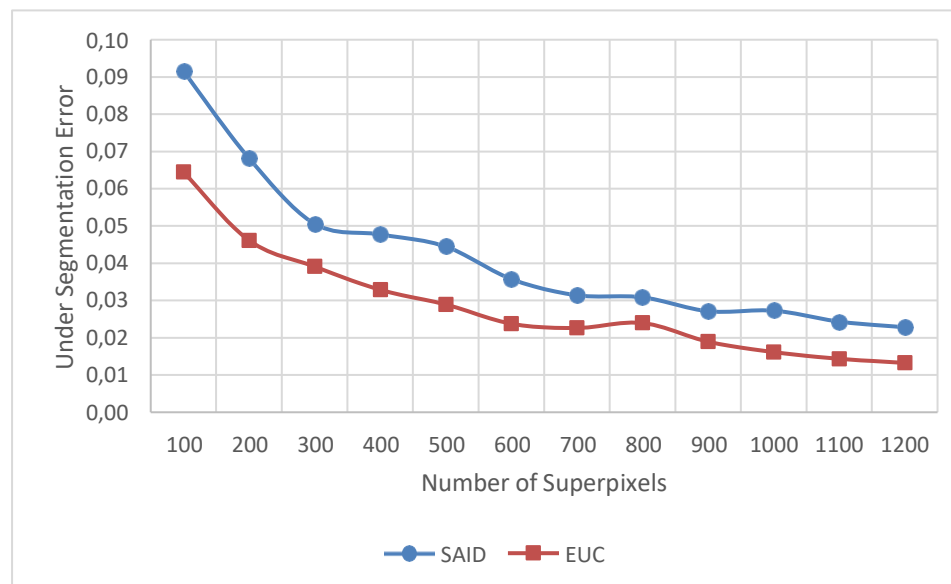


Figure 4.4a: Under-segmentation error against the number of superpixels for Centred object images with regular compactness

However, Figure 4.4b further shows the Euclidean outperforming SAID when segmenting Centred object images with irregular compactness. Hence it means that the Euclidean distance is best suited for images with Centred objects regardless of the regular or the irregular compactness.

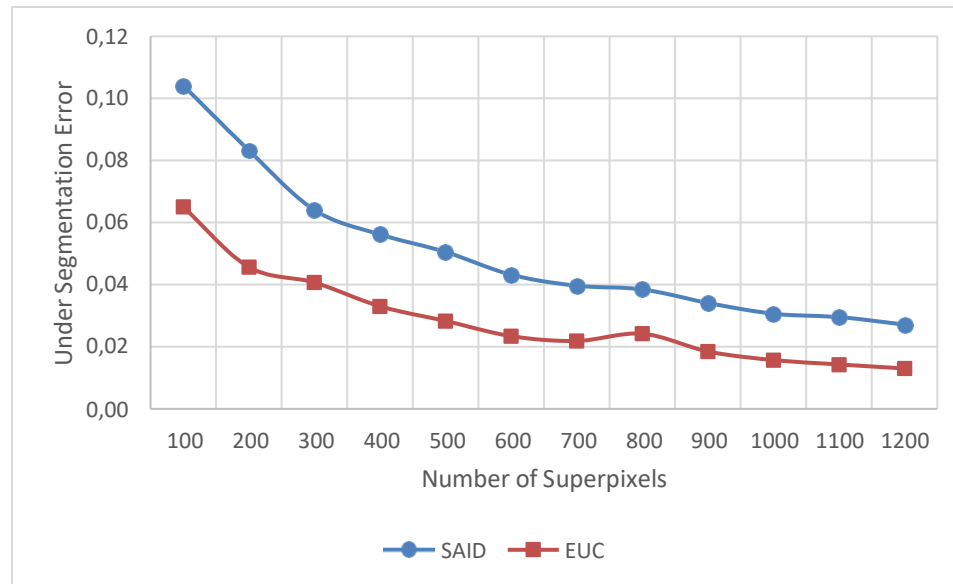


Figure 4.4b: Under-segmentation error against the number of superpixels for Centred object images with irregular compactness

Consequently, further experiments were carried out for images with low contrast, Figure 4.5a and Figure 4.5b shows a similar result of Euclidean distance performing better than SAID regardless of the regular or the irregular superpixel compactness a contradiction to when the images were viewed perceptually.

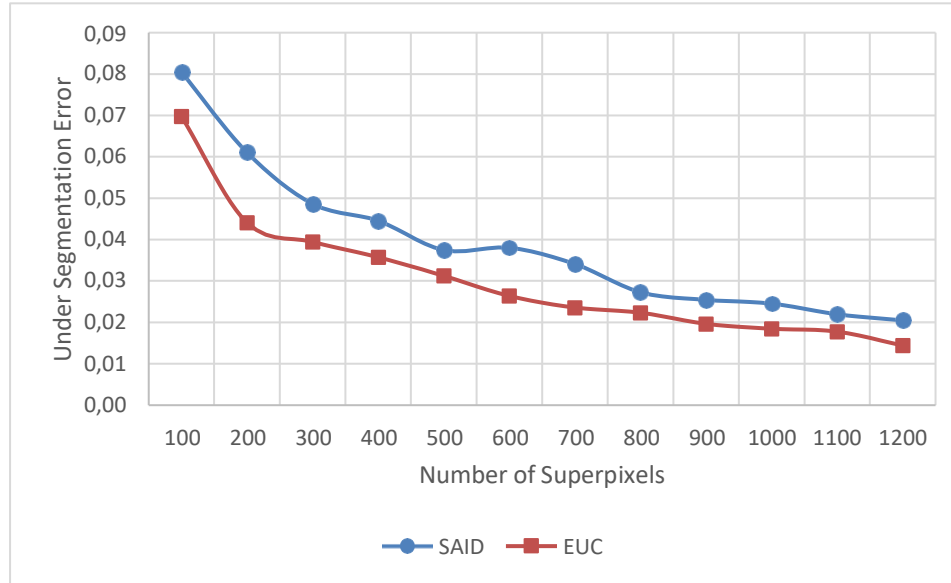


Figure 4.5a: Under-segmentation error against the number of superpixels for low contrast images with regular compactness

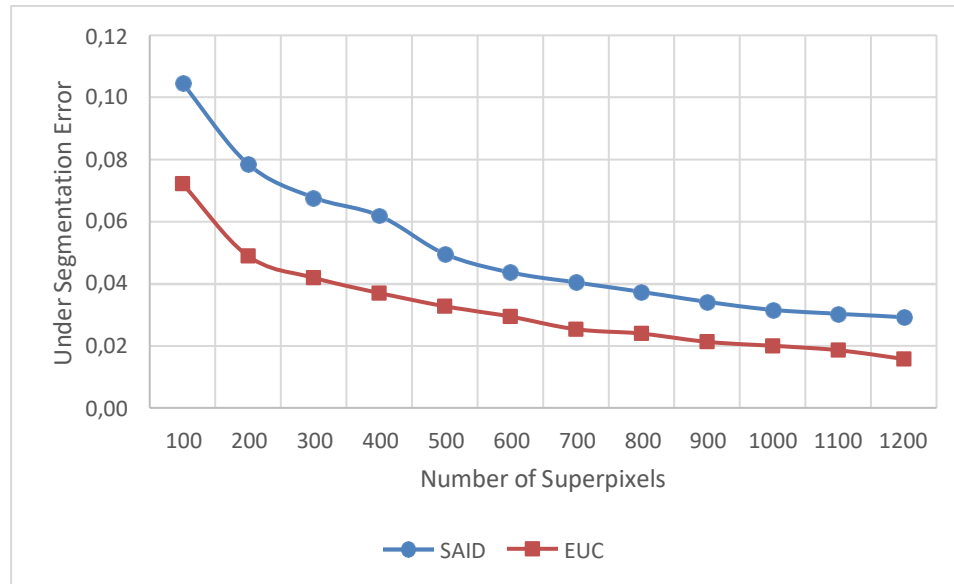


Figure 4.5b: Under-segmentation error against the number of superpixels for low contrast images with irregular compactness

Achievable segmentation accuracy (ASA) metrics that correctly label clusters are classified as achievable accuracy. As the number of superpixels grows, an excellent ASA emerges. (Liu et al., 2016). In Figure 4.6a SAID outperformed the Euclidean distance when segmenting images overlapping objects with regular superpixel compactness. However, in Figure 4.6b Euclidean

distance outperformed SAID with irregular superpixel compactness.

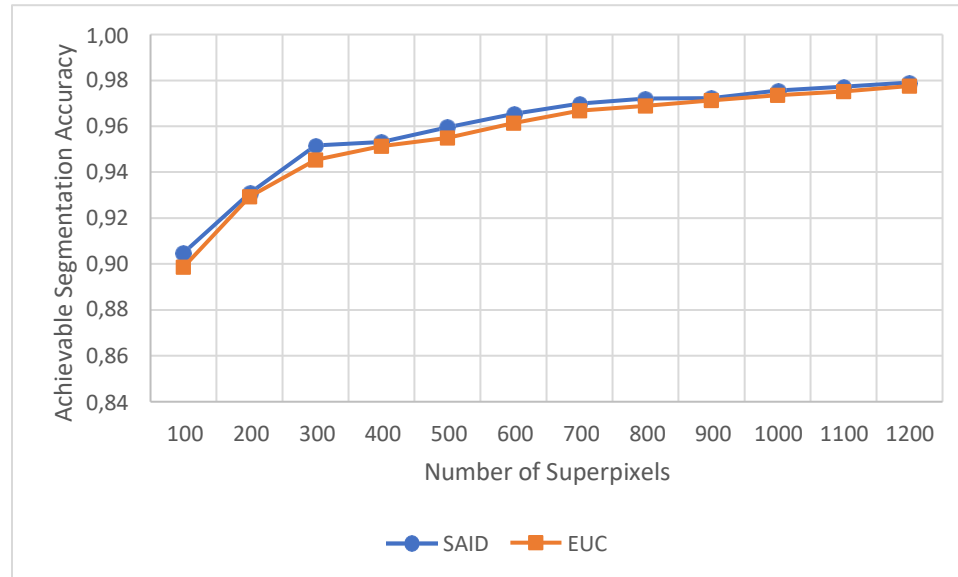


Figure 4.6a: Achievable segmentation accuracy against the number of superpixels for overlapping images with regular compactness

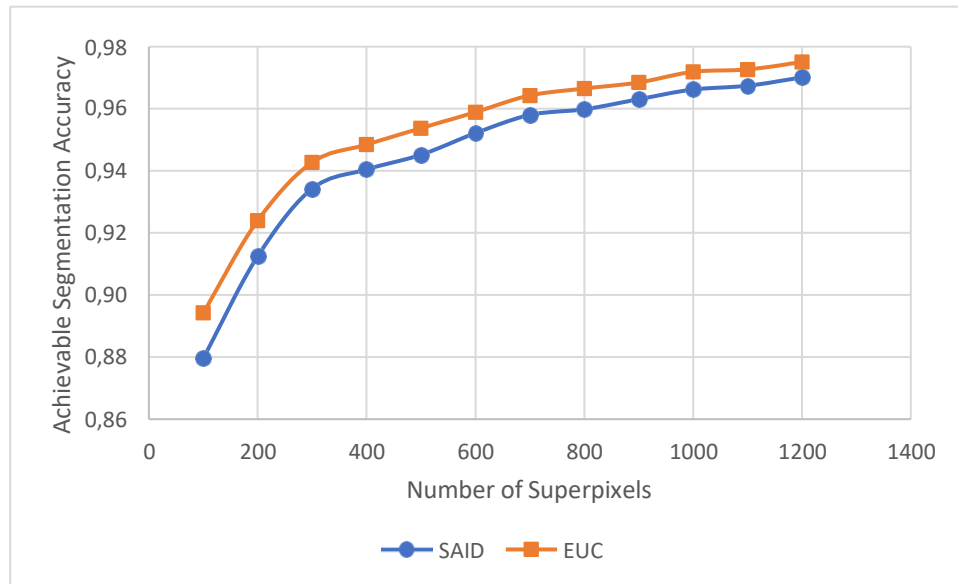


Figure 4.6b: Achievable segmentation accuracy against the number of superpixels for overlapping images with irregular compactness

In Figure, 4.7a SAID performed better than Euclidean distance when calculating the ASA for complex images with foreground and background colour complexity for regular compactness. Consequently, the reversal is the case in Figure 4.7b with irregular compactness as EUC

outperformed SAID.

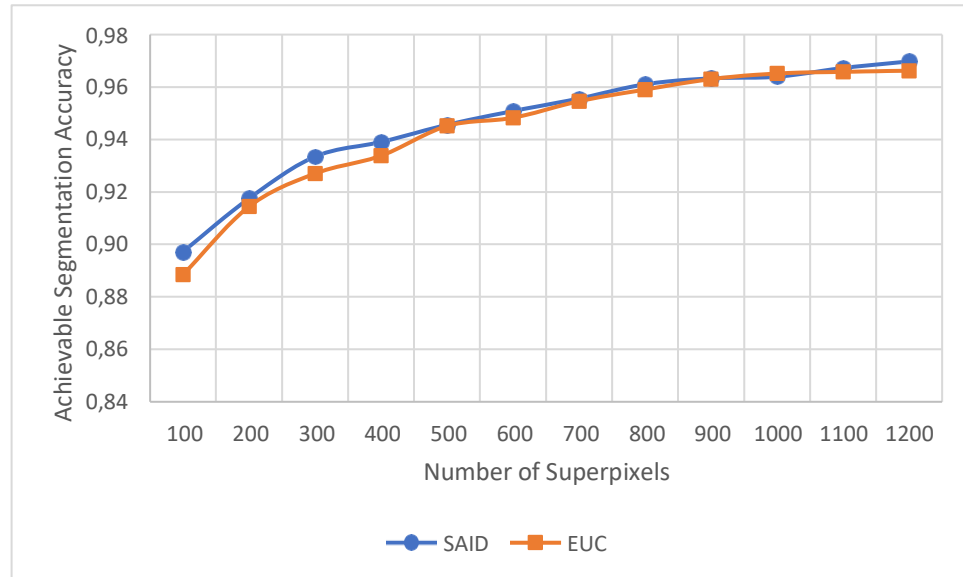


Figure 4.7a: Achievable segmentation accuracy against the number of superpixels for complex images with regular compactness

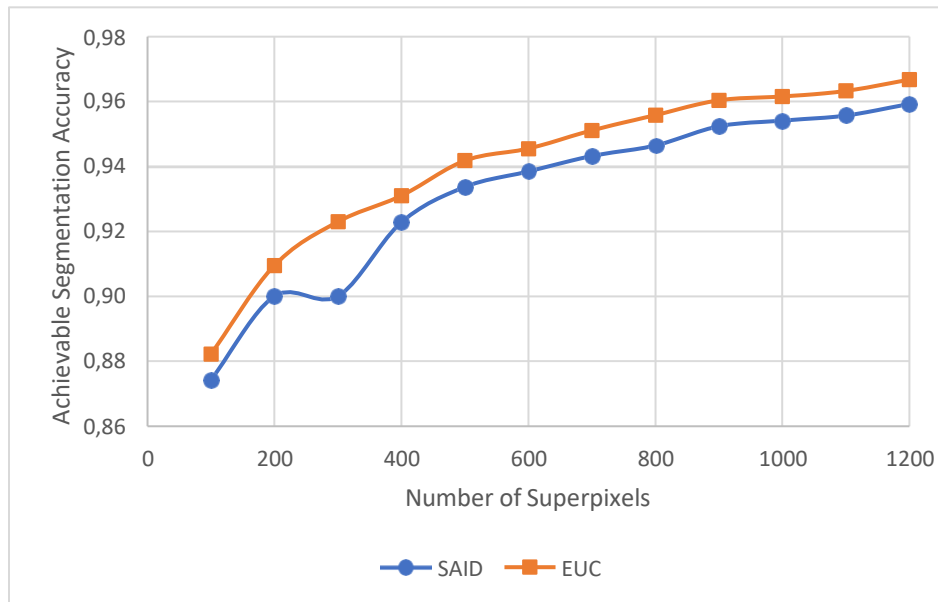


Figure 4.7b: Achievable segmentation accuracy against the number of superpixels for complex images with irregular compactness

However, in Figures, 4.8a and 4.8b Euclidean distance performed better than SAID when calculating the ASA for multiple object images regardless of the regular and irregular

compactness.

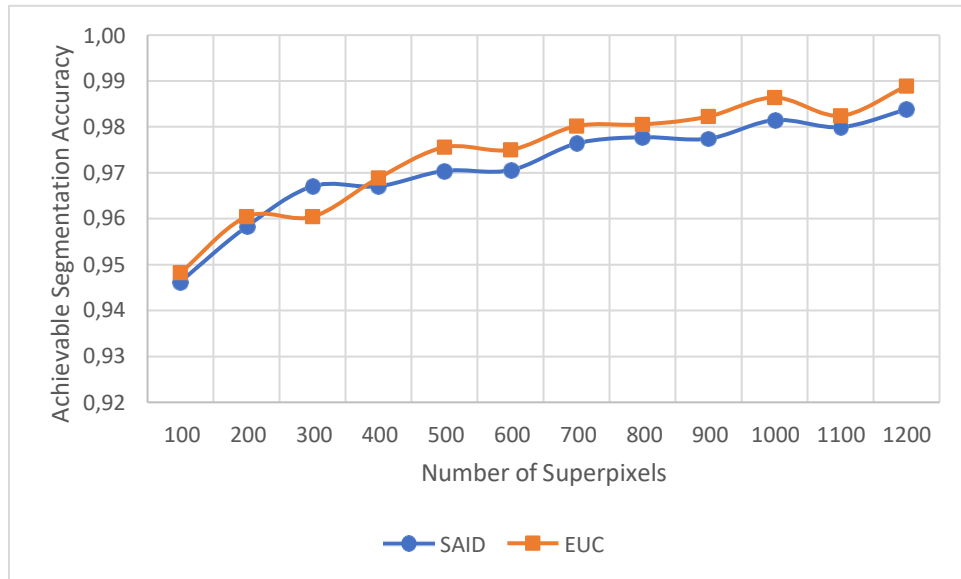


Figure 4.8a: Achievable segmentation accuracy against the number of superpixels for multiple object images with regular compactness

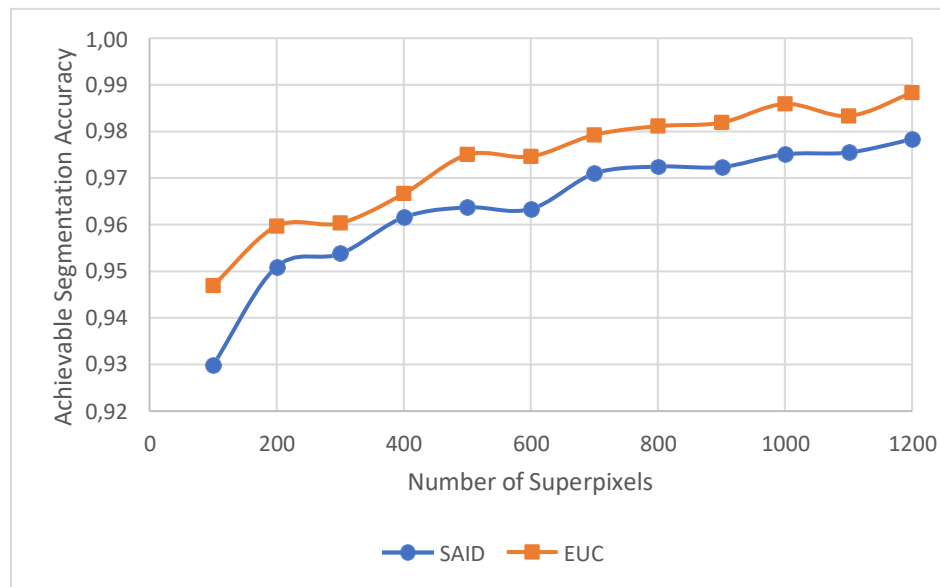


Figure 4.8b: Achievable segmentation accuracy against the number of superpixels for multiple object images with irregular compactness

While experimenting with images with Centred objects for both regular and irregular compactness as shown in Figures, 4.9a and 4.9b Euclidean distance performed better than SAID when calculating the ASA.

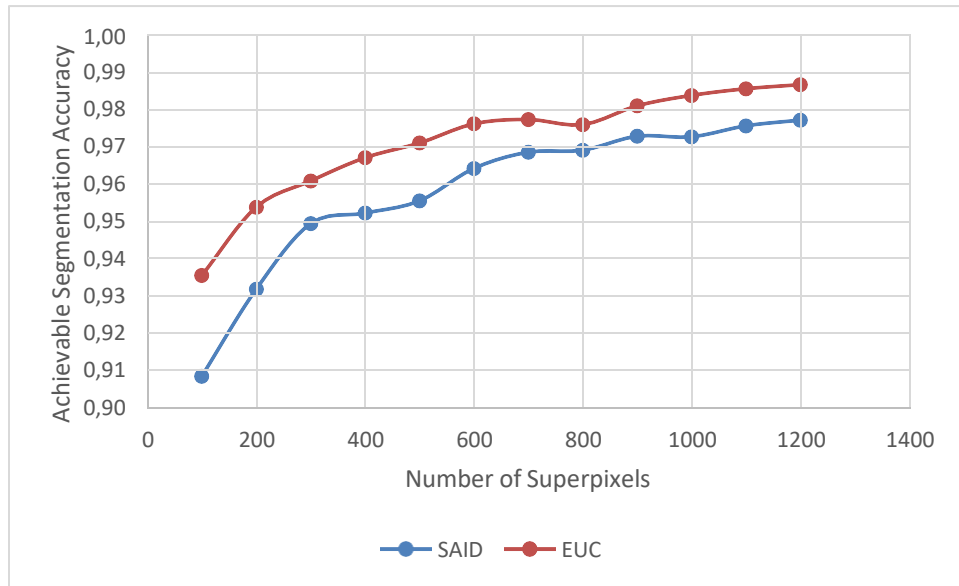


Figure 4.9a: Achievable segmentation accuracy against the number of superpixels for Centred object images with regular compactness

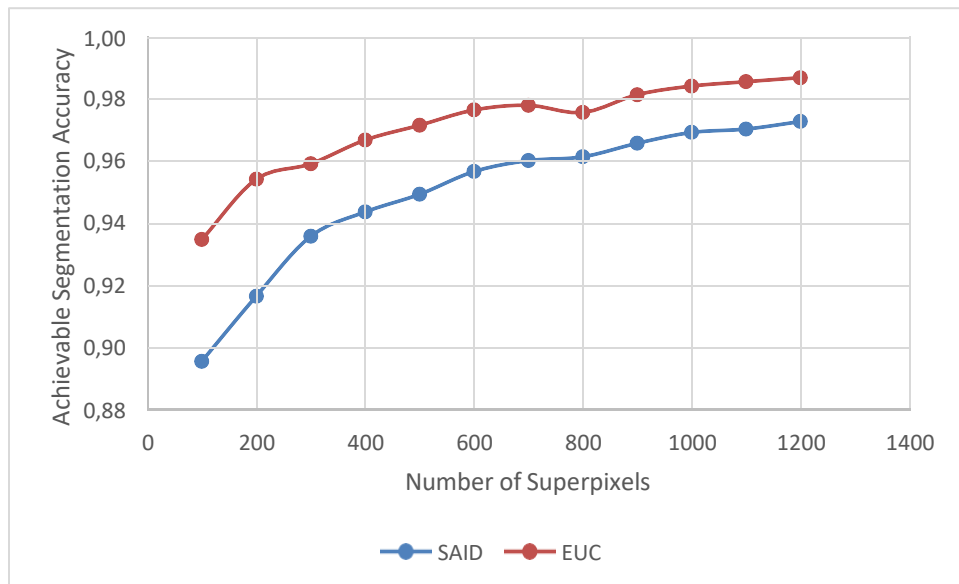


Figure 4.9b: Achievable segmentation accuracy against the number of superpixels for Centred object images with irregular compactness

A further experiment was considered for images with low contrast considering the regular and the irregular compactness. However, the same result was gathered as shown in Figures

4.10a and 4.10b, the Euclidean distance outperformed the SAID for the ASA performance metrics.

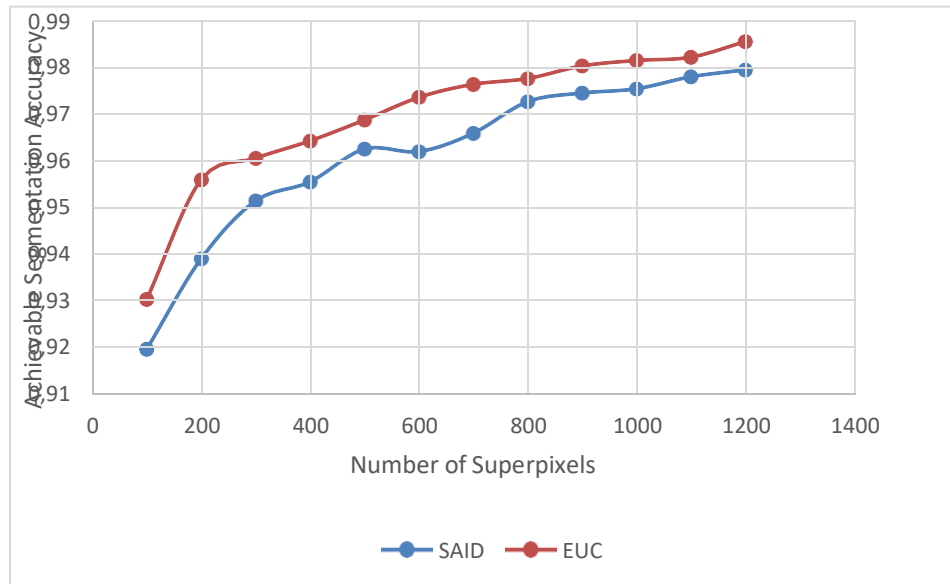


Figure 4.10a: Achievable segmentation accuracy against the number of superpixels for low contrast images with regular compactness

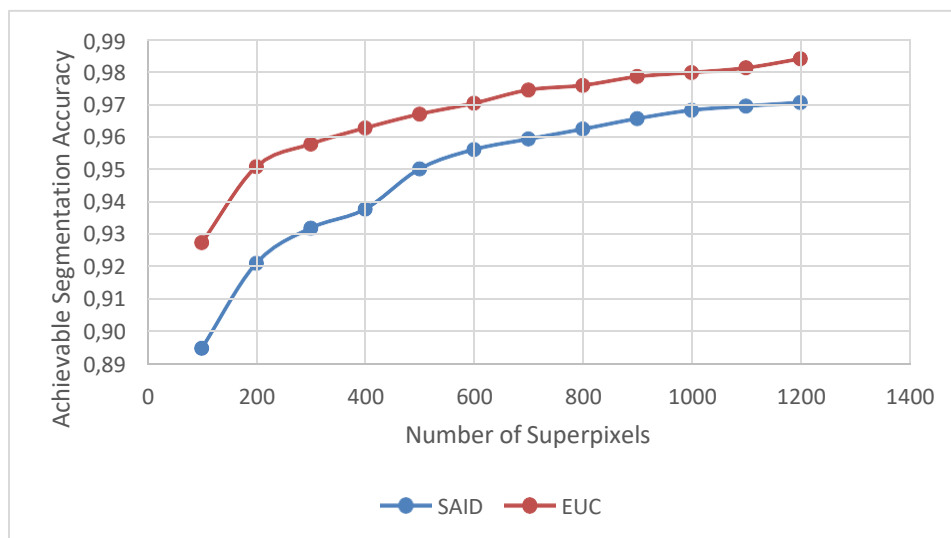


Figure 4.10b: Achievable segmentation accuracy against the number of superpixels for low contrast images with regular compactness

Compactness is a metric that helps cluster digital images with similar sizes, thus aiding high perceptual boundaries of clustered images and favouring superpixels overlapping with only a single object (Schick et al., 2014). Figures 4.11a to 4.15b shows that SAID and Euclidean distance has equal compactness metric values for images with overlapping,

multiple, complex, Centred and low contrast images. However, the trade-off for compactness for Euclidean distance is boundary adherence.

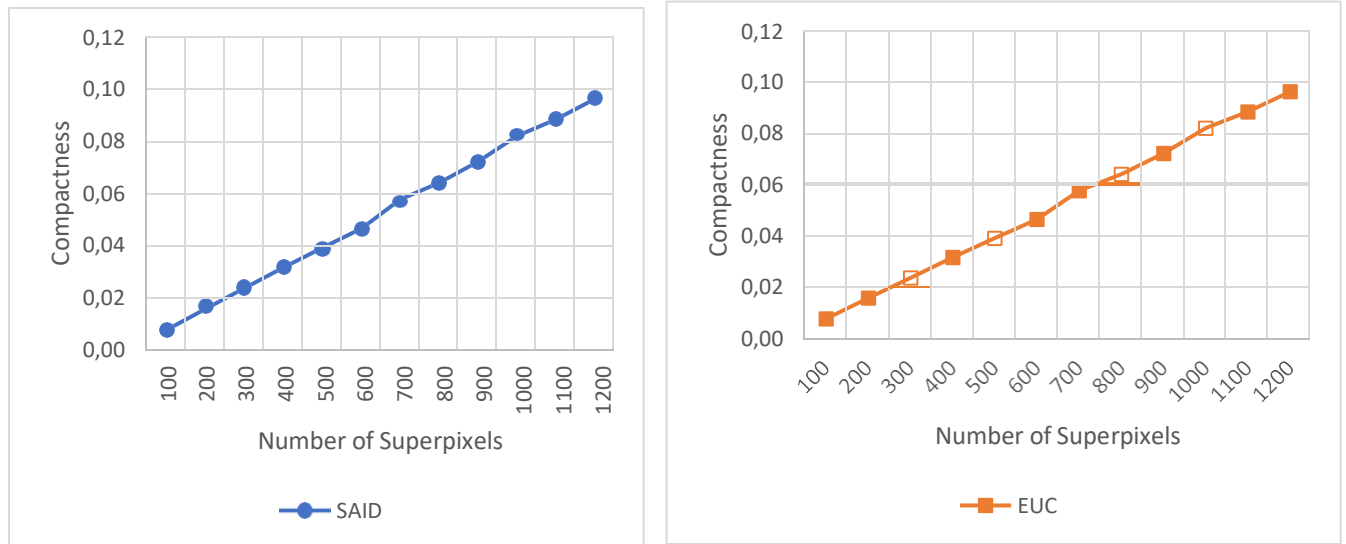


Figure 4.11a: Compactness against the number of superpixels for overlapping images with regular compactness

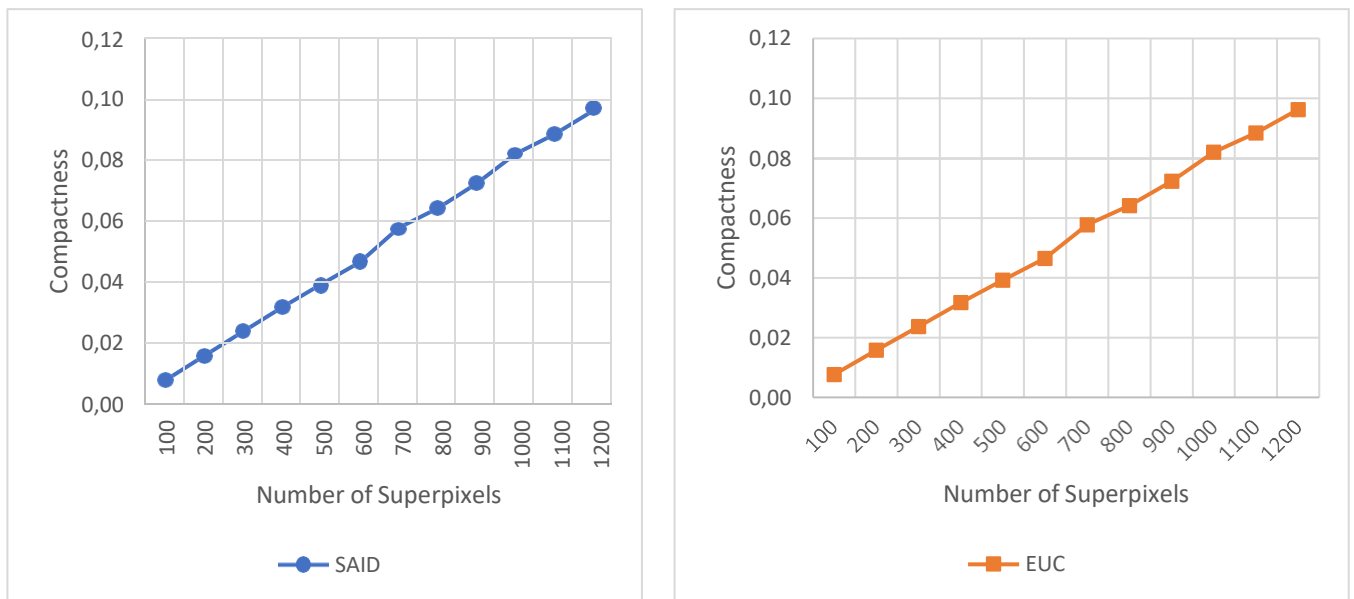


Figure 4.11b: Compactness against the number of superpixels for overlapping images with irregular compactness

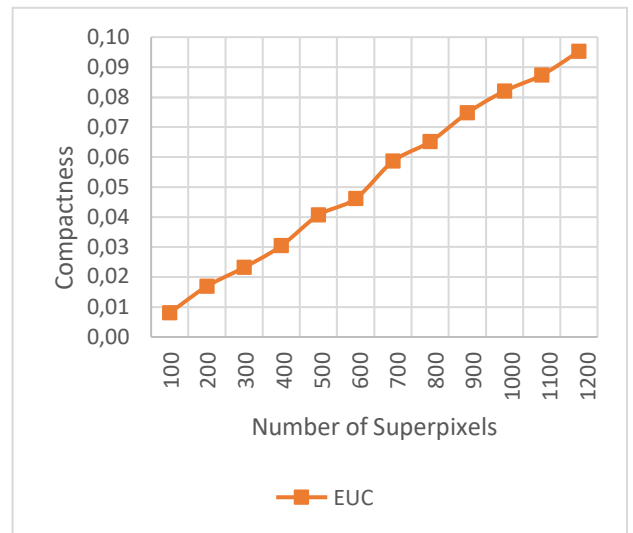
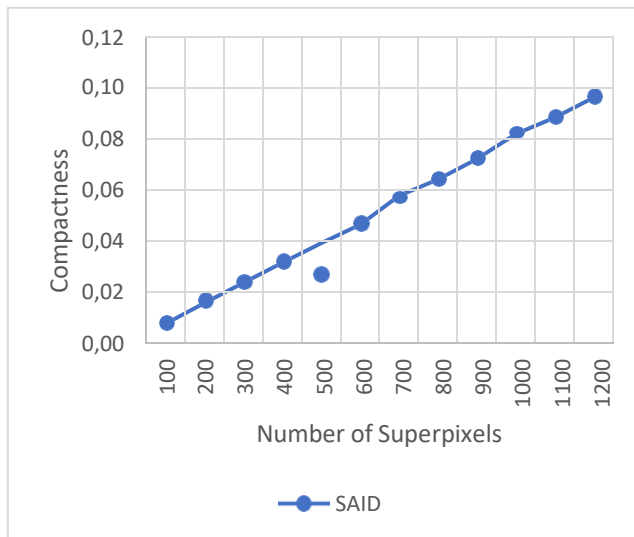


Figure 4.12a: Compactness against the number of superpixels for complex images with regular compactness

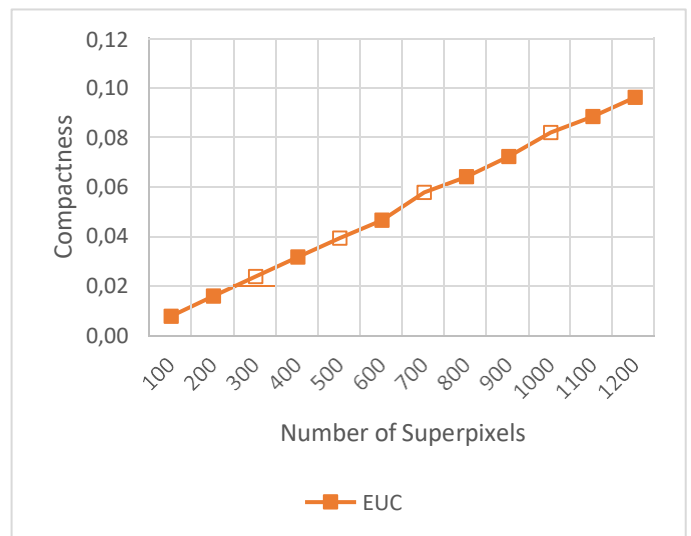
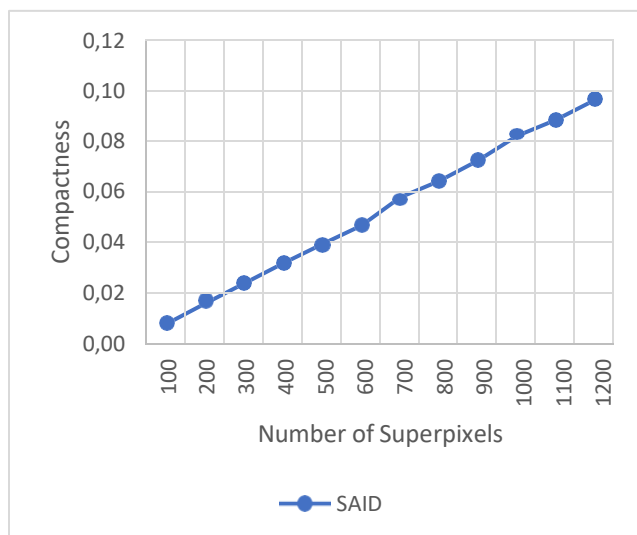


Figure 4.12b: Compactness against the number of superpixels for complex images with irregular compactness

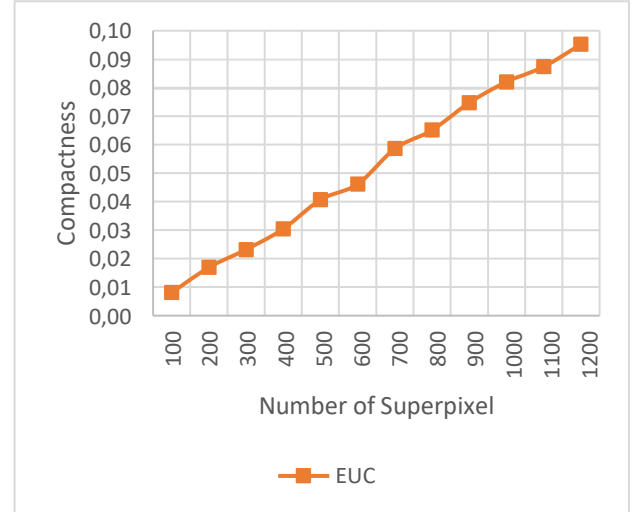
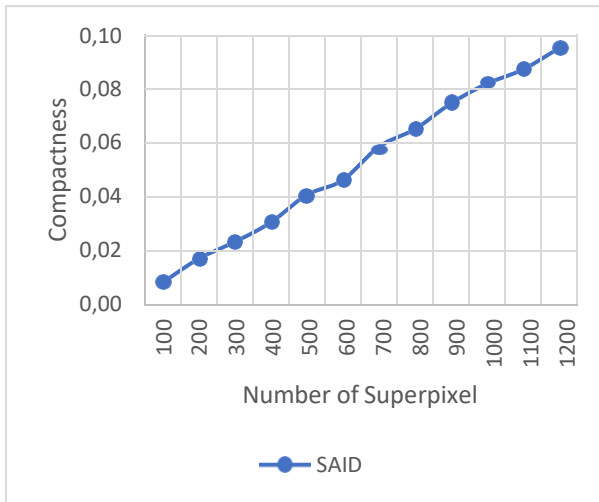


Figure 4.13a: Compactness against the number of superpixels for multiple object images with regular compactness

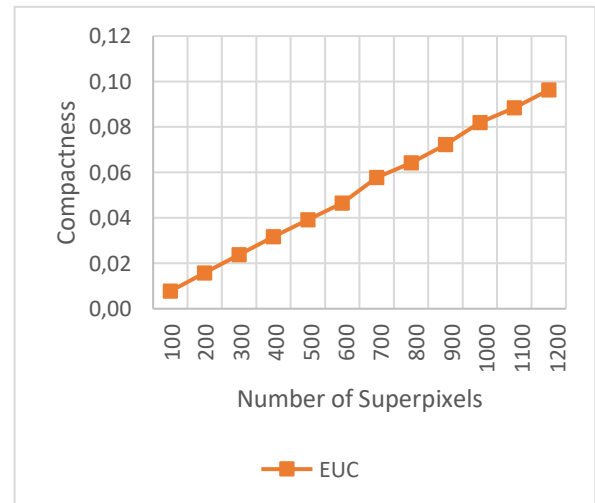
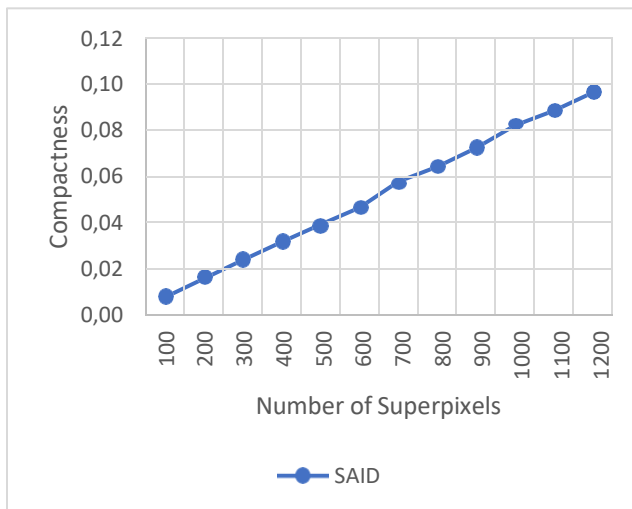


Figure 4.13b: Compactness against the number of superpixels for multiple object images with irregular compactness

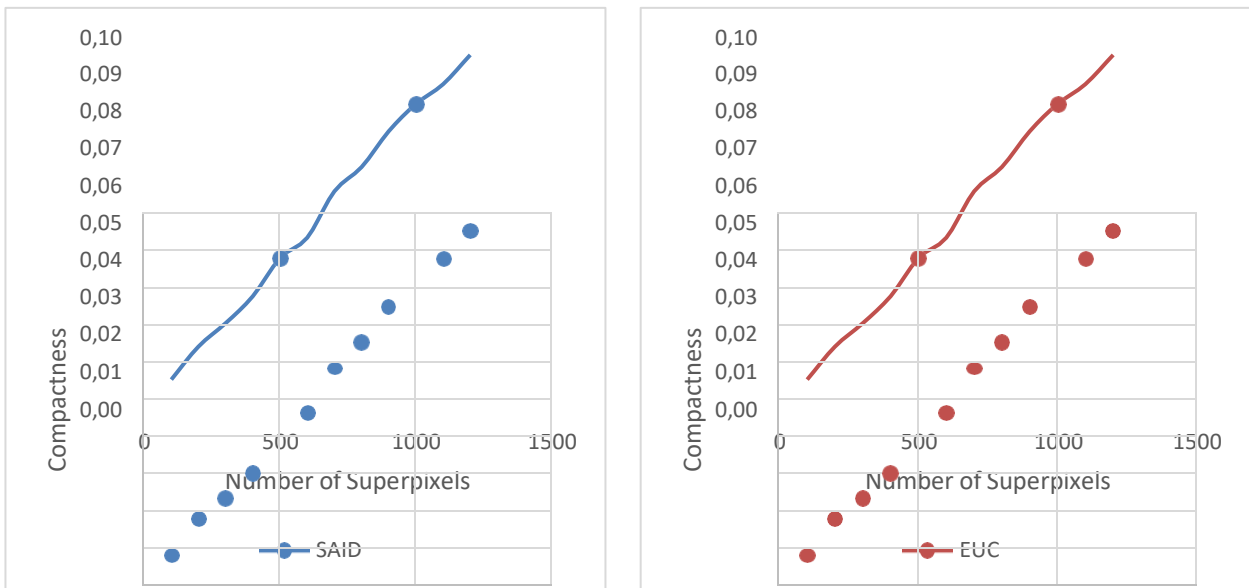


Figure 4.14a: Compactness against the number of superpixels for Centred object images with regular compactness

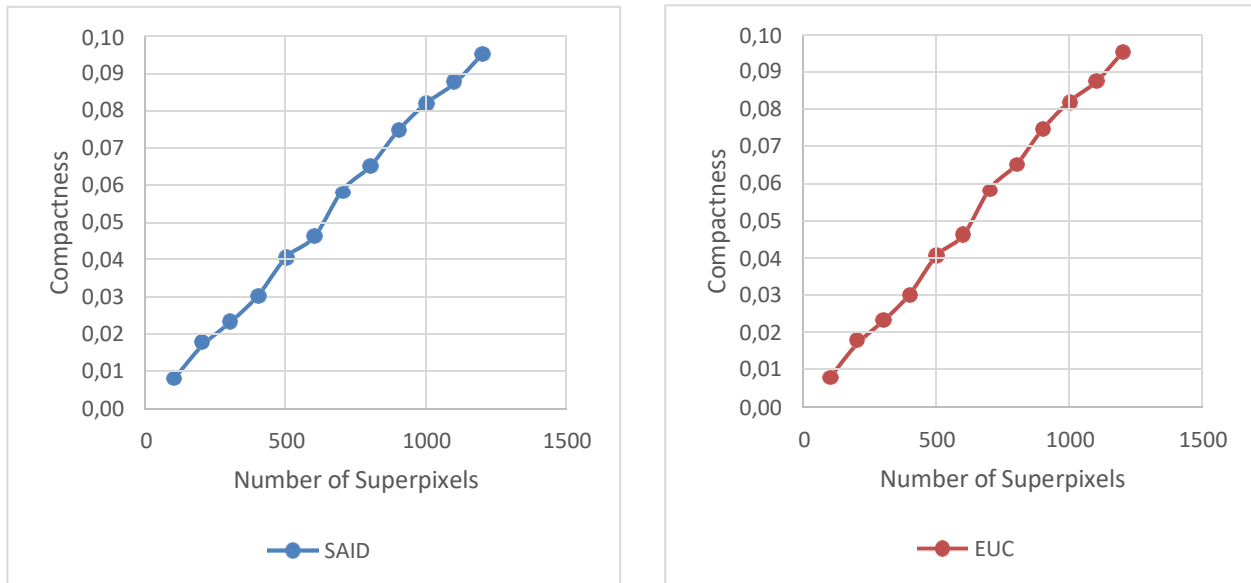


Figure 4.14b: Compactness against the number of superpixels for Centred object images with irregular compactness

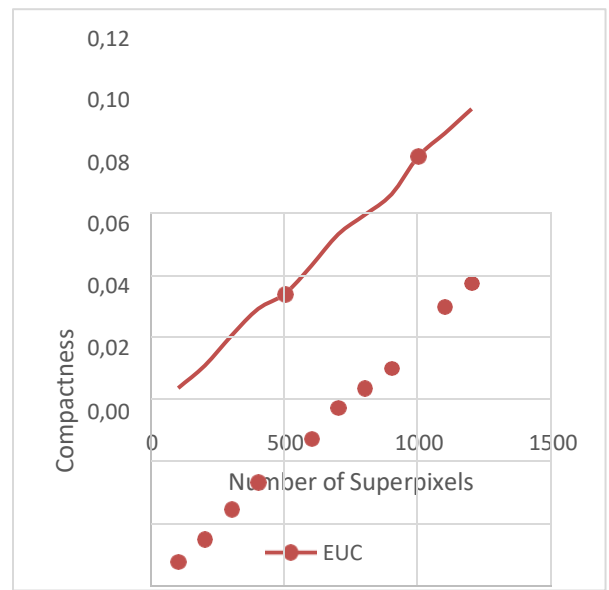
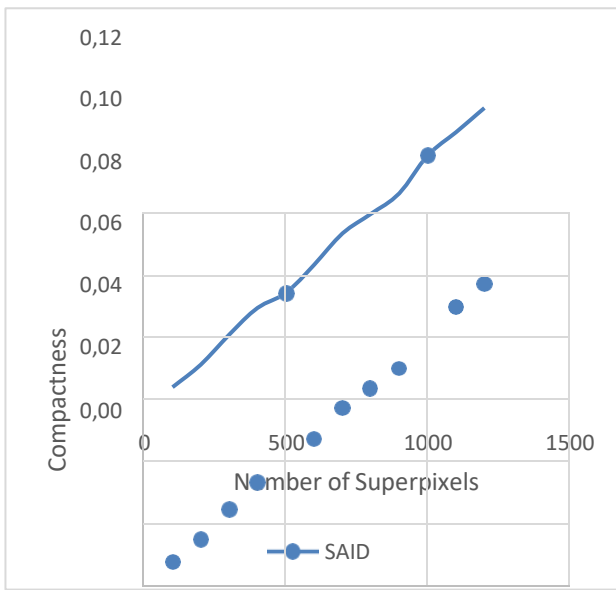


Figure 4.15a: Compactness against the number of superpixels for low contrast images with regular compactness

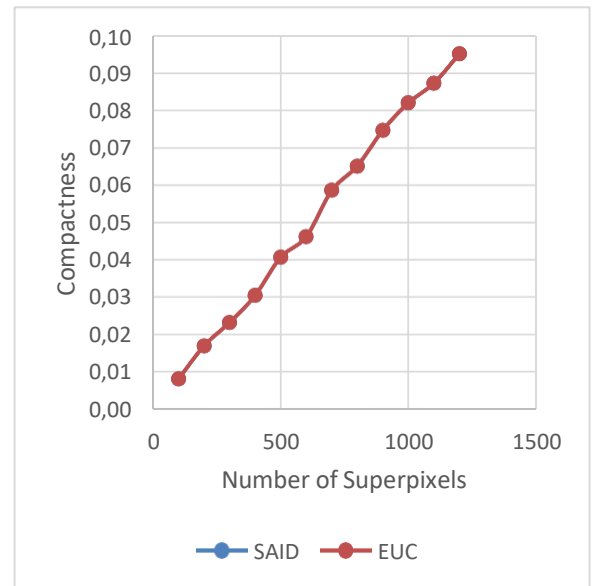
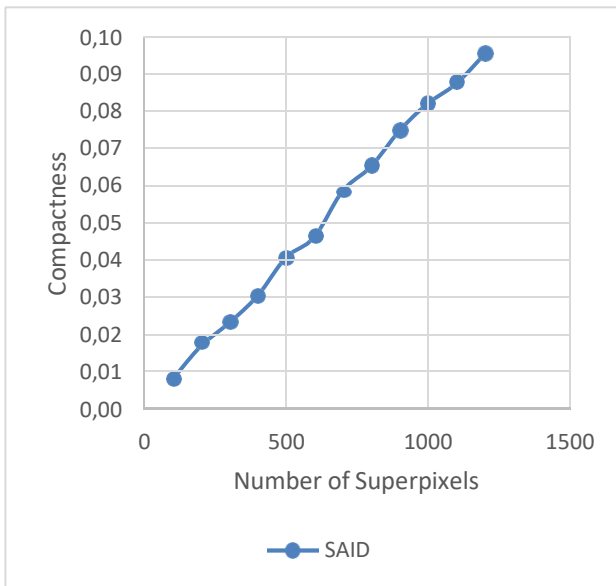


Figure 4.15b: Compactness against the number of superpixels for low contrast images with irregular compactness

As shown in Figures 4.16a to 4.20a, Euclidean offers better boundary recall than SAID with regular compactness. However, it is worth noting that Euclidean doesn't require its superpixels to be compact, allowing it to better catch the edges of thin, non-compact regions (Levenshtein et al.,

2009). However, for Figures 4.16b to 4.20b, SAID gave a better performance when compared with Euclidean distance for images with irregular compactness.

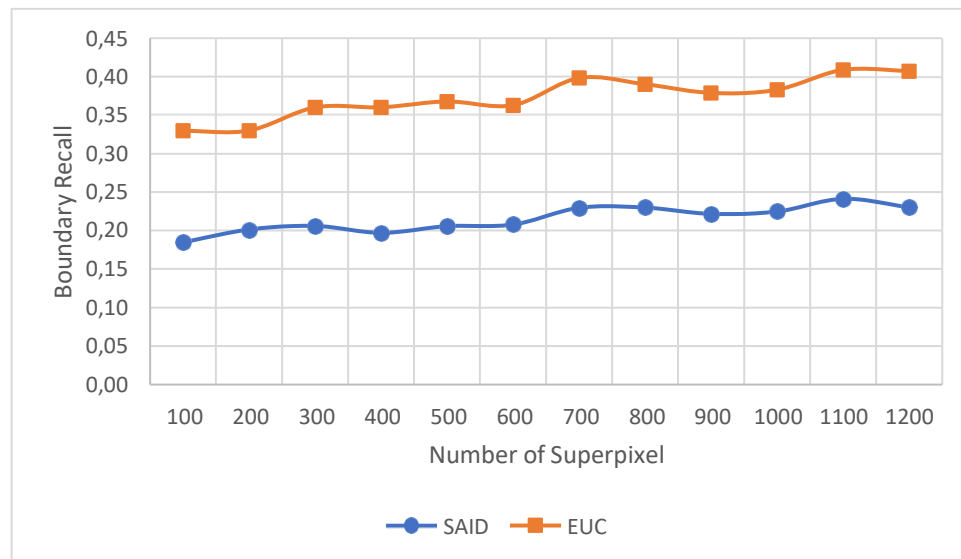


Figure 4.16a: Boundary recall against the number of superpixels for overlapping images with regular compactness

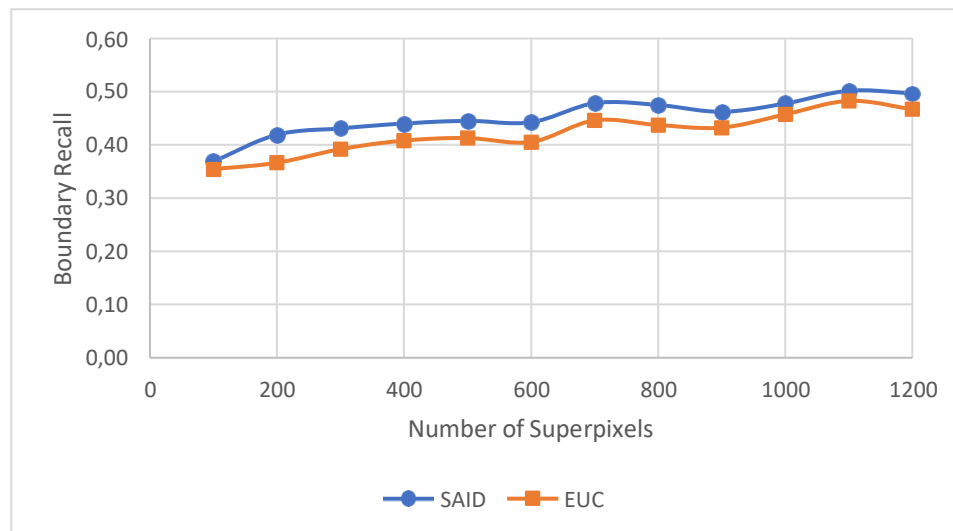


Figure 4.16b: Boundary recall against the number of superpixels for overlapping images with irregular compactness

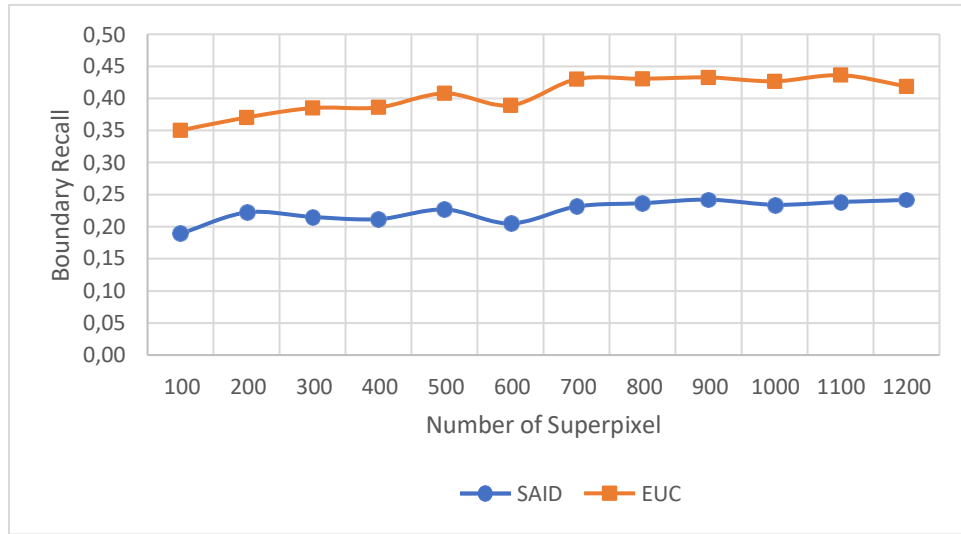


Figure 4.17a: Boundary recall against the number of superpixels for complex images with regular compactness

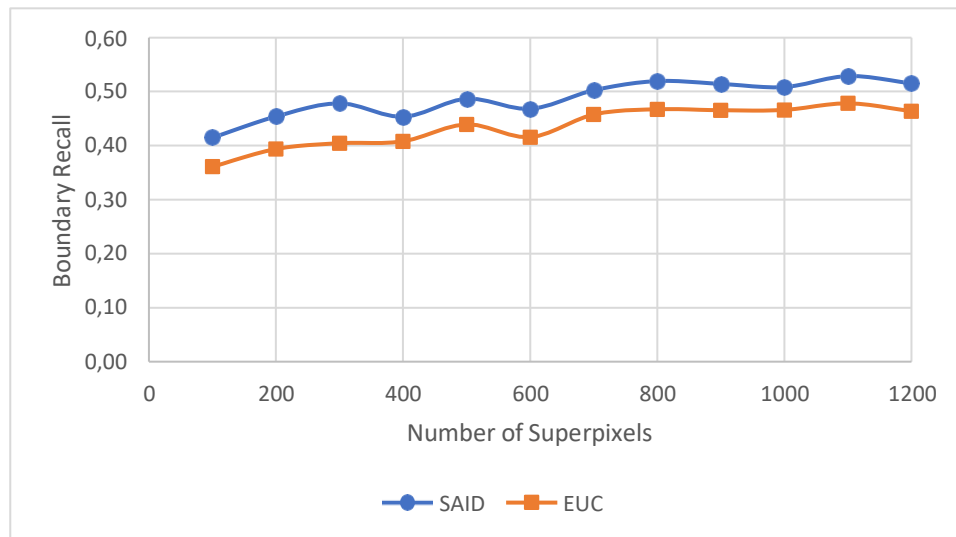


Figure 4.17b: Boundary recall against the number of superpixels for complex images with irregular compactness

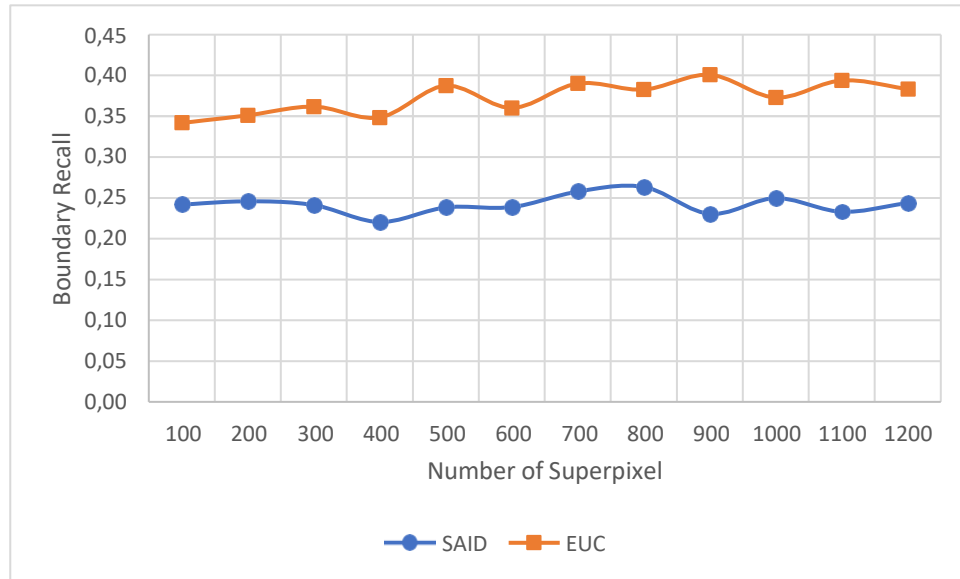


Figure 4.18a: Boundary recall against the number of superpixels for multiple object images with regular compactness

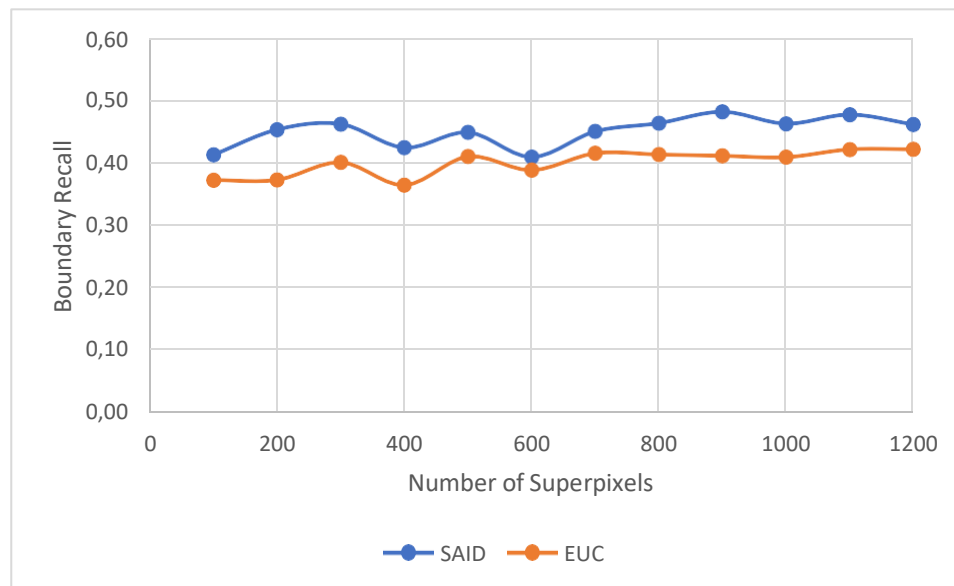


Figure 4.18b: Boundary recall against the number of superpixels for multiple object images with irregular compactness

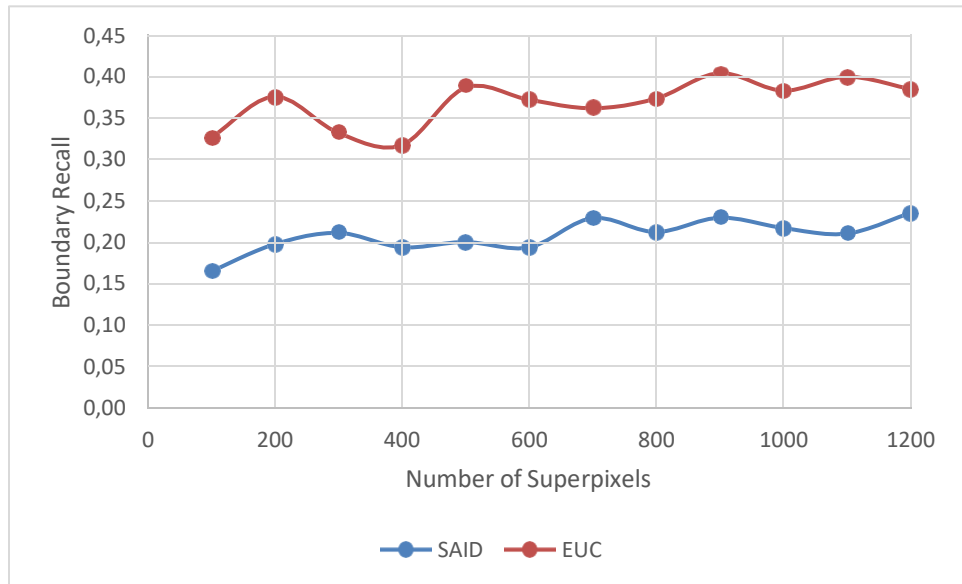


Figure 4.19a: Boundary recall against the number of superpixels for Centred object images with regular compactness

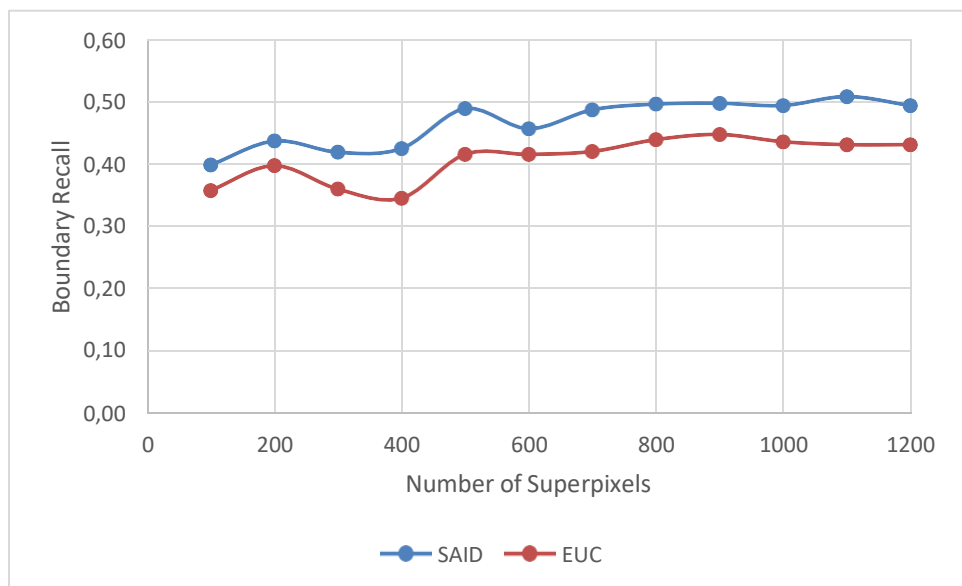


Figure 4.19b: Boundary recall against the number of superpixels for Centred object images with irregular compactness

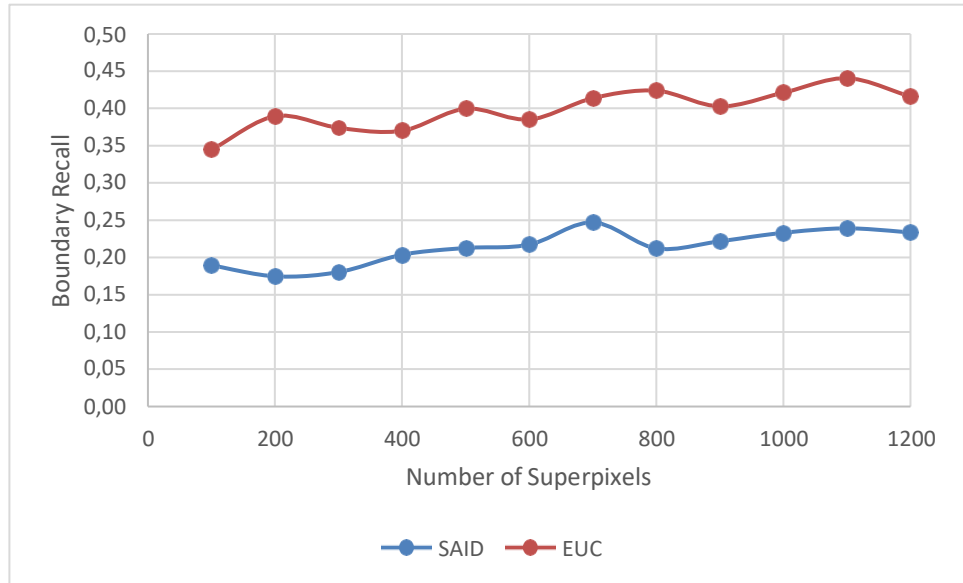


Figure 4.20a: Boundary recall against the number of superpixels for low contrast images with regular compactness

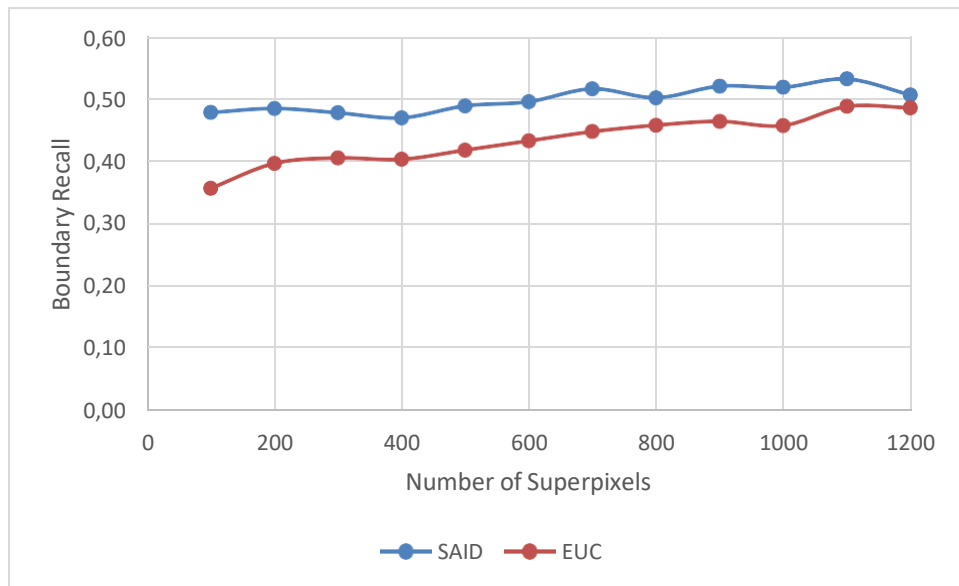


Figure 4.20b: Boundary recall against the number of superpixels for low contrast images with irregular compactness

Contour density was used to measure border adherence to avoid intentionally overestimating boundary recall. Figures 4.21a to 4.25a show that the contour density of SAID is more stable and outperformed for the given number of superpixels, that is 100 to 1200 when compared to Euclidean

distance. The opposite can be observed when Euclidean distance is compared with SAID in Figures 4.21b to 4.25b. EUC is more stable than SAID while segmenting images with irregular compactness because EUC traded boundary adherence with compactness

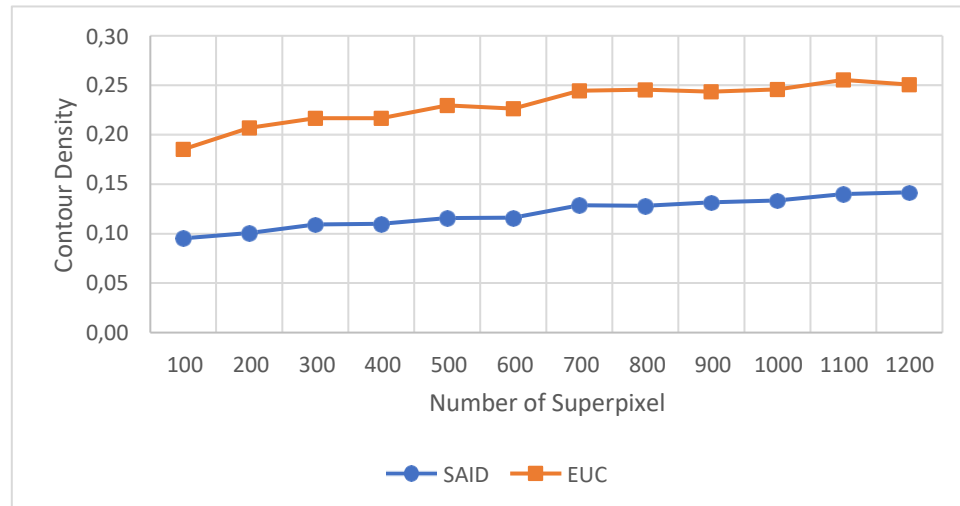


Figure 4.21a: Contour density against the number of superpixels for overlapping images with regular compactness

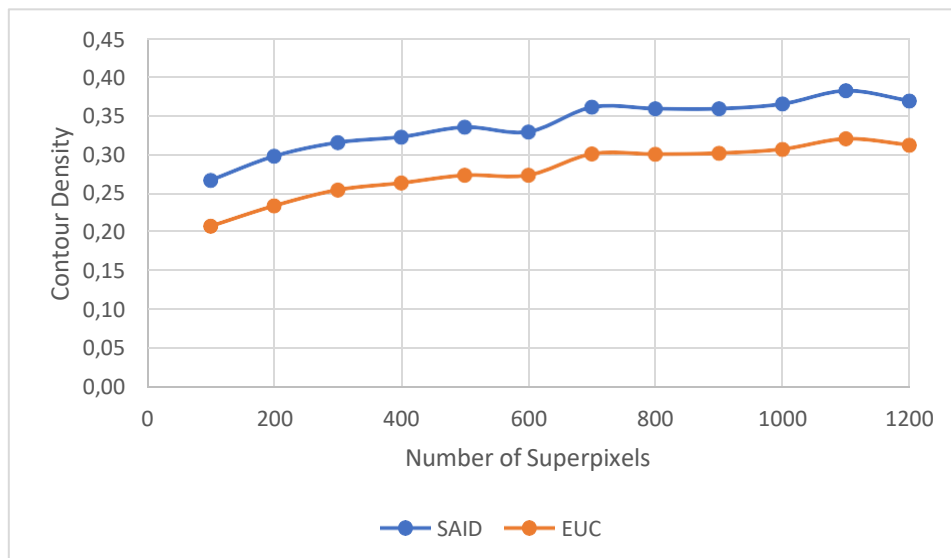


Figure 4.21b: Contour density against the number of superpixels for overlapping images with irregular compactness

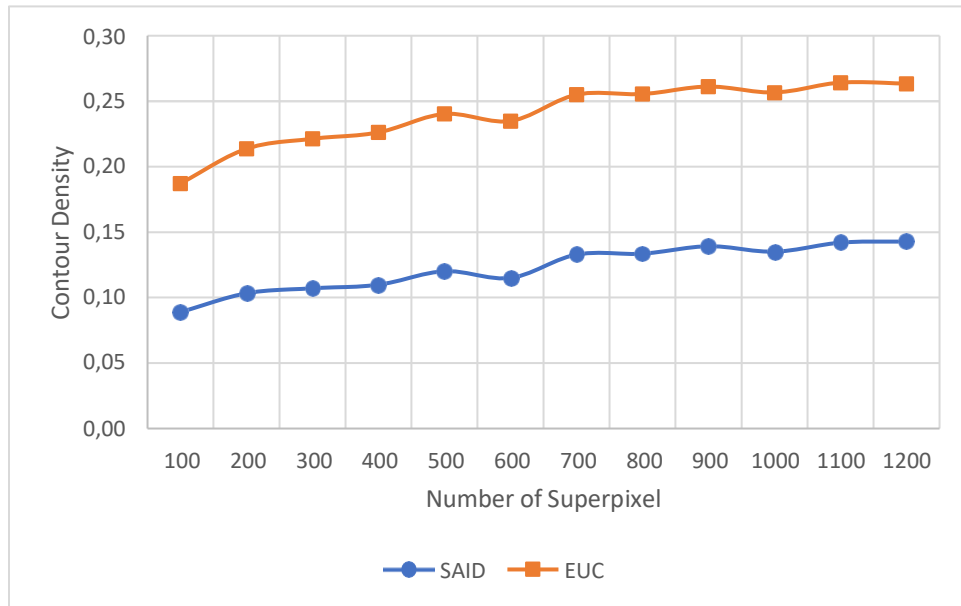


Figure 4.22a: Contour density against the number of superpixels for complex images with regular compactness

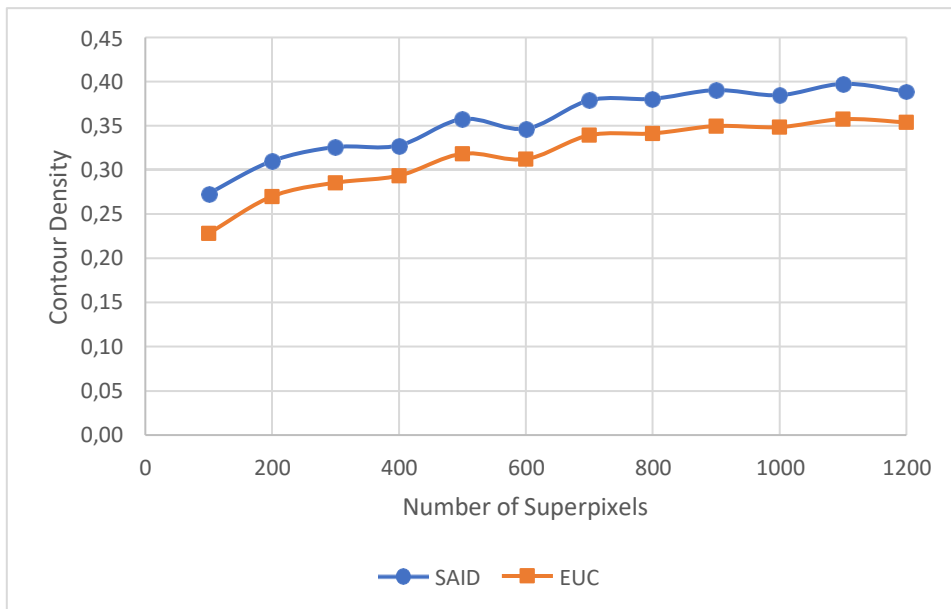


Figure 4.22b: Contour density against the number of superpixels for complex images with irregular compactness

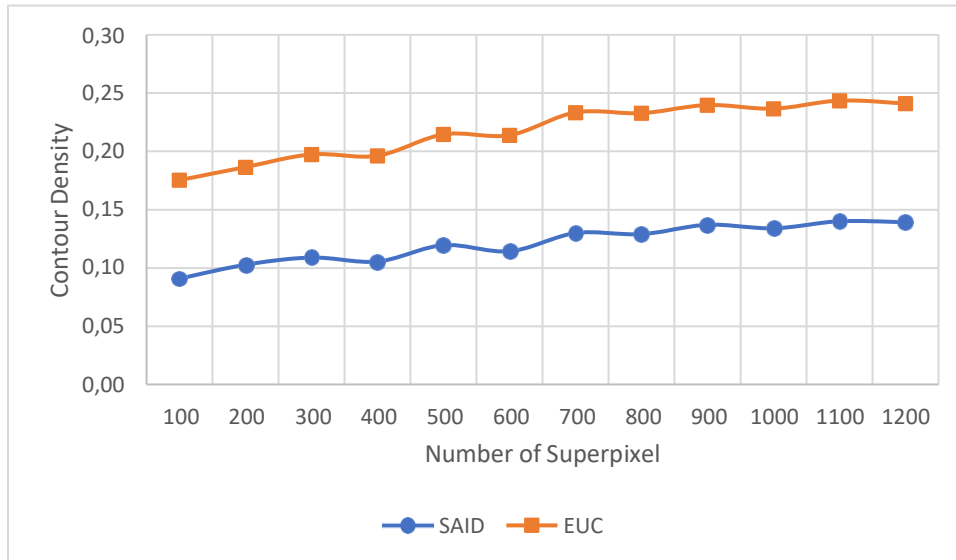


Figure 4.23a: Contour density against the number of superpixels for multiple object images with regular compactness

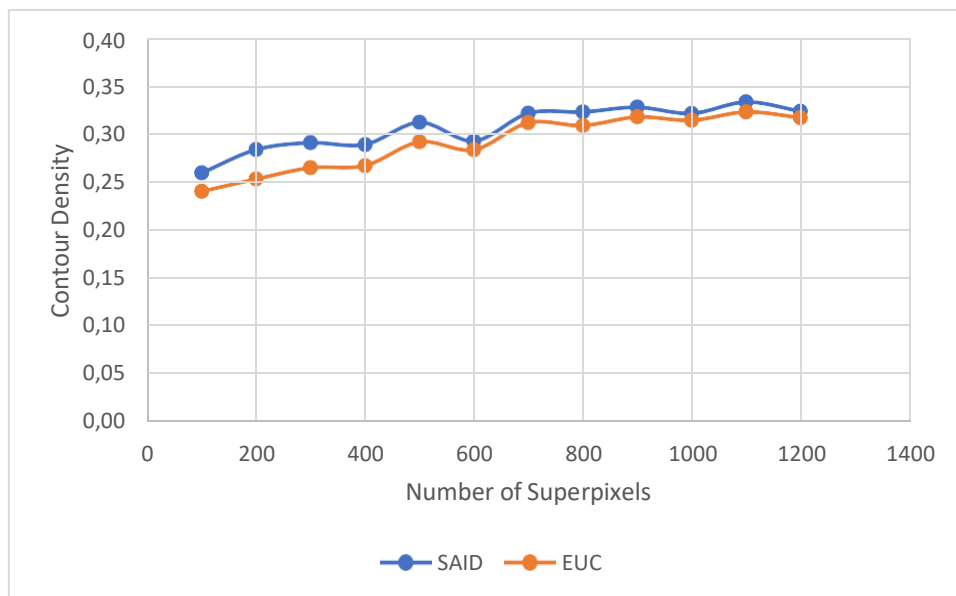


Figure 4.23b: Contour density against the number of superpixels for multiple object images with irregular compactness

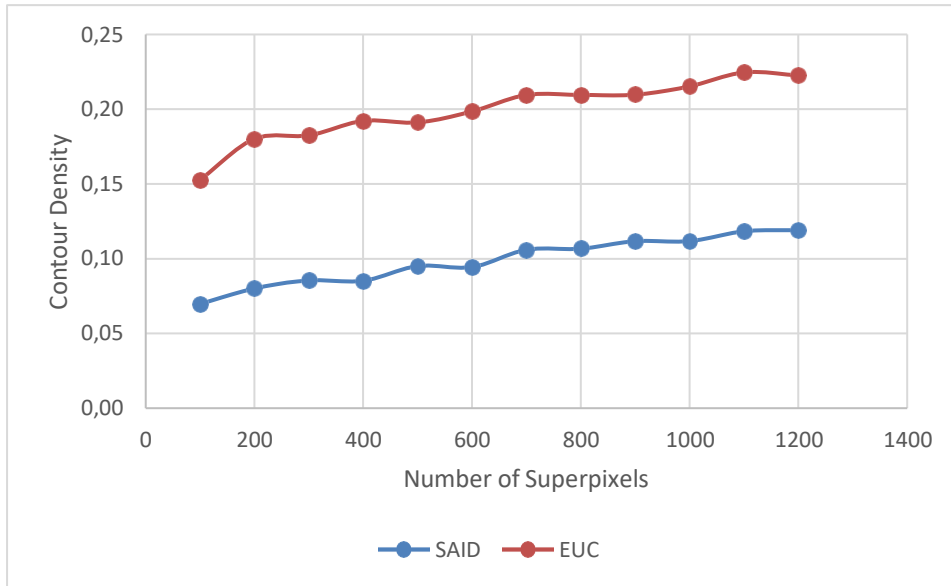


Figure 4.24a: Contour density against the number of superpixels for Centred object images with regular compactness

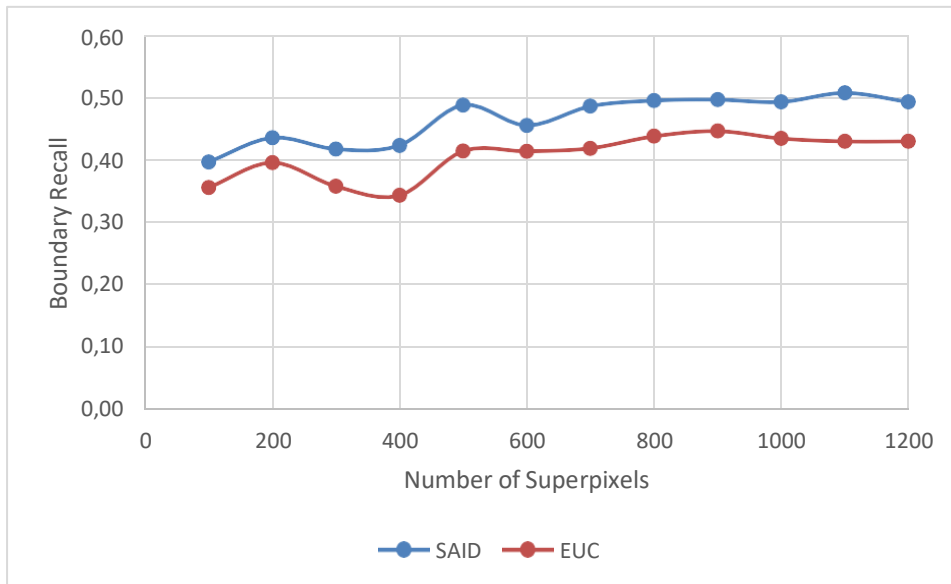


Figure 4.24b: Contour density against the number of superpixels for Centred object images with irregular compactness

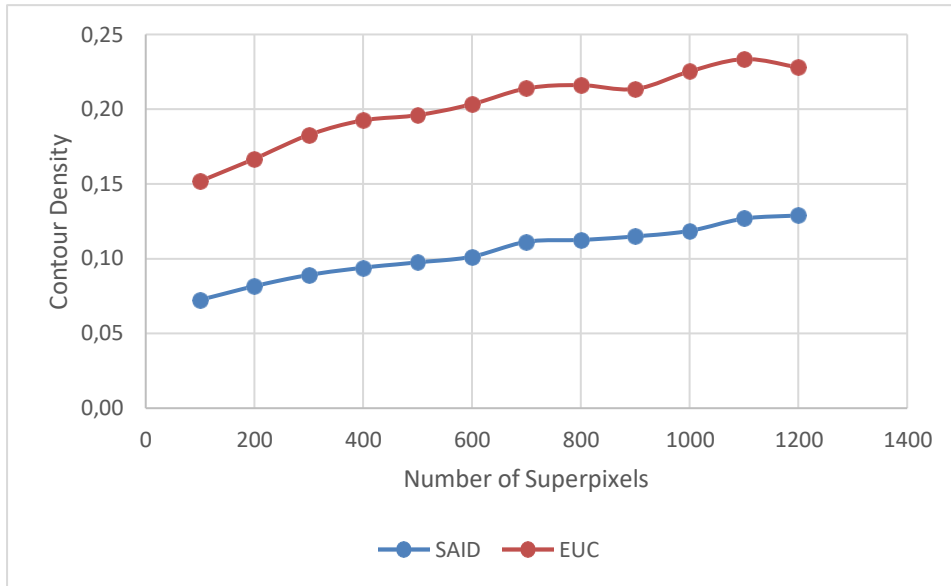


Figure 4.25a: Contour density against the number of superpixels for low contrast images with regular compactness

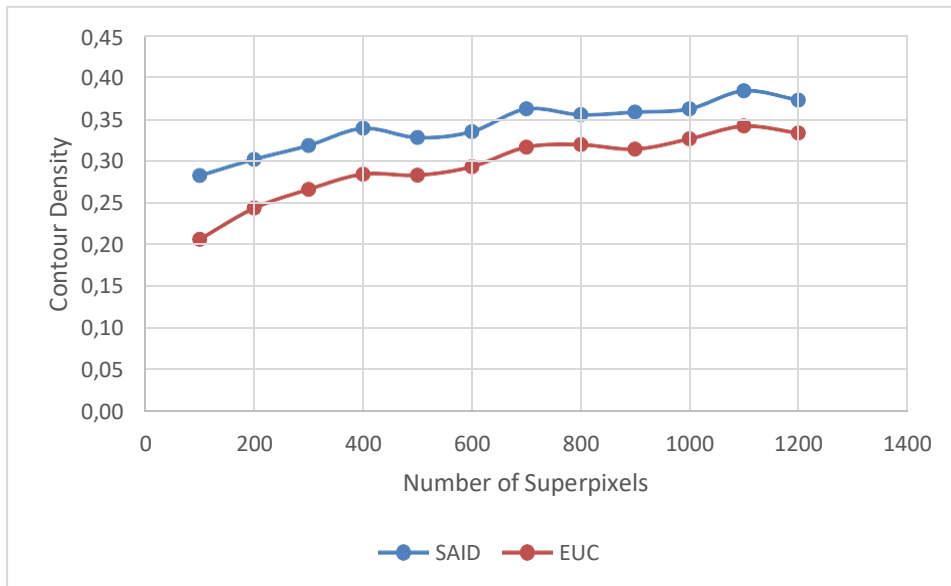


Figure 4.25b: Contour density against the number of superpixels for low contrast images with irregular compactness

In comparison to the variants of the selected superpixel segmentation algorithm, SLIC with Euclidean distance measure has a lot of opportunity for improvement on all five performance evaluation metrics, especially when segmenting complex images.

4.4 Quantitative Evaluation for HSV Colour Model

The under-segmentation error, shown in Figure 4.26, is a key evaluation metric that identifies algorithmic segmentation flaws. The under-segmentation error for overlapping images with regular compactness is shown in Figure 4.26a; the result reveals that the SAID distance measure and the Euclidean (EUC) distance performed equally when segmenting.

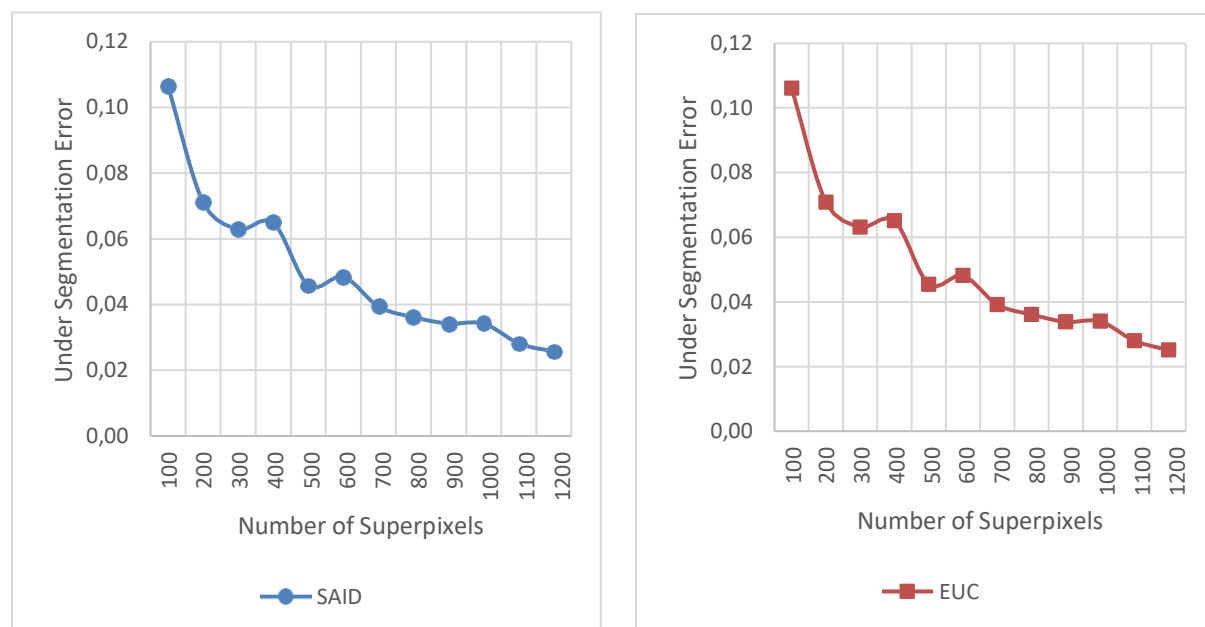


Figure 4.26a: Under-segmentation error against the number of superpixels for overlapping images with regular compactness

Figure 4.26b, on the other hand, shows that SAID struggled to accurately detect salient image structure for overlapping images with irregular compactness. As a result of the irregularity of compactness, the region may appear unclear. As a result, while segmenting overlapping images with irregular compactness, EUC performed better.

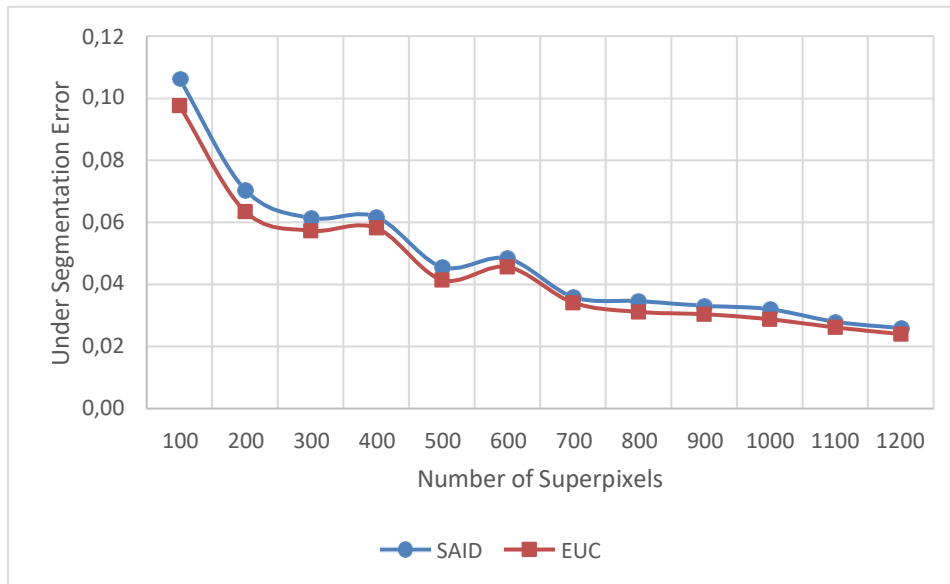


Figure 4.26b: Under-segmentation error against the number of superpixels for overlapping images with irregular compactness

Similarly, Figure 4.27a confirms that SAID and Euclidean performed equally well when segmenting complicated images with regular compactness, as shown in Figure 4.26a. Images featuring irregularly shaped objects, complicated foreground and background colour complexity are examples of complex images.

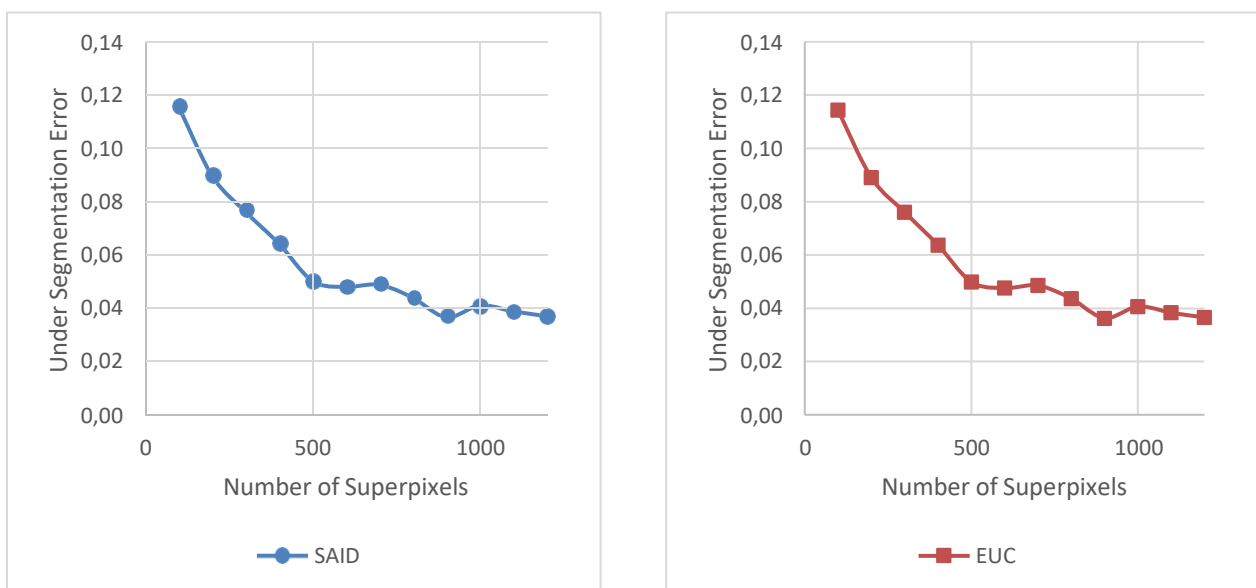


Figure 4.27a: Under-segmentation error against the number of superpixels for complex images with regular compactness

However, as presented in Figure 4.27b, Euclidean distance outperformed SAID for complex images with irregular compactness.

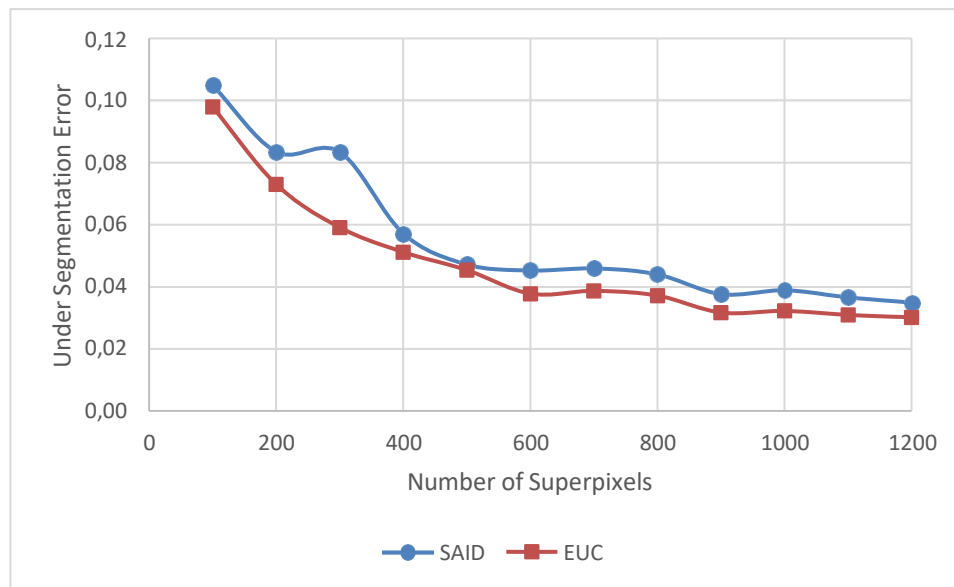


Figure 4.27b: Under-segmentation error against the number of superpixels for complex images with irregular compactness

Furthermore, when segmenting multiple images with regular compactness, Figure 4.28a displays a consistent result that illustrates Euclidean distance at par SAID. Figure 4.28b, on the other hand, illustrates that when segmenting complex images with irregular compactness, Euclidean distance catches the conspicuous object better than SAID.

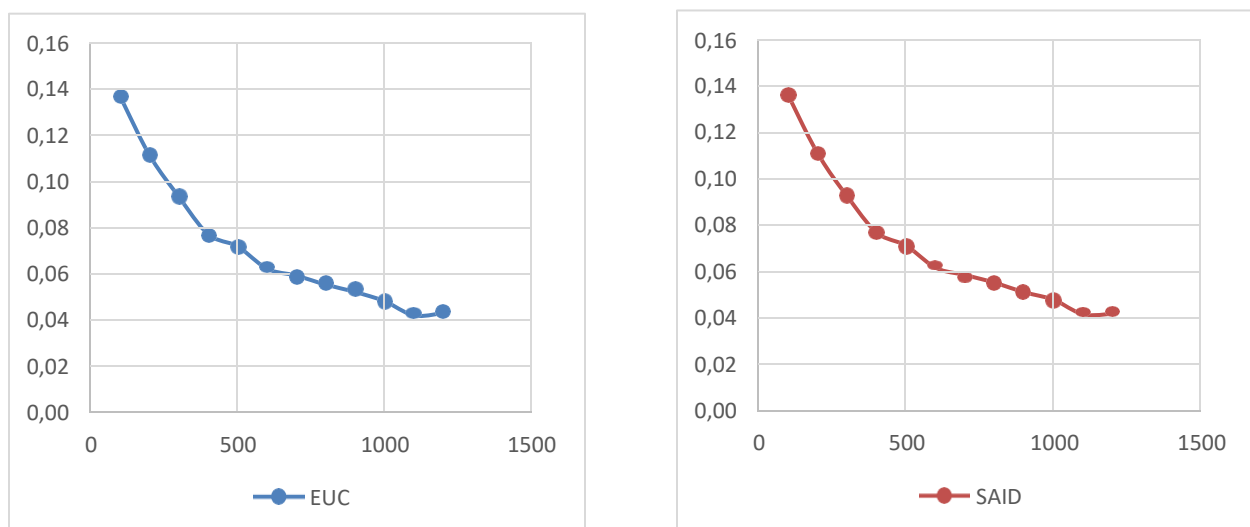


Figure 4.28a: Under-segmentation error against the number of superpixels for multiple object images with regular compactness

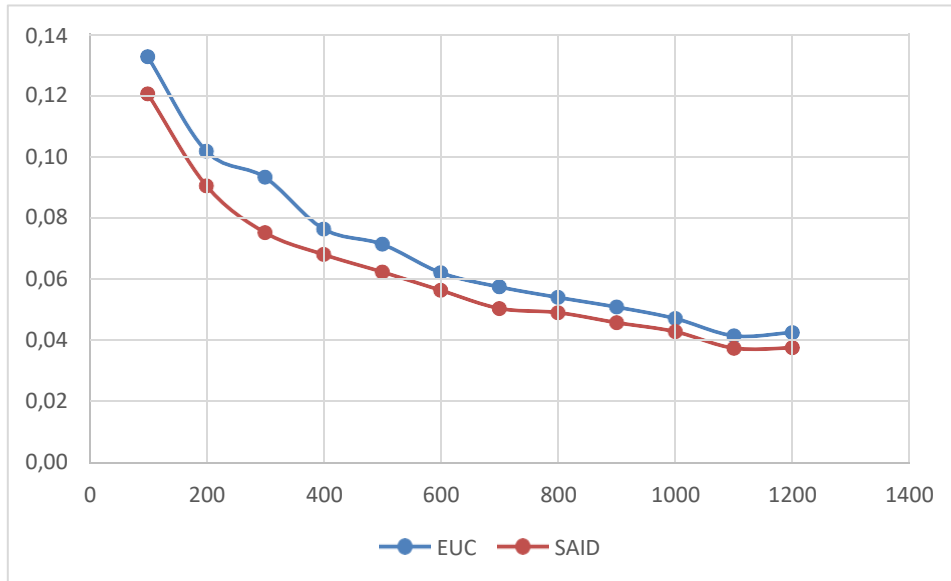


Figure 4.28b: Under-segmentation error against the number of superpixels for multiple object images with irregular compactness

When the object is in the Centred of the image with irregular compactness superpixel, Figure 4.29a displays the under-segmentation error metric. The experimental result demonstrates that Euclidean distance performed similarly well as SAID.

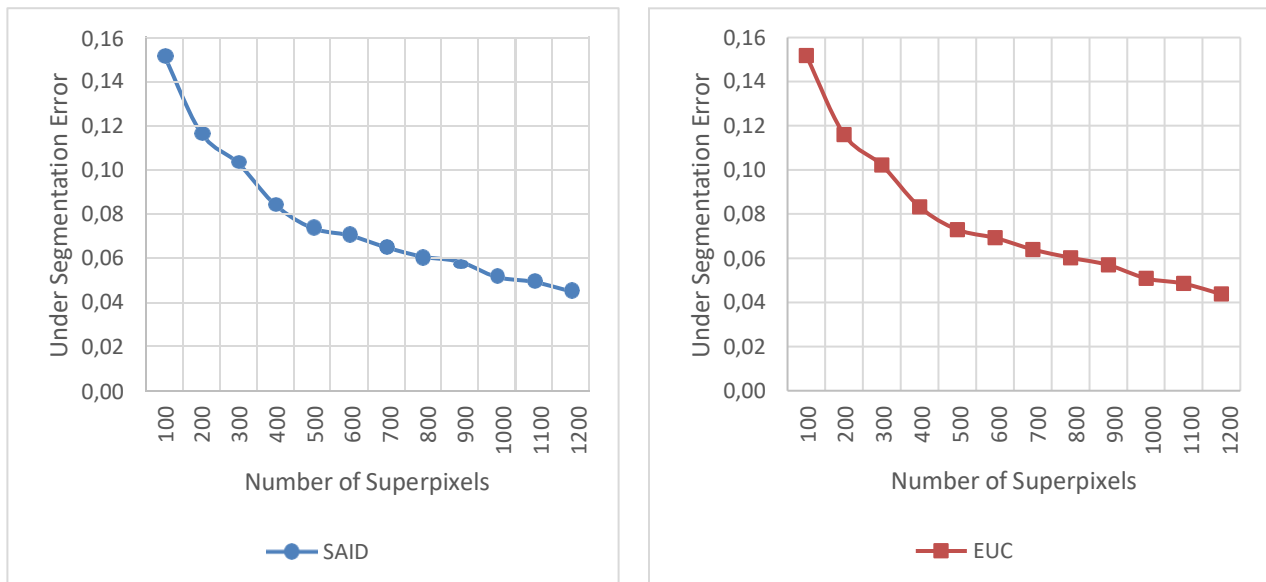


Figure 4.29a: Under-segmentation error against the number of superpixels for Centred object images with regular compactness

Figure 4.29b, on the other hand, indicates that when segmenting Centred object images with irregular compactness, the Euclidean outperforms SAID.

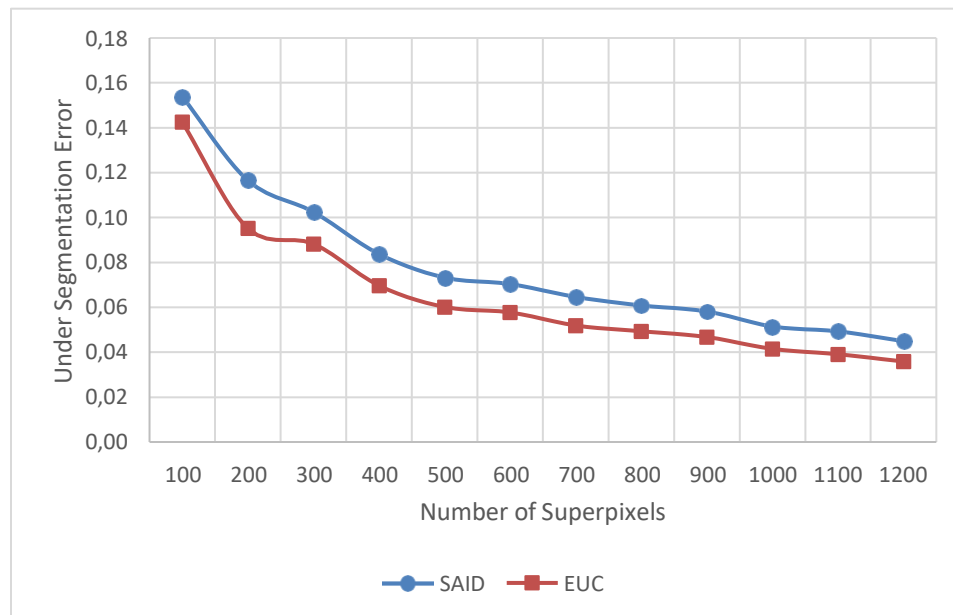


Figure 4.29b: Under-segmentation error against the number of superpixels for Centred object images with irregular compactness

As a result, more experiments were carried out for low-contrast images; Figure 4.30a shows Euclidean distance and SAID at par. Figure 4.30b, on the other hand, indicates that Euclidean distance outperformed SAID for irregular superpixel compactness, even though the images were seen perceptually during the qualitative analysis favours SAID.

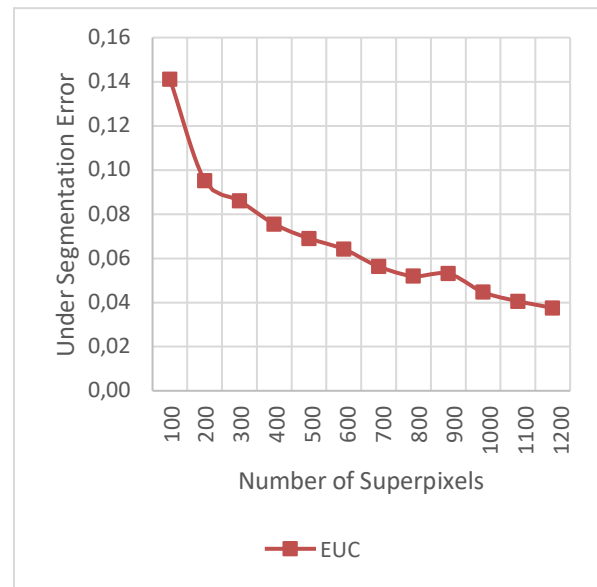
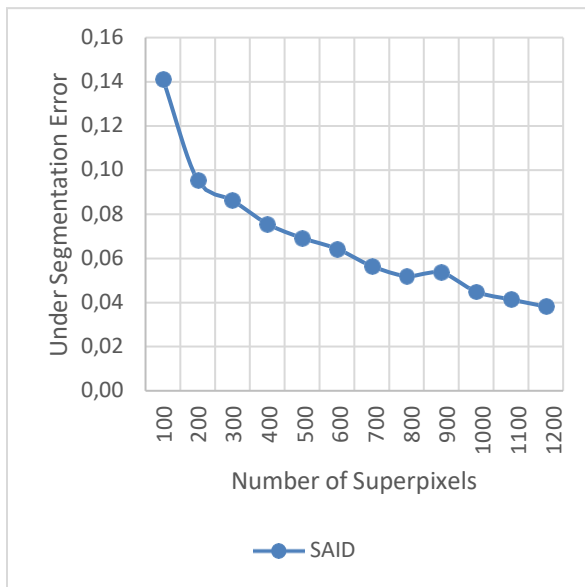


Figure 4.30a: Under-segmentation error against the number of superpixels for low contrast images with regular compactness

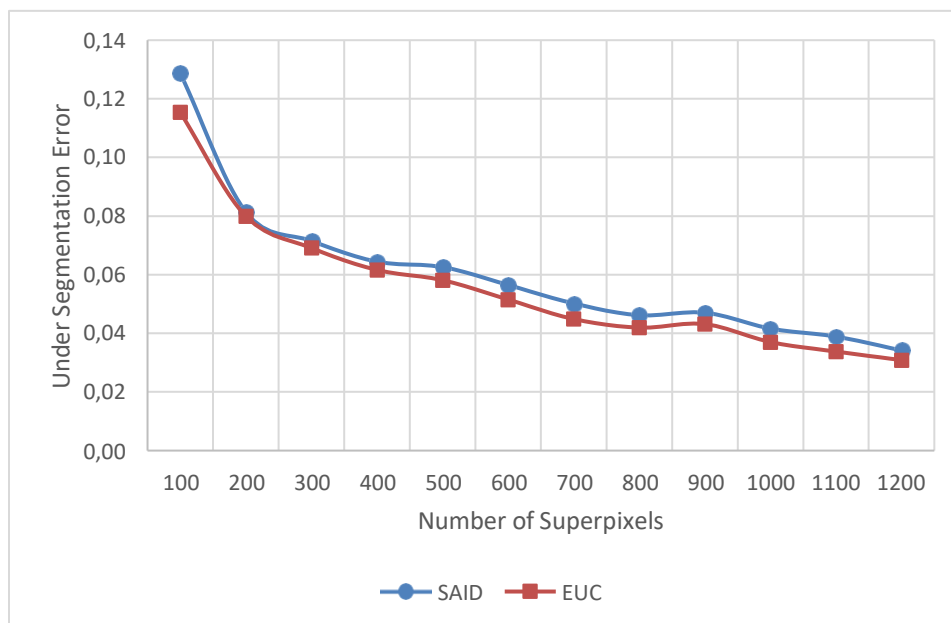


Figure 4.30b: Under-segmentation error against the number of superpixels for low contrast images with irregular compactness

In Figure, 4.31a SAID and Euclidean distance was of equal performance when segmenting images overlapping objects with regular superpixel compactness. However, in Figure 4.31b Euclidean distance outperformed SAID with irregular superpixel compactness.

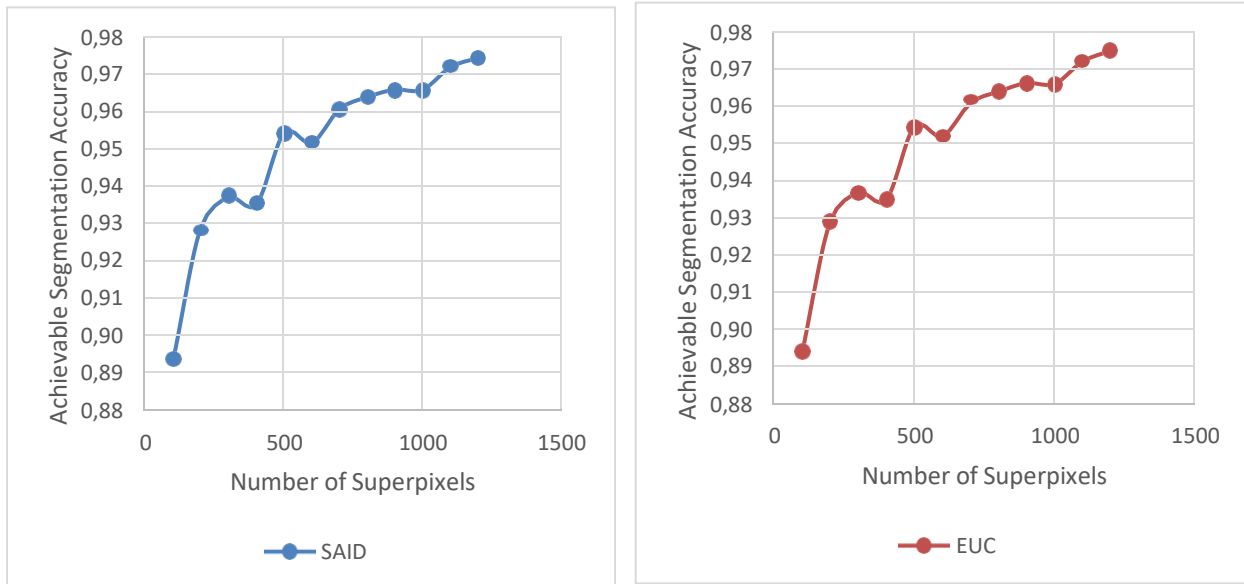


Figure 4.31a: Achievable segmentation accuracy against the number of superpixels for overlapping images with regular compactness

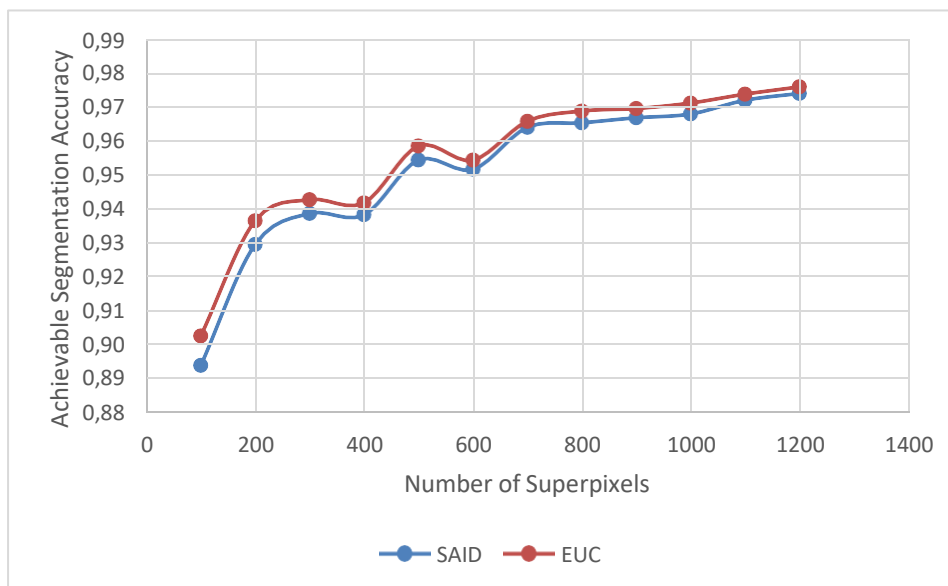


Figure 4.31b: Achievable segmentation accuracy against the number of superpixels for overlapping images with irregular compactness

When computing the ASA for complex images with foreground and background colour complexity for regular compactness, Figure 4.32a depicts that SAID and Euclidean distance

performed equally well. As a result, as seen in Figure 4.32b, the reversal occurs with irregular compactness, as EUC outperforms SAID.

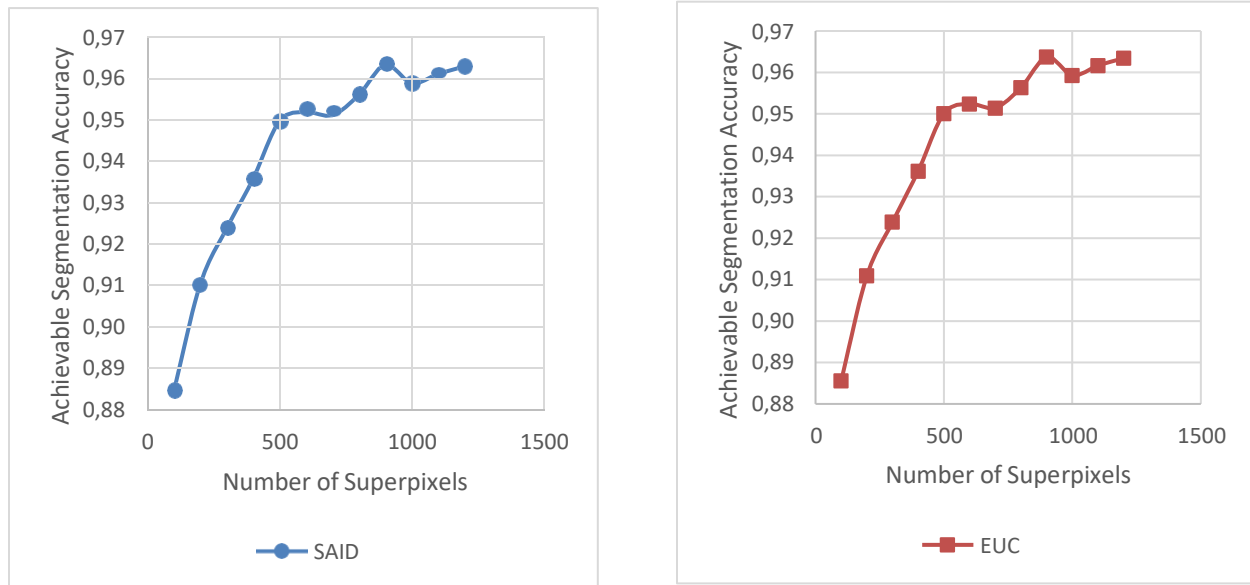


Figure 4.32a: Achievable segmentation accuracy against the number of superpixels for complex images with regular compactness

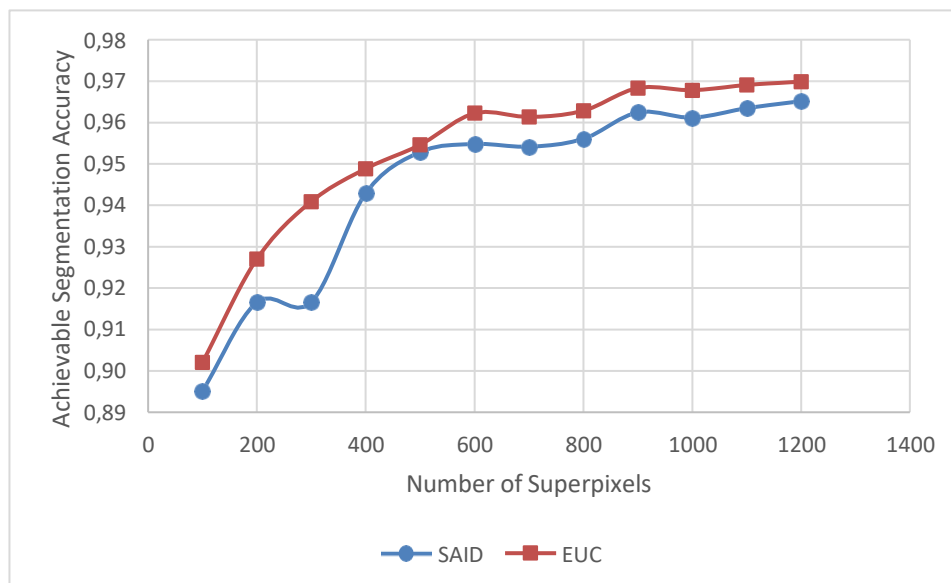


Figure 4.32b: Achievable segmentation accuracy against the number of superpixels for complex images with irregular compactness

However, in Figure, 4.33a Euclidean distance was at par with SAID when calculating the ASA for multiple object images regardless of the regular and irregular compactness. However, in Figure

4.33b EUC outperforms SAID

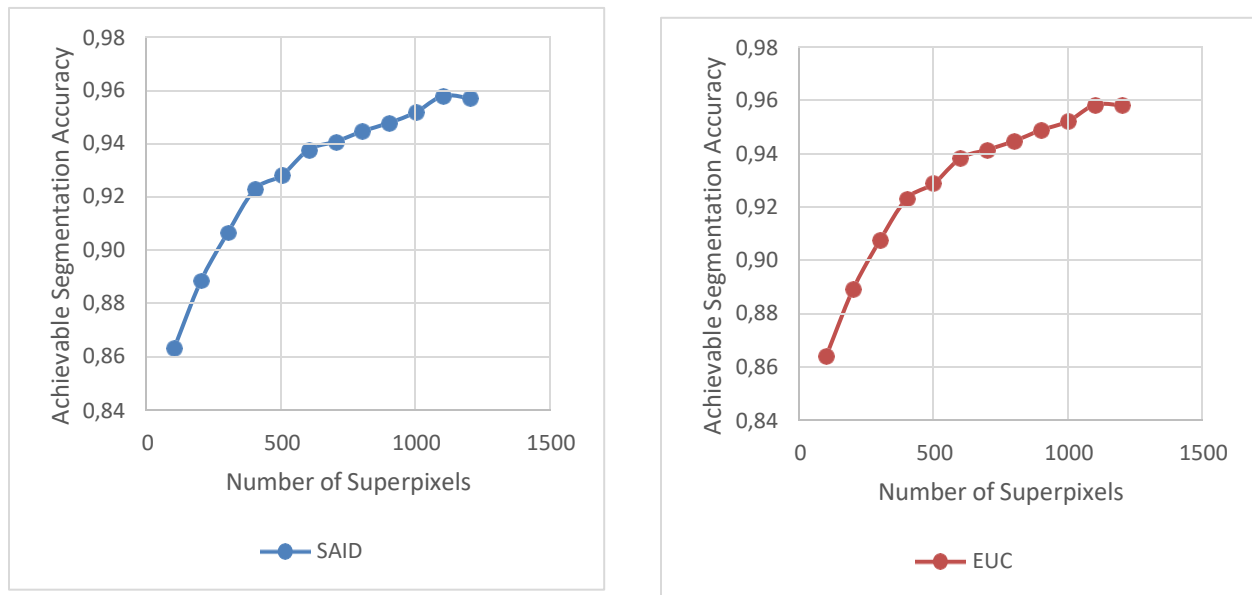


Figure 4.33a: Achievable segmentation accuracy against the number of superpixels for multiple object images with regular compactness

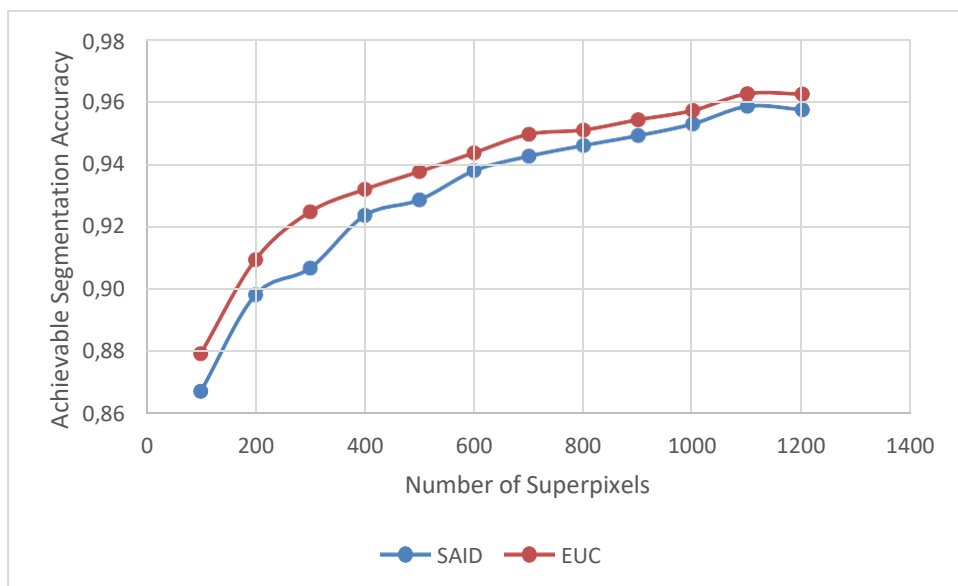


Figure 4.33b: Achievable segmentation accuracy against the number of superpixels for multiple object images with irregular compactness

While experimenting with images with Centred objects for regular compactness Figures, 4.34a depicts that Euclidean distance and SAID performance was at par when calculating the ASA. However, for irregular compactness, as shown in Figures 4.34b Euclidean distance performed better than SAID when calculating the ASA.

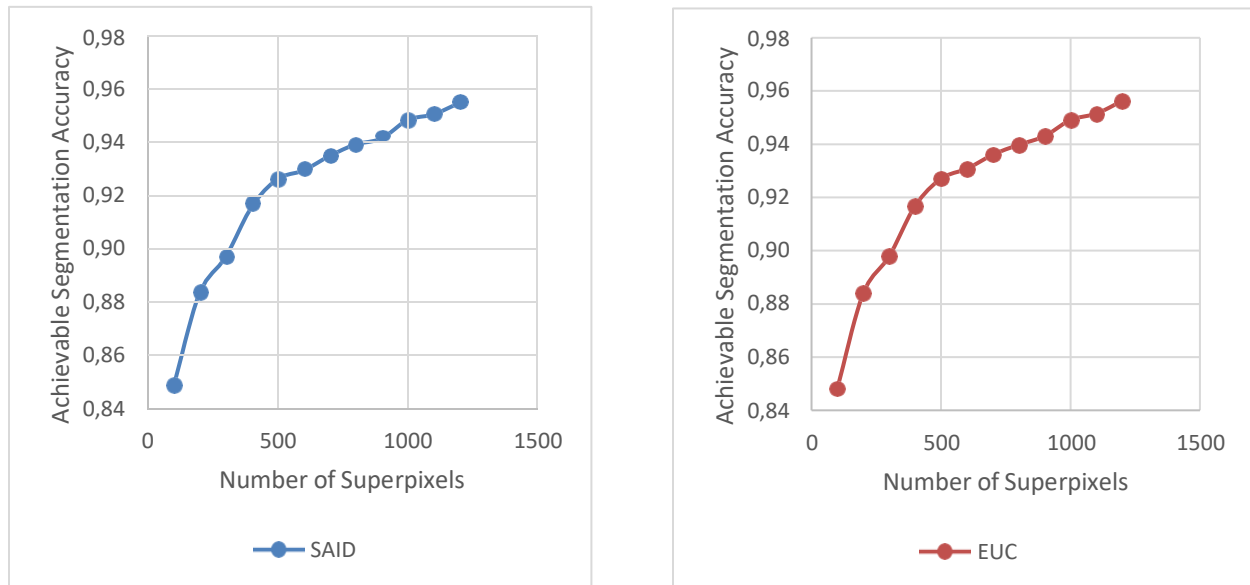


Figure 4.34a: Achievable segmentation accuracy against the number of superpixels for Centred object images with regular compactness

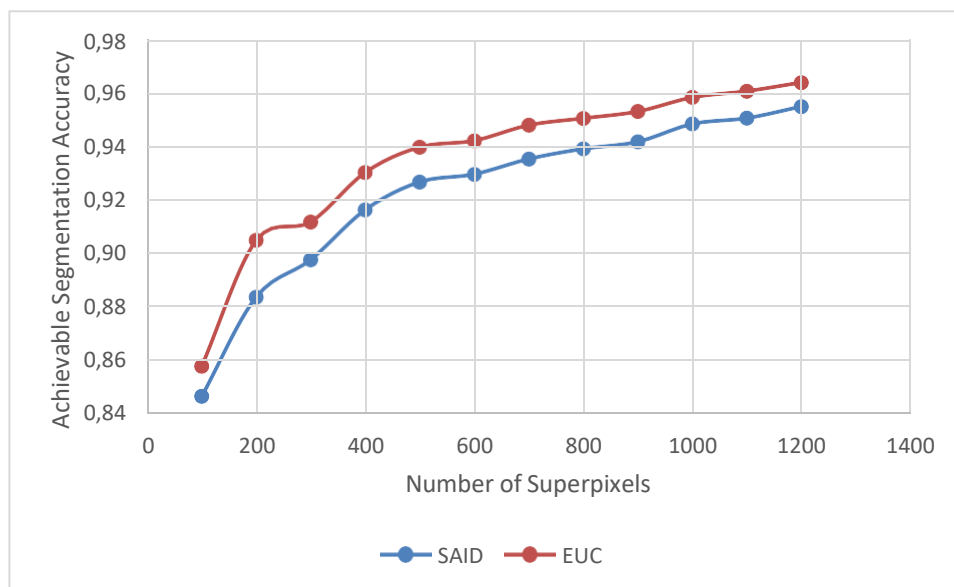


Figure 4.34b: Achievable segmentation accuracy against the number of superpixels for Centred object images with irregular compactness

A further experiment was considered for images with low contrast considering the regular compactness. The result presented in Figures 4.35a depicts that SAID and Euclidean distance performed equally. However, as shown in Figures 4.35b, the Euclidean distance outperformed the SAID with irregular compactness for the ASA performance metrics.

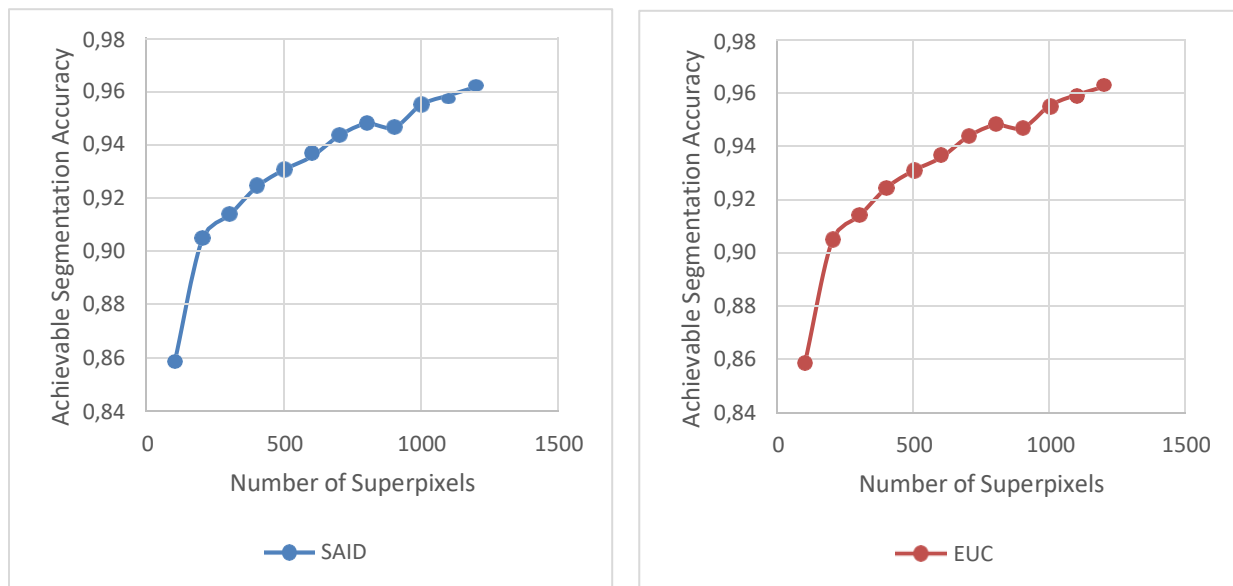


Figure 4.35a: Achievable segmentation accuracy against the number of superpixels for low contrast images with regular compactness

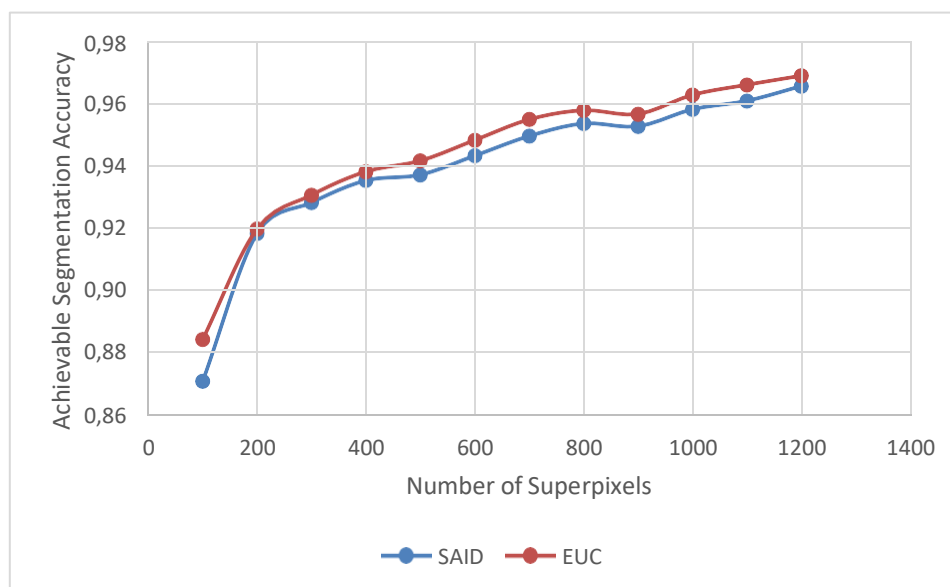


Figure 4.35b: Achievable segmentation accuracy against the number of superpixels for low contrast images with regular compactness

For images with overlapping, multiple, complex, centre, and low contrast images, SAID and Euclidean distance has comparable compactness metric values, as shown in Figures 4.36a to 4.40b. However, boundary adherence is a trade-off for Euclidean distance compactness.

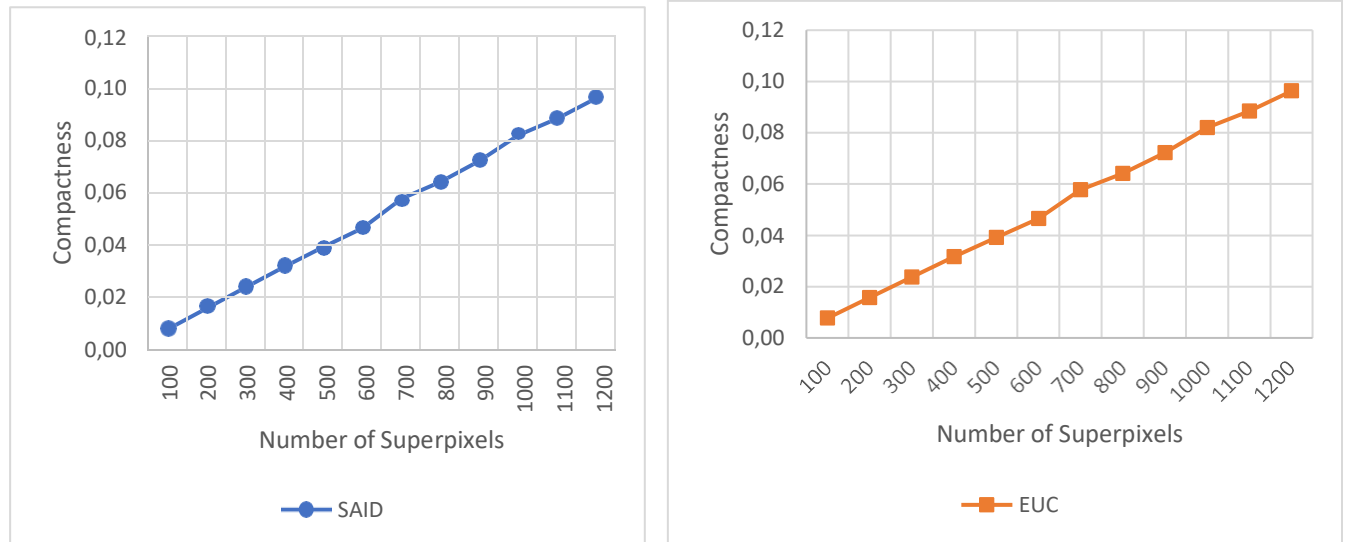


Figure 4.36a: Compactness against the number of superpixels for overlapping images with regular compactness

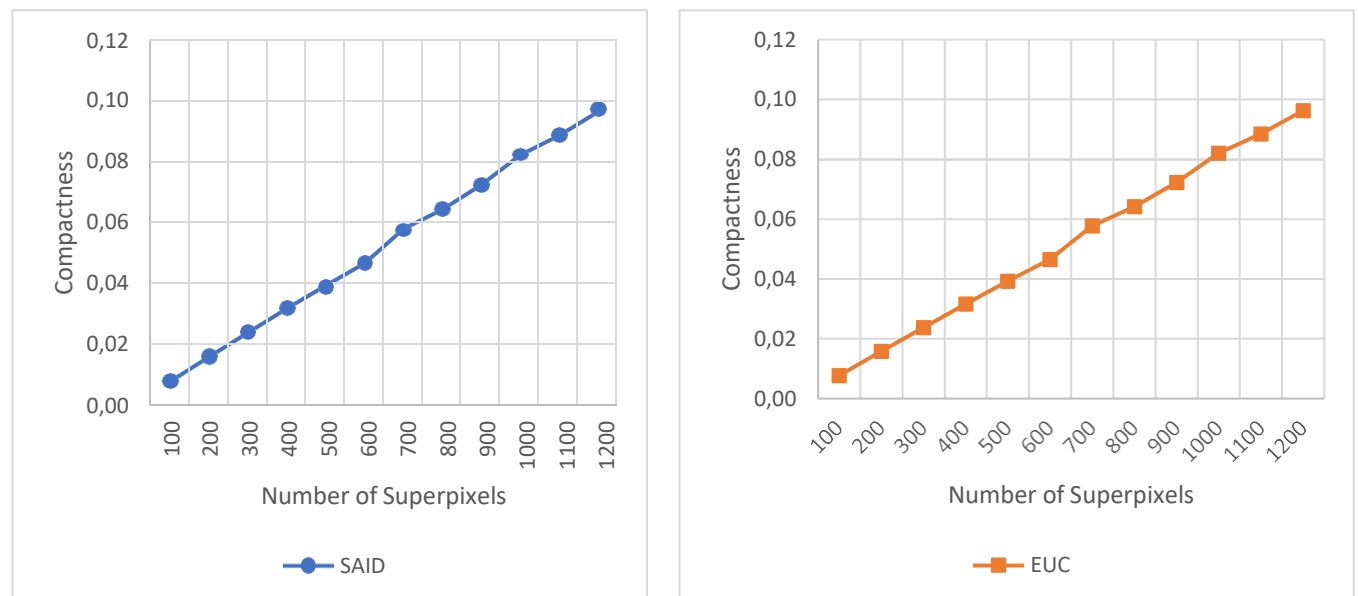


Figure 4.36b: Compactness against the number of superpixels for overlapping images with irregular compactness

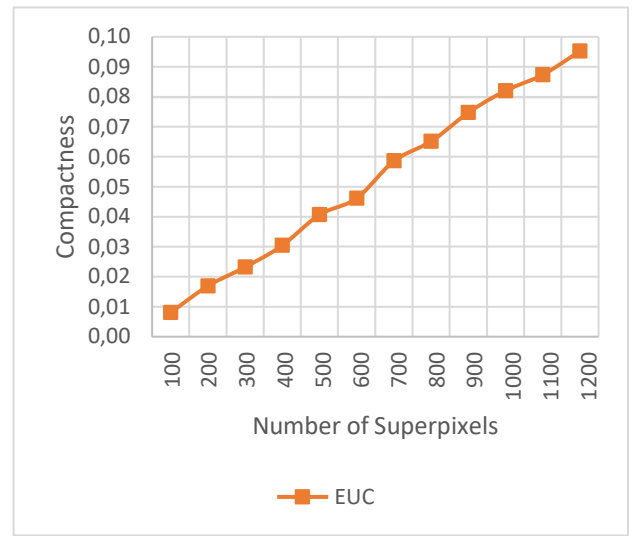
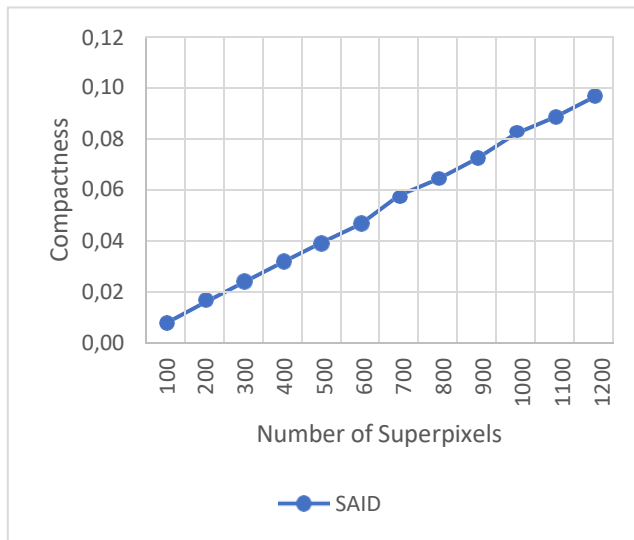


Figure 4.37a: Compactness against the number of superpixels for complex images with regular compactness

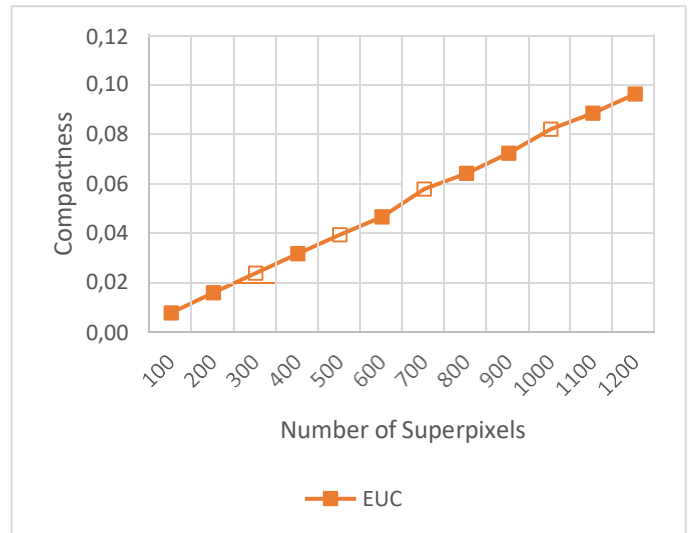
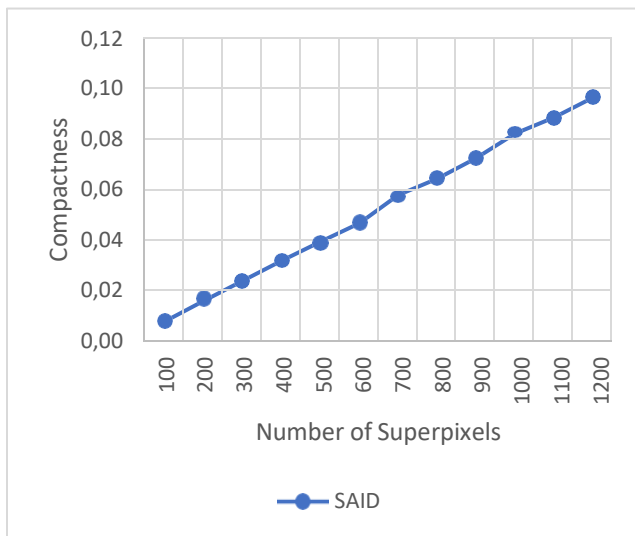


Figure 4.37b: Compactness against the number of superpixels for complex images with irregular compactness

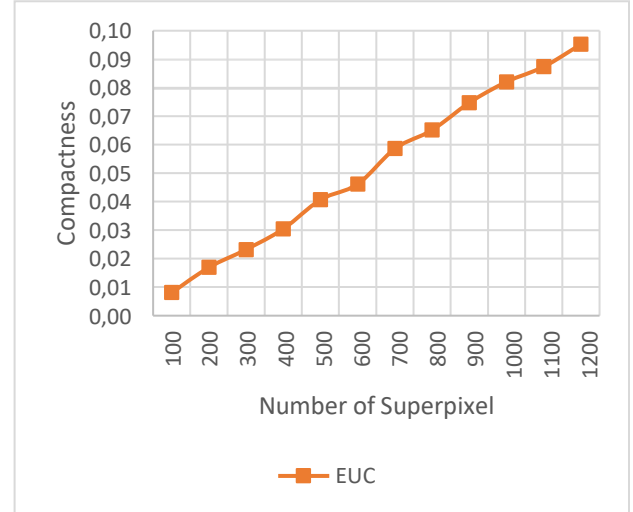
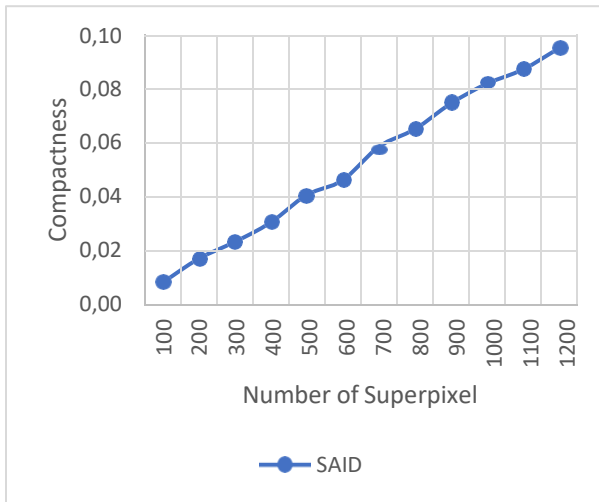


Figure 4.38a: Compactness against the number of superpixels for multiple object images with regular compactness

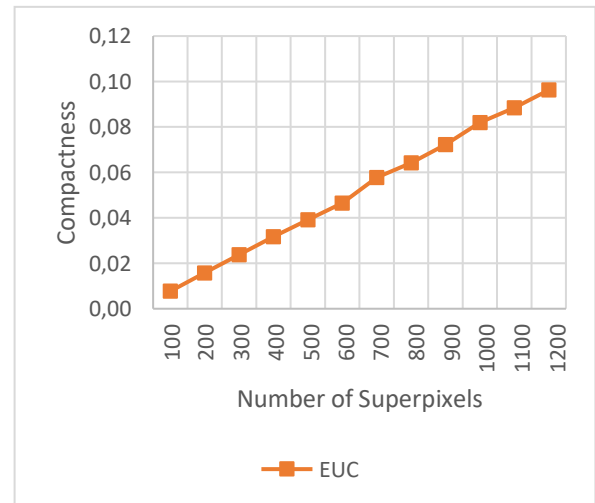
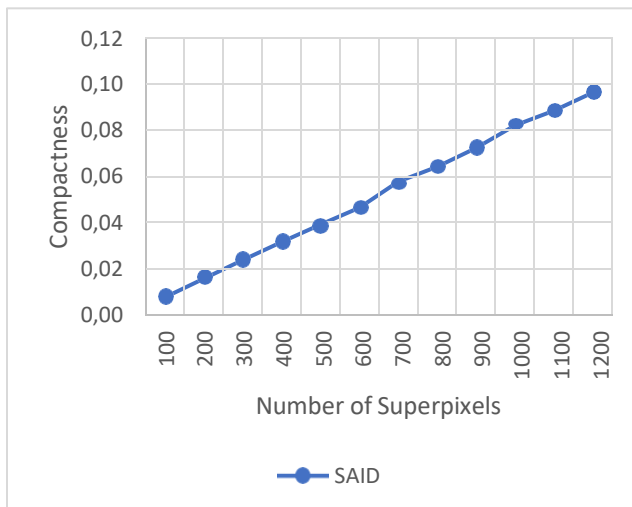


Figure 4.38b: Compactness against the number of superpixels for multiple object images with irregular compactness

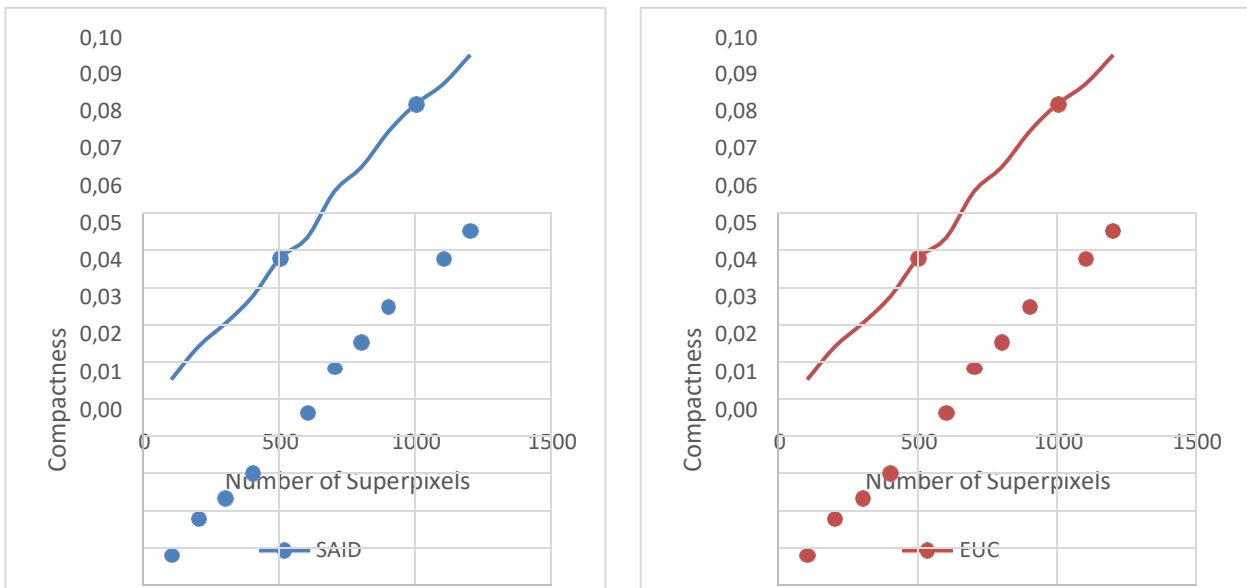


Figure 4.39a: Compactness against the number of superpixels for Centred object images with regular compactness

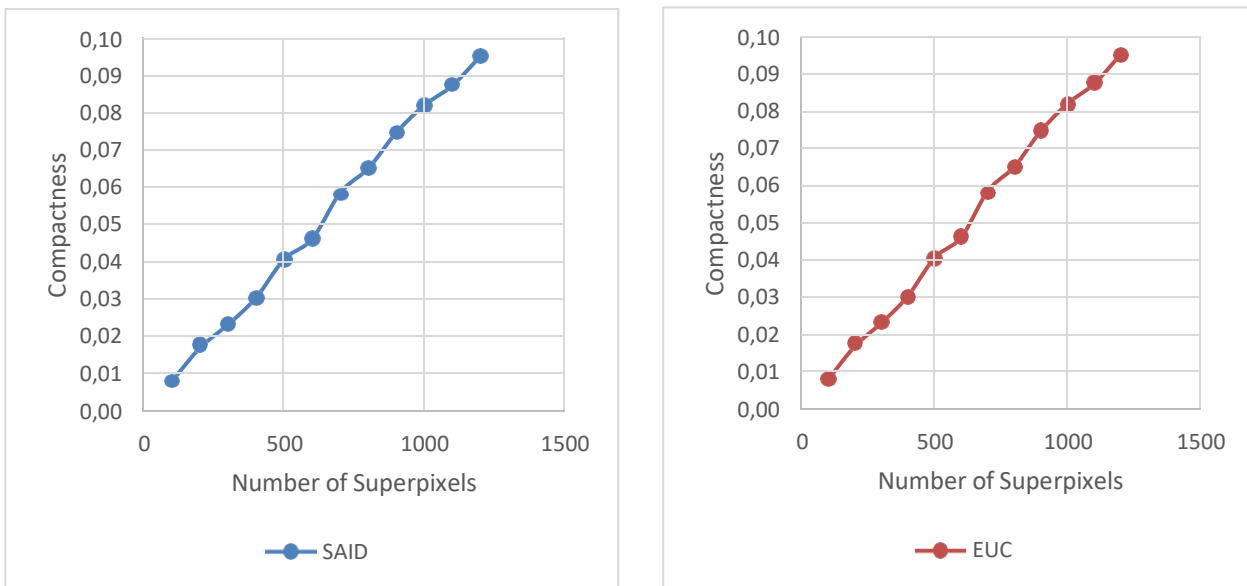


Figure 4.39b: Compactness against the number of superpixels for Centred object images with irregular compactness

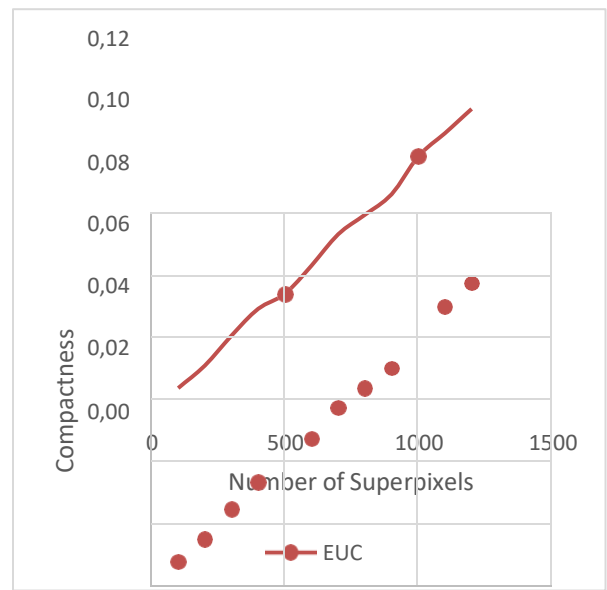
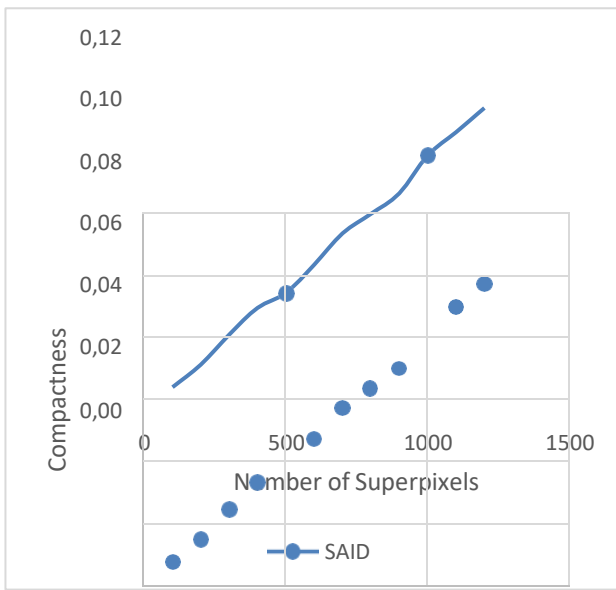


Figure 4.40a: Compactness against the number of superpixels for low contrast images with regular compactness

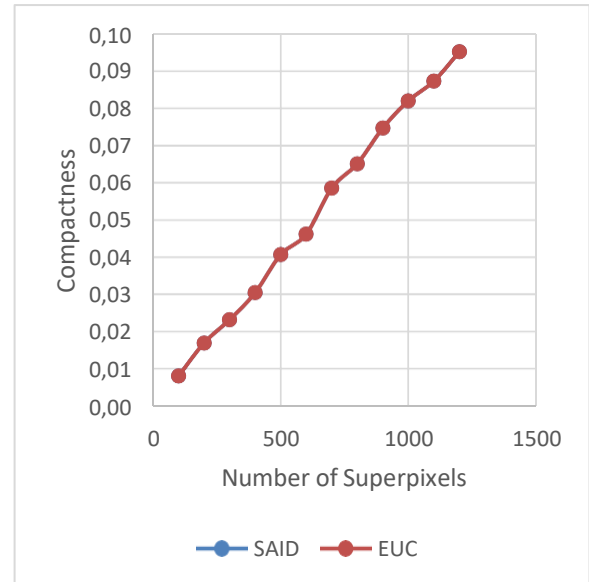
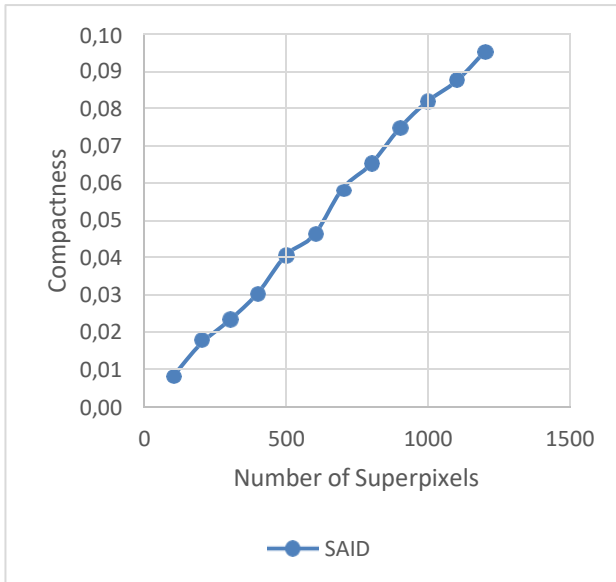


Figure 4.40b: Compactness against the number of superpixels for low contrast images with irregular compactness

With regular compactness, Euclidean offers a slightly higher boundary recall than SAID, as illustrated in Figures 4.41a to 4.45b. It is worth noting, though, that Euclidean's superpixels do not have to be compact, allowing it to better catch the borders of thin, non-compact regions

(Levinshtein et al., 2009).

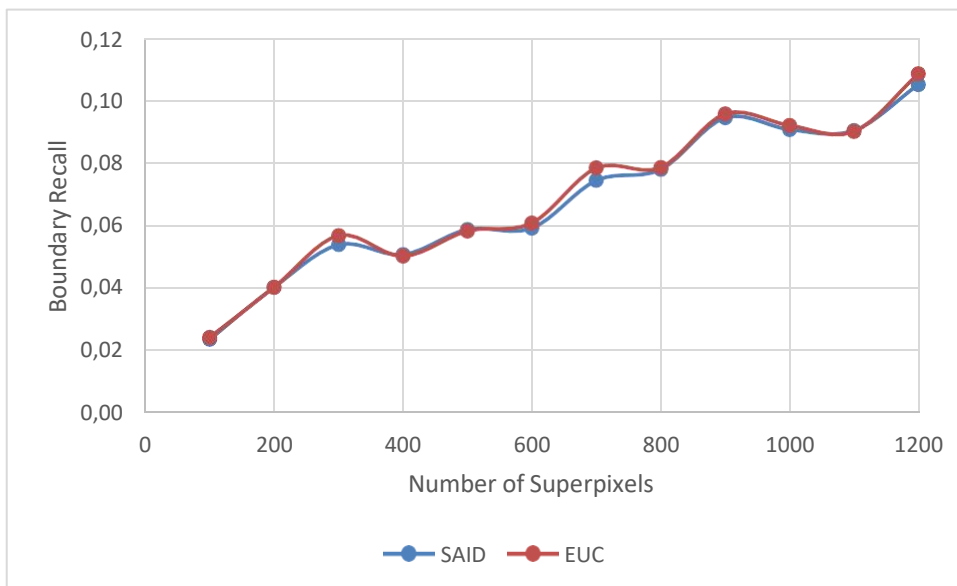


Figure 4.41a: Boundary recall against the number of superpixels for overlapping images with regular compactness

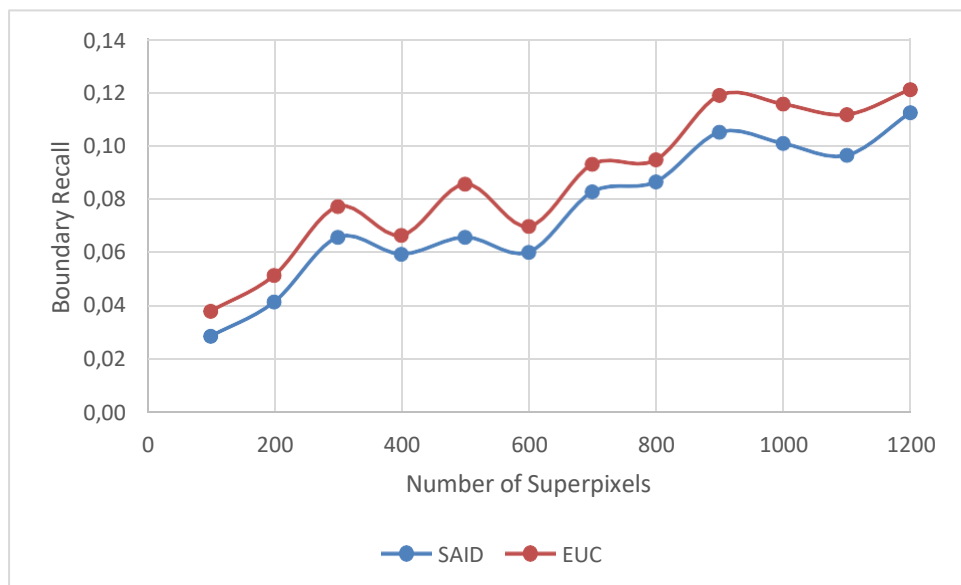


Figure 4.41b: Boundary recall against the number of superpixels for overlapping images with irregular compactness

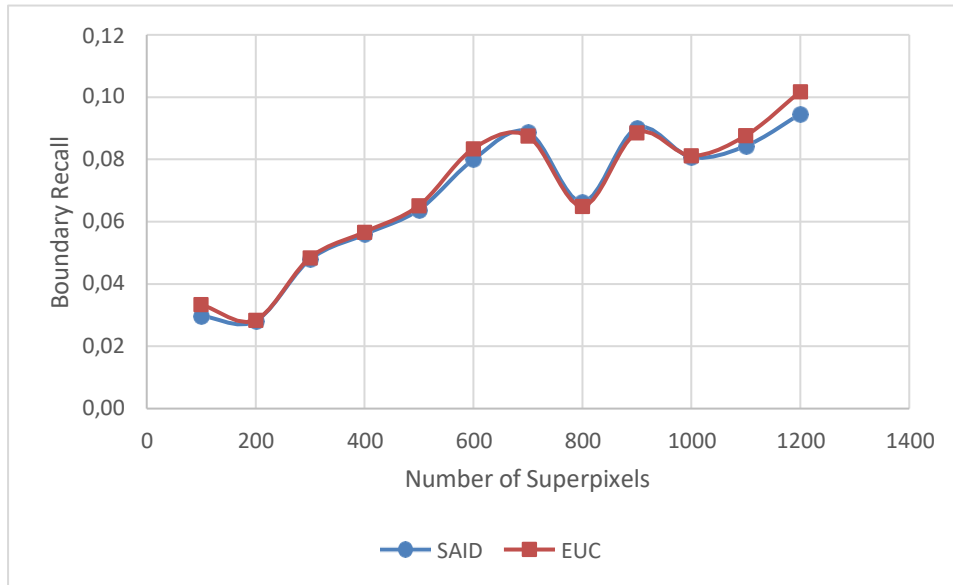


Figure 4.42a: Boundary recall against the number of superpixels for complex images with regular compactness

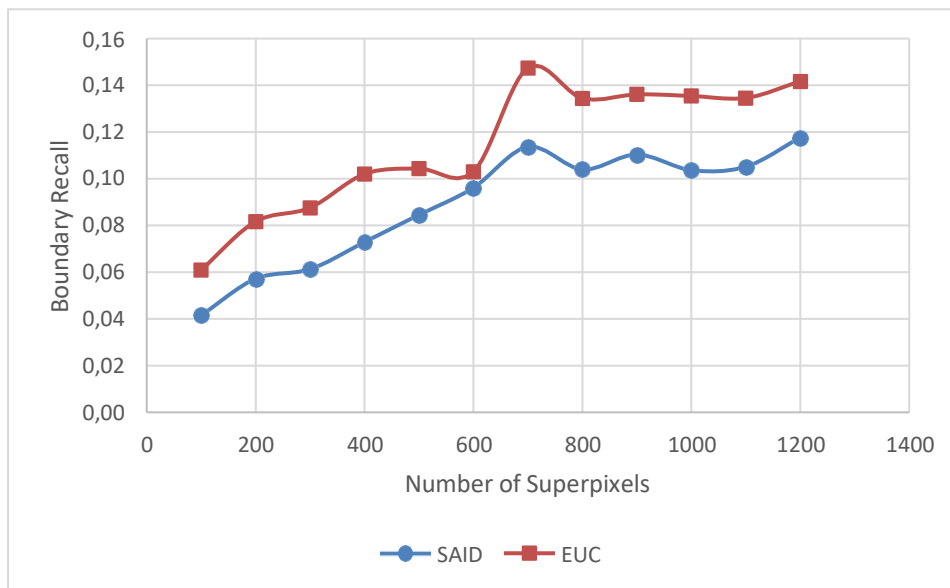


Figure 4.42b: Boundary recall against the number of superpixels for complex images with irregular compactness

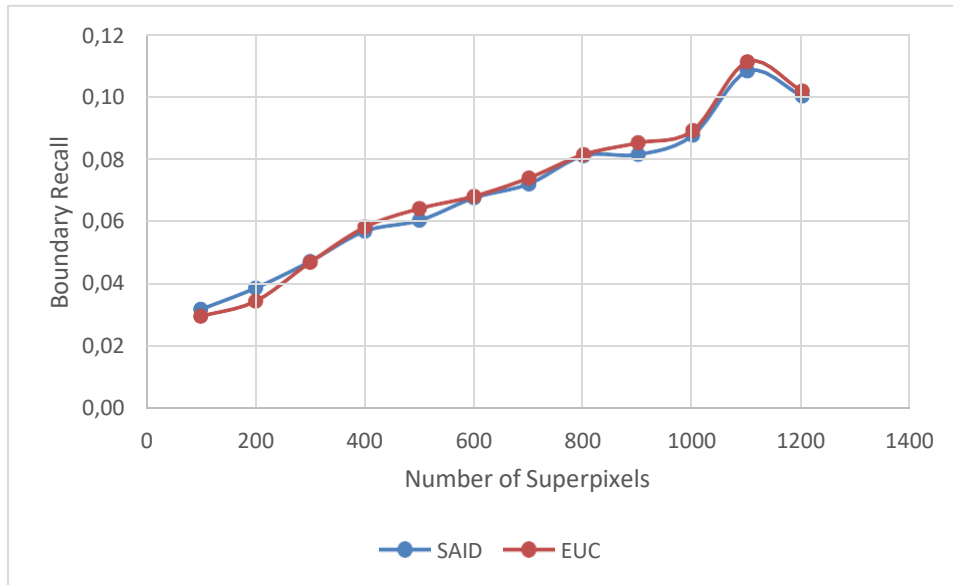


Figure 4.43a: Boundary recall against the number of superpixels for multiple object images with regular compactness

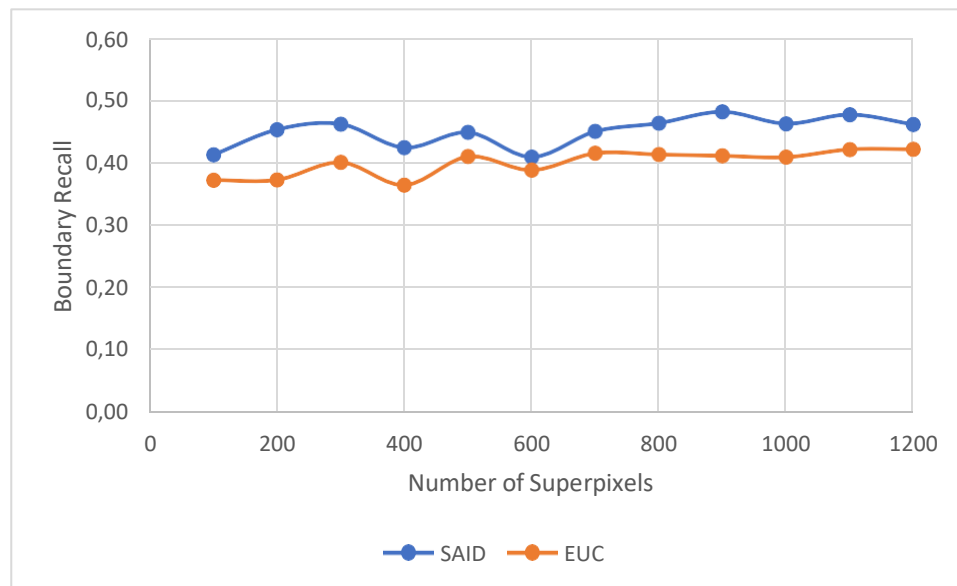


Figure 4.43b: Boundary recall against the number of superpixels for multiple object images with irregular compactness

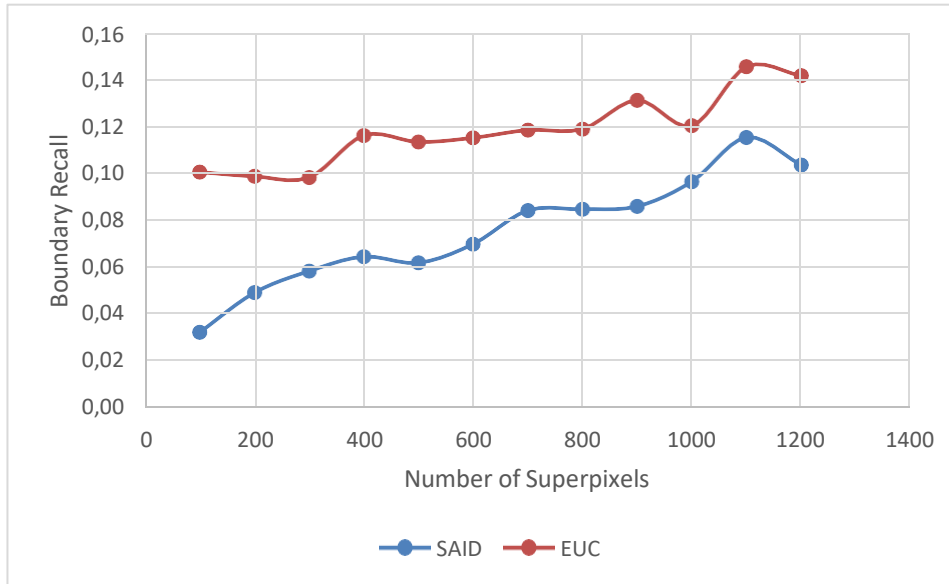


Figure 4.44a: Boundary recall against the number of superpixels for Centred object images with regular compactness

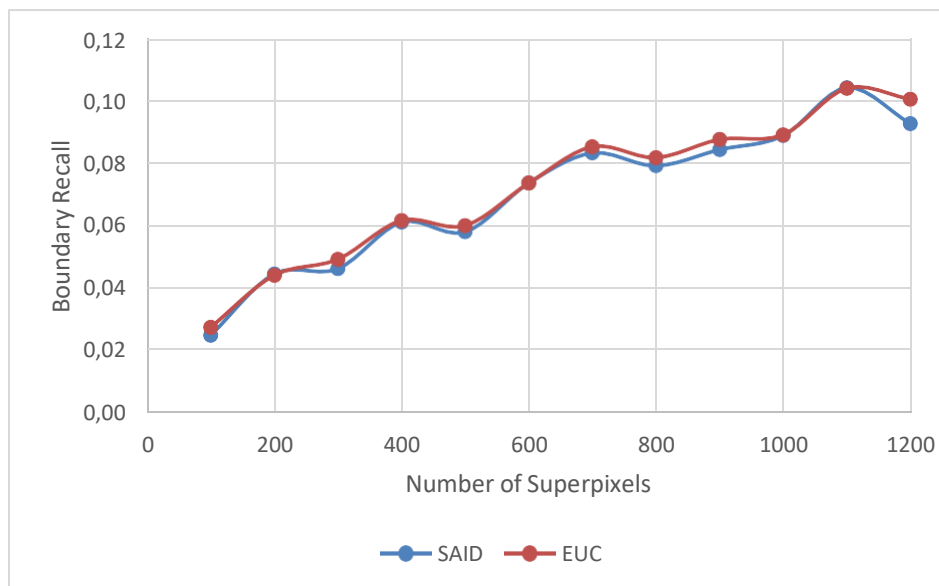


Figure 4.44b: Boundary recall against the number of superpixels for Centred object images with irregular compactness

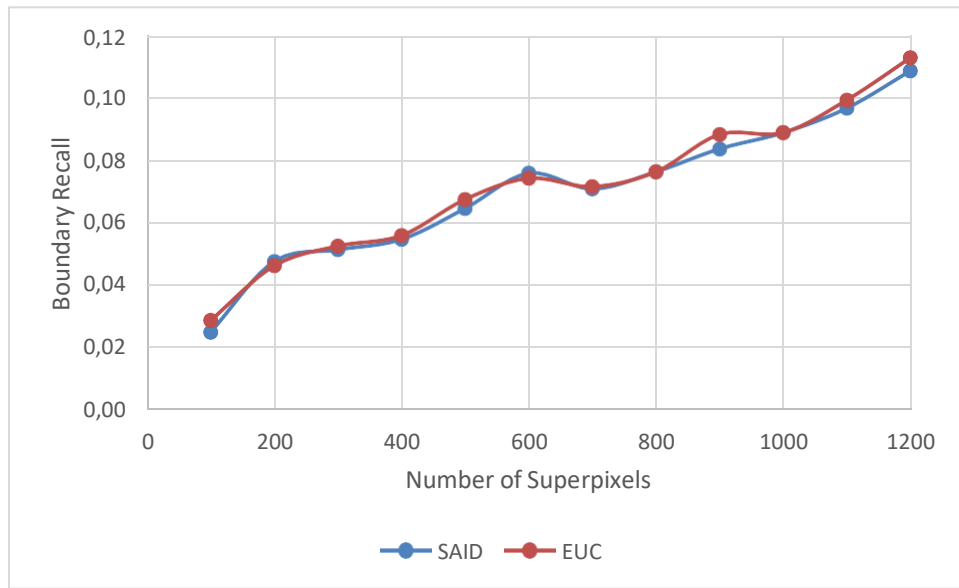


Figure 4.45a: Boundary recall against the number of superpixels for low contrast images with regular compactness

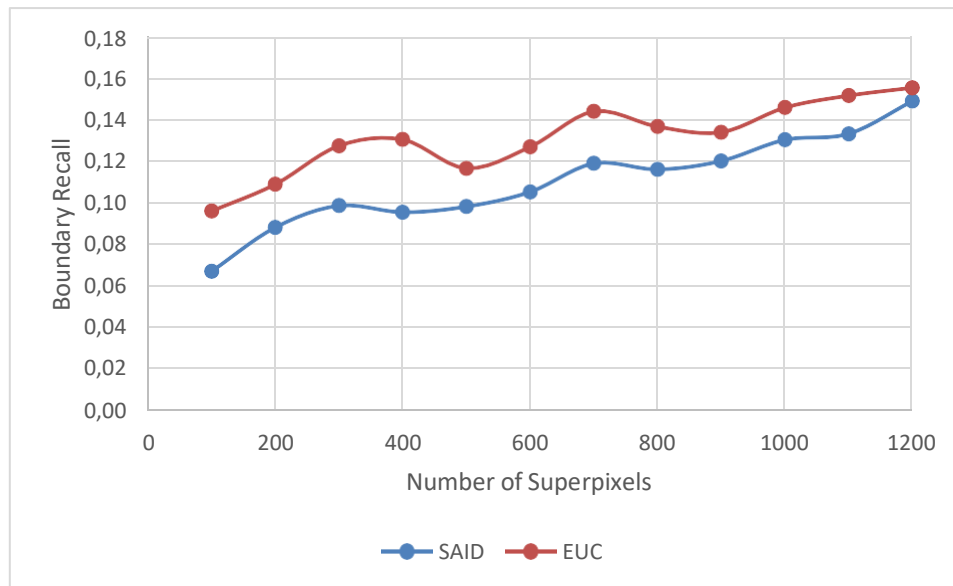


Figure 4.45b: Boundary recall against the number of superpixels for low contrast images with irregular compactness

Figures 4.46a to 4.50b shows that the contour density of EUC is more stable and outperformed SAID for the given number of superpixels, that is 100 to 1200 for both regular and irregular compactness when segmenting images with overlapping, multiple, complex, Centred and low

contrast objects.

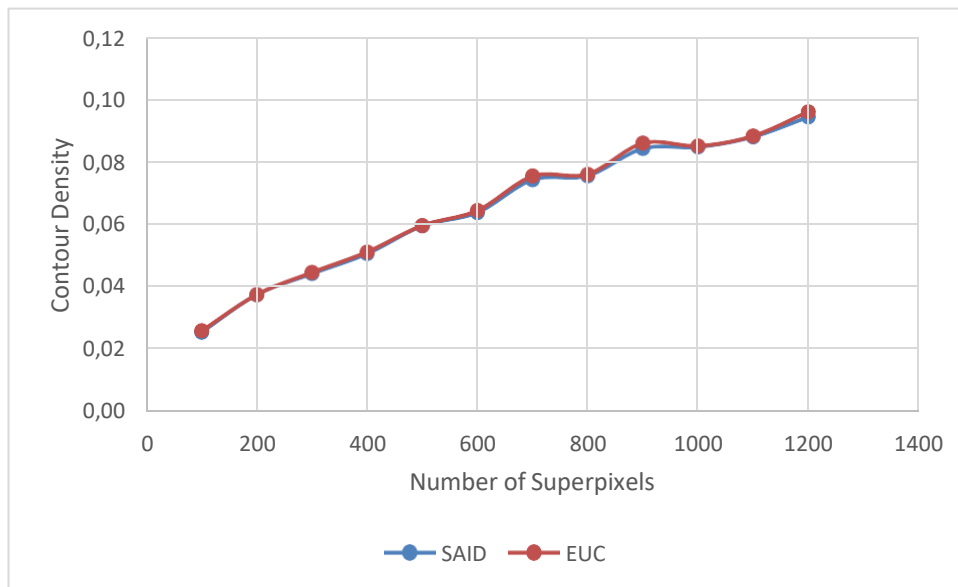


Figure 4.46a: Contour density against the number of superpixels for overlapping images with regular compactness

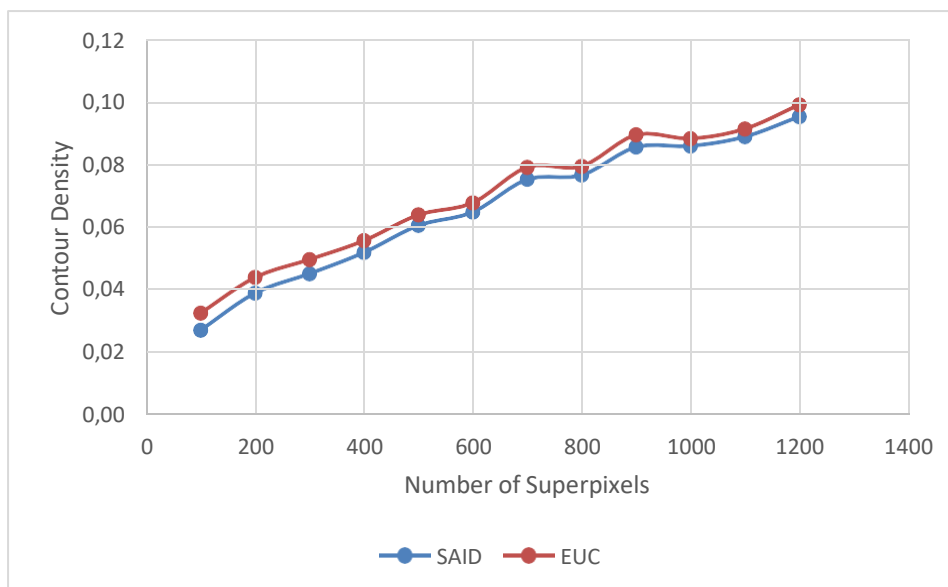


Figure 4.46b: Contour density against the number of superpixels for overlapping images with irregular compactness

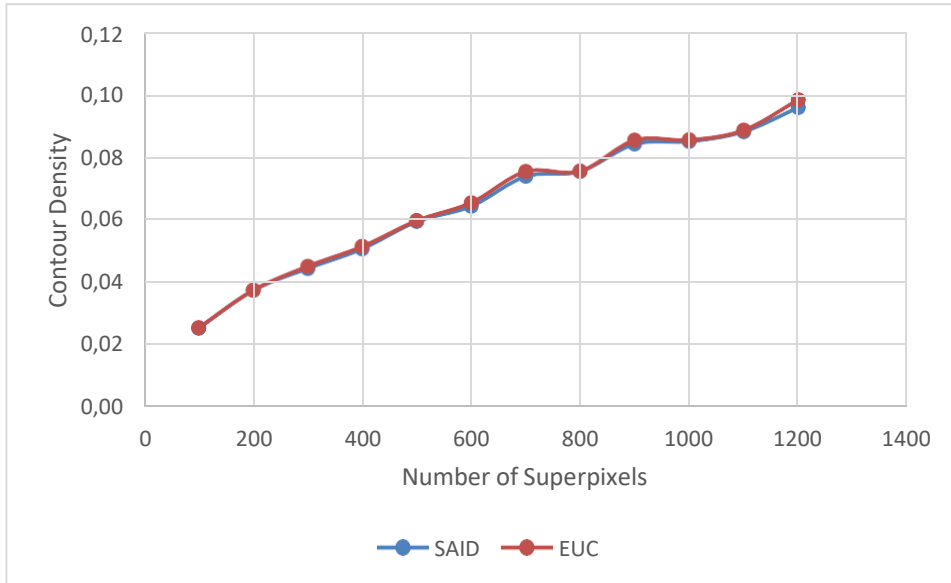


Figure 4.47a: Contour density against the number of superpixels for complex images with regular compactness

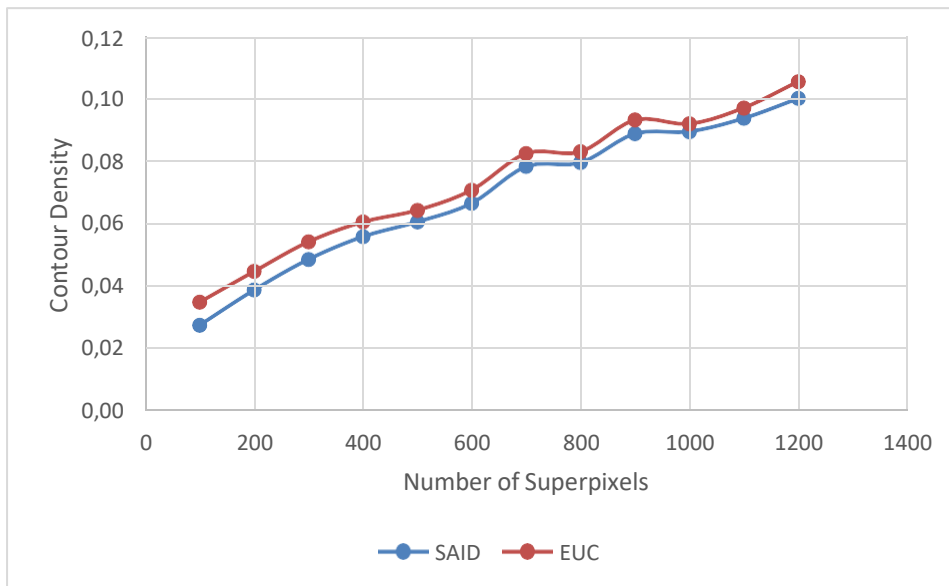


Figure 4.47b: Contour density against the number of superpixels for complex images with irregular compactness

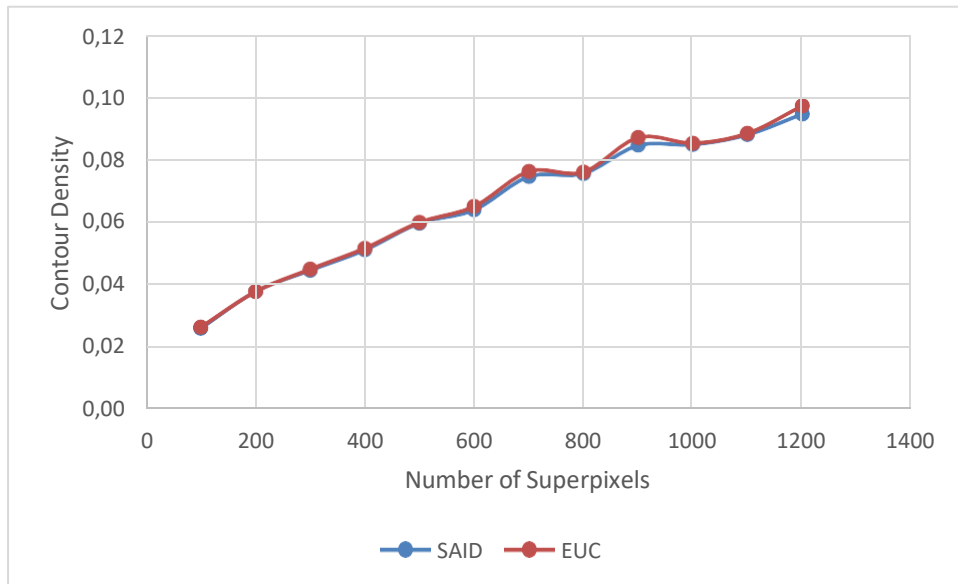


Figure 4.48a: Contour density against the number of superpixels for multiple object images with regular compactness

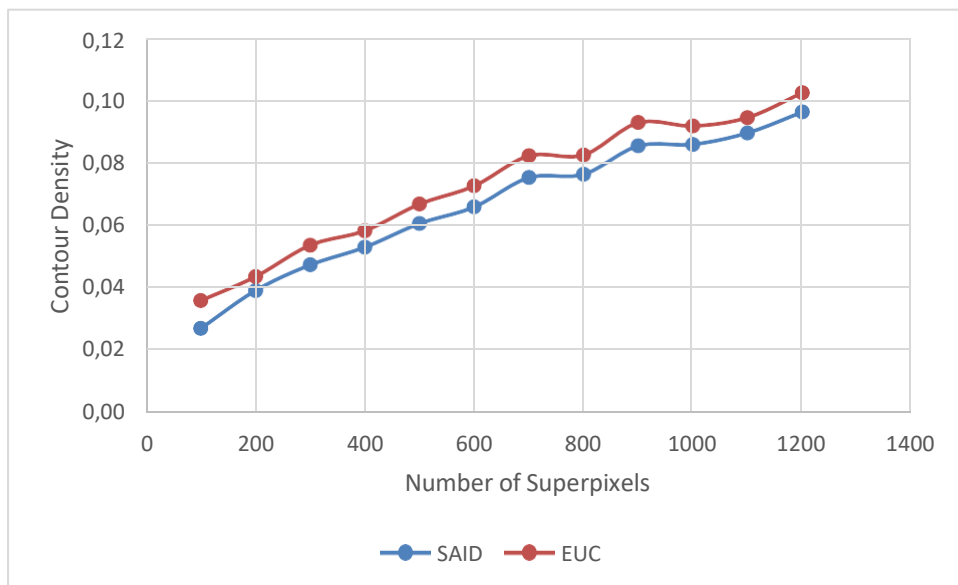


Figure 4.48b: Contour density against the number of superpixels for multiple object images with irregular compactness

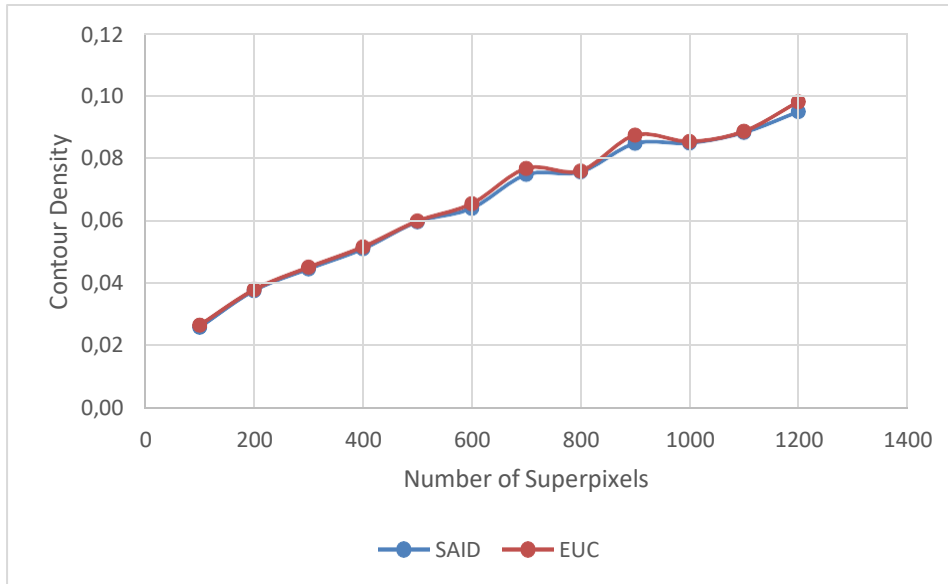


Figure 4.49a: Contour density against the number of superpixels for Centred object images with regular compactness

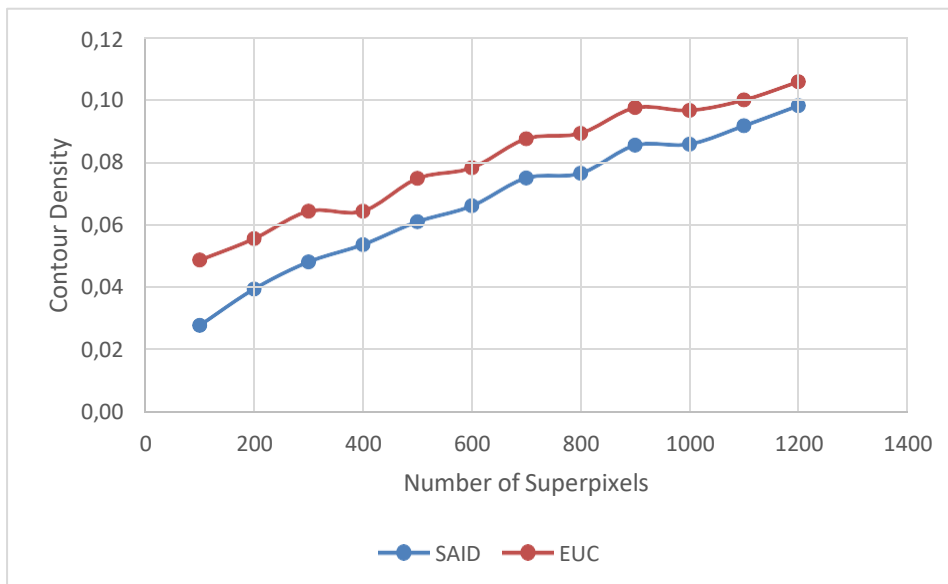


Figure 4.49b: Contour density against the number of superpixels for Centred object images with irregular compactness

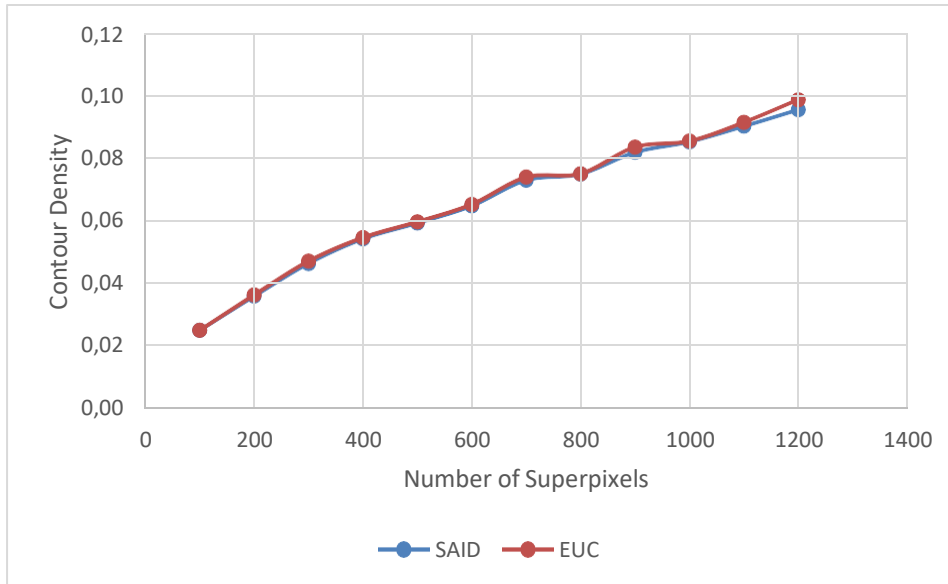


Figure 4.50a: Contour density against the number of superpixels for low contrast images with regular compactness

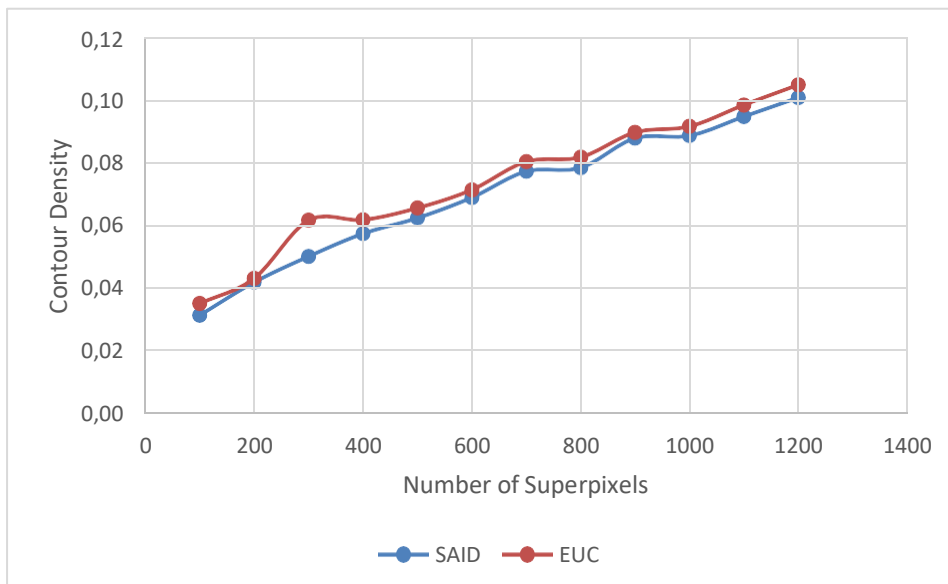


Figure 4.50b: Contour density against the number of superpixels for low contrast images with irregular compactness

4.5 Chapter Summary

Chapter four examines the variants of the selected superpixel segmentation algorithm. This chapter presents the examination of experiments, their outcomes, and their related interpretations to realize the third goal of the study. The chapter begins with a discussion of performance evaluation. Furthermore, the qualitative analysis of the superpixel image result is presented for the animal, human, object categories. The variants of the selected superpixel segmentation algorithm performance are then evaluated using quantitative analysis using well-known performance evaluation indicators.

CHAPTER FIVE

SUMMARY AND CONCLUSIONS

This chapter reflects on the entire study summarizing the work completed, identifying the research gap and reports on the exceptional contributions of this study. The thesis concludes with possible research recommendations and future developments based on this study.

5.1 Summary

The overall goal of this research was to test a new saliency segmentation algorithm to increase the effectiveness of the perceptual colour difference saliency approach and colour picture segmentation performance. The research goal has been met to achieve the following objectives.

1. To comprehensively review the relevant primary studies based on the existing superpixel image segmentation algorithms.

The first objective comprehensively reviewed relevant publications based on superpixel segmentation algorithms which are presented in Chapter two of this study. Chapter two presented a comprehensive review of literature which is divided into eight sections beginning with the first presenting the digital image segmentation setting and going on to present the non-superpixel image segmentation which includes edge-based and region-based image segmentation while the third section emphasized superpixel segmentation. The fourth section presents statistical data analysis through meta-analysis to guide us in the best approach for image segmentation based on literature. The fifth and sixth section discusses the clustering algorithms and distance measure for image segmentation. The seventh section discusses colour models and finally, the last section presents the performance evaluation that will be used in measuring the performance of the variants of the selected superpixel segmentation algorithm across two colour models.

2. To experiment with the variants of a selected superpixel image segmentation algorithm realised by utilising the strong attribute concurrence influence distance and Euclidean distance in two colour models.

The Matlab programming environment was used to implement the variants of the selected superpixel image segmentation algorithm that were used to experiment with a sample of images collected from the Berkeley 500 dataset. The images presented complicated backgrounds. These included the following categories of images Human, Animal and Objects. The variants of the superpixel image segmentation algorithms incorporated the selected SLIC algorithm that performed local clustering of pixels in the 5-D space defined by L, a, b values of the CIELAB colour model with SAID to address the gap and produced high-quality compact superpixels.

3. To compare the performances of variants of the selected superpixel segmentation algorithm based on the standard superpixel evaluation measures.

A quantitative performance evaluation was completed using under-segmentation error, Achievable segmentation accuracy, compactness, boundary recall and contour density with under-segmentation error as a vital metric that reveals errors made by an algorithm while segmenting. The use of SAID in the perceptual colour segmentation algorithm gave a better performance when compared with SLIC with Euclidean distance measure for overlapping and complex images with regular compactness while considering under segmentation algorithm achievable segmentation accuracy and contour density. However, for boundary recall, the perceptual colour segmentation algorithm outperformed SLIC for overlapping and complex images with irregular compactness. Although looking at the superpixel segmented images perceptually the variants of the selected superpixel segmentation algorithm seems to outperform SLIC however while evaluating quantitatively the compactness of the variants of the selected superpixel segmentation algorithm and SLIC are the same.

5.2 Future Work

Despite significant progress in the field of superpixel image segmentation, there is always room for improvement in the field of image processing as a whole. The researcher outlines a few of the many exciting future work that will provide numerous applications and extensions using the preliminary version of the suggested perceptual colour superpixel algorithm in this study. The following studies, in the opinion of the researcher, are worth continuing.

1. The variants of the selected superpixel segmentation algorithm can be extended by trying a different variation of distance measures to improve the compactness of superpixel image segmentation.
2. The variants of the selected superpixel segmentation algorithm can also be validated on more challenging application areas such as video images.
3. The computational cost of the variants of the selected superpixel segmentation algorithm can also be improved.

5.3 Conclusion

This study has presented superpixel compactness of perceptual colour difference segmentation for digital images which is aimed to investigate the performance of an attribute concurrence influence distance metric on image compactness in a superpixel segmentation algorithm. The SAID distance measure was benchmarked with the Euclidean distance measure as distance metrics in the selected superpixel segmentation algorithm using the BSD500 dataset across two colour models of LAB and HSV. The experiment used LAB and HSV colour models. The results presented for the LAB colour model concluded that SAID outperformed Euclidean distance for images with overlapping and complex objects with regular compactness across the under segmentation error, achievable segmentation accuracy and contour density performance evaluation metrics except for boundary recall. However, Euclidean distance performed better than SAID for images with multiple, Centred and low contrast objects with regular compactness across the under segmentation error, achievable segmentation accuracy, boundary recall and contour density performance evaluation metrics. Consequently, for irregular compactness SAID further outperformed Euclidean distance for images with overlapping, complex, multiple, Centred and low contrast objects for boundary recall performance evaluation metrics, however, for under segmentation error, achievable segmentation

accuracy and contour density Euclidean distance performed better than SAID. Furthermore, the compactness performance metrics for SAID and Euclidean distance gave the same compactness value for both regular and irregular compactness.

Consequently, based on the result analysis for the HSV colour model SAID and Euclidean distance performance with regular compactness was at par across all the performance evaluation metrics used for images with overlapping, complex, multiple, centred and low contrast objects. However Euclidean distance outperformed SAID with irregular compactness for images with overlapping, complex, multiple, centred and low contrast objects. Finally, while several algorithms have acceptable under segmentation error and boundary recall, they lack control over the number of superpixels and a compactness parameter. As a result of this research, variants of the selected superpixel segmentation algorithm has been experimented with and presented as an alternative to the well-known SLIC superpixel segmentation techniques.

REFERENCES

- Abdulrahman, S.A., Khalifa, W., Roushdy, M. and Salem, A.B.M., 2020. Comparative study for 8 computational intelligence algorithms for human identification. *Computer Science Review*, 36, p.100237.
- Achanta, R., Shaji, A., Smith, K., Lucchi, A., Fua, P. and Süsstrunk, S., 2010. *Slic superpixels*. Available: https://www.iro.umontreal.ca/~mignotte/IFT6150/Articles/SLIC_Superpixels.pdf (Accessed 10 January 2021).
- Achanta, R., Shaji, A., Smith, K., Lucchi, A., Fua, P. and Süsstrunk, S., 2012. SLIC superpixels compared to state-of-the-art superpixel methods. *IEEE Transactions on Pattern Analysis and Machine Intelligence*, 34(11): 2274-2282.
- Acharjya, P.P. and Ghoshal, D., 2012. Watershed segmentation based on distance transform and edge detection techniques. *International Journal of Computer Applications*, 52(13).
- Adetiba, E. and Olugbara, O. O. 2015. Improved classification of lung cancer using radial basis function neural network with affine transforms of Voss representation. *PloS One*, 10 (12): e0143542.
- Ahn, E., Bi, L., Jung, Y.H., Kim, J., Li, C., Fulham, M. and Feng, D.D., 2015, August. Automated saliency-based lesion segmentation in dermoscopic images. In 2015 37th annual international conference of the IEEE Engineering in Medicine and Biology Society (EMBC) (pp. 3009-3012). IEEE.
- Ahn, E., Kim, J., Bi, L., Kumar, A., Li, C., Fulham, M. and Feng, D. D., 2017. Saliency-based lesion segmentation via background detection in dermoscopic images. *IEEE Journal of Biomedical and Health Informatics*, 21(6): 1685-1693.
- Ajala Funmilola, A., Oke, O.A., Adedeji, T.O., Alade, O.M. and Adewusi, E.A., 2012. Fuzzy kc-means clustering algorithm for medical image segmentation. *Journal of Information Engineering and Applications*, 2(6): 21-32.
- Al-Amri, S.S., Kalyankar, N.V. and Khamitkar, S.D., 2010. Image segmentation by using edge detection. *International Journal on Computer Science and Engineering*, 2(3): 804- 807.
- Alexe, Bogdan, Thomas Deselaers, and Vittorio Ferrari. "What is an object?." 2010 IEEE Computer Society Conference on Computer Vision and Pattern Recognition. IEEE.
- Alias, M.S.A., Ibrahim, N. and Zin, Z.M., 2019. Comparative study of machine learning algorithms and correlation between input parameters. *International Journal of Integrated Engineering*, 11(4): 81-90.
- AlQadi, Z. and Hussein, M.E., 2017. Window averaging method to create a feature vector for RGB colour image. *International Journal of Computer Science and Mobile Computing*, 6(2): 60-66.
- Al-Sbou, Y. 2020. Minkowski distance as quality of service assessment tool. *International Journal of Engineering Research and Technology*, 13(5): 947-952. Available: DOI:10.37624/IJERT/13.5.2020.947-952 (Accessed 21 February 2021).

- Al-Tairi, Z.H., Rahmat, R.W., Saripan, M.I. and Sulaiman, P.S., 2014. Skin segmentation using YUV and RGB colour spaces. *Journal of Information Processing Systems*, 10(2): 283-299.
- Arbelaez, P., Maire, M., Fowlkes, C. and Malik, J., 2010. Contour detection and hierarchical image segmentation. *IEEE Transactions on Pattern Analysis and Machine Intelligence*, 33(5): 898-916.
- Bai, C., Chen, J.N., Huang, L., Kpalma, K. and Chen, S., 2018. Saliency-based multi- feature modeling for semantic image retrieval. *Journal of Visual Communication and Image Representation*, 50: 199-204.
- Baldevbhai, P.J. and Anand, R.S., 2012. Colour image segmentation for medical images using $L^* a^* b^*$ colour space. *IOSR Journal of Electronics and Communication Engineering*, 1(2):.24-45.
- Basilio, J.A.M., Torres, G.A., Perez, G.S., Medina, L.K.T. and Meana, H.M.P., 2011. Explicit image detection using YCbCr space colour model as skin detection. *Applications of Mathematics and Computer Engineering*, 123-128.
- Berrendero, J.R., Bueno-Larraz, B. and Cuevas, A., 2020. On Mahalanobis Distance in Functional Settings. *Journal of Machine Learning Research*, 21: 9-1.
- Bianco, G., Muzzupappa, M., Bruno, F., Garcia, R. and Neumann, L., 2015. A new colour correction method for underwater imaging. *The International Archives of Photogrammetry, Remote Sensing and Spatial Information Sciences*, 40(5): 25.
- Bora, D.J. and Gupta, A.K., 2014. A new approach towards clustering based colour image segmentation. *International Journal of Computer Applications*, 107(12): 23-30.
- Bora, D.J., Gupta, A.K. and Khan, F.A., 2015. Comparing the performance of $L^* A^* B^*$ and HSV colour spaces with respect to colour image segmentation. arXiv preprint arXiv:1506.01472.
- Borel-Donohue, C. and Young, S.S., 2019. Image quality and super resolution effects on object recognition using deep neural networks. In: *Artificial Intelligence and Machine Learning for Multi-Domain Operations Applications* (Vol. 11006, p. 110061M). International Society for Optics and Photonics.
- Boykov, Y., Veksler, O. and Zabih, R., 2001. Fast approximate energy minimization via graph cuts. *IEEE Transactions on Pattern Analysis and Machine Intelligence*, 23(11): 1222-1239.
- Bruce, J., Balch, T. and Veloso, M., 2000. Fast and inexpensive colour image segmentation for interactive robots. In *Proceedings. 2000 IEEE/RSJ International Conference on Intelligent Robots and Systems (IROS 2000)(Cat. No. 00CH37113)* (Vol. 3, pp. 2061-2066). IEEE.
- Buciu, I. and Gacsadi, A., 2011. Directional features for automatic tumor classification of mammogram images. *Biomedical Signal Processing and Control*, 6(4): 370-378.
- Bukola, T.T., 2017. *Colour image segmentation using perceptual colour difference saliency algorithm* (Doctoral dissertation).

- Cao, J. and Wu, X., 2017. A novel level set method for image segmentation by combining local and global information. *Journal of Modern Optics*, 64(21): 2399- 2412.
- Cao, K. and Jain, A. K. 2017. Automated Latent Fingerprint Recognition. *arXiv preprint arXiv:1704.01925*.
- Chang, Y.L. and Li, X., 1994. Adaptive image region-growing. *IEEE Transactions on Image Processing*, 3(6): 868-872.
- Chéhikian, A., 1999. Image segmentation by contours and regions cooperation. *Signal Processing*, 78(3): 329-347.
- Chen, G., Hu, T., Guo, X. and Meng, X., 2009. A fast region-based image segmentation based on least square method. In *2009 IEEE International Conference on Systems, Man and Cybernetics* (pp. 972-977). IEEE.
- Chen, G., Weng, Q., Hay, G.J. and He, Y., 2018. Geographic Object-based Image Analysis (GEOBIA): Emerging trends and future opportunities. *GIScience & remote sensing*, 55(2): 159-182.
- Chen, J., Li, Z. and Huang, B., 2017. Linear spectral clustering superpixel. *IEEE Transactions on Image Processing*, 26(7): 3317-3330.
- Cheng, H.D., Jiang, X.H., Sun, Y. and Wang, J., 2001. Colour image segmentation: advances and prospects. *Pattern Recognition*, 34(12): 2259-2281.
- Chikando, A. and Kinser, J., 2005. Optimizing image segmentation using colour model mixtures. In *34th Applied Imagery and Pattern Recognition Workshop (AIPR'05)* (pp. 6-pp). IEEE.
- Cong, L., Ding, S., Wang, L., Zhang, A. and Jia, W., 2018. Image segmentation algorithm based on superpixel clustering. *IET Image Processing*, 12(11): 2030-2035.
- Connolly, C. and Fleiss, T., 1997. A study of efficiency and accuracy in the transformation from RGB to CIELAB colour space. *IEEE Transactions on Image Processing*, 6(7): 1046-1048.
- Deborah, H., Richard, N. and Hardeberg, J.Y., 2015. A comprehensive evaluation of spectral distance functions and metrics for hyperspectral image processing. *IEEE Journal of Selected Topics in Applied Earth Observations and Remote Sensing*, 8(6): 3224- 3234.
- Dehariya, V.K., Shrivastava, S.K. and Jain, R.C., 2010. Clustering of image data set using k-means and fuzzy k-means algorithms. In *2010 International Conference on Computational Intelligence and Communication Networks* (pp. 386-391). IEEE.
- Delmerico, J.A., David, P. and Corso, J.J., 2011. Building facade detection, segmentation, and parameter estimation for mobile robot localization and guidance.
- Deng, H., Wu, J., Zhu, L., Yan, Z. and Yu, L., 2017. Texture edge-guided depth recovery for structured light-based depth sensor. *Multimedia Tools and Applications*, 76(3): 4211-4226.

- DerSimonian, R. and Laird, N., 1986. Meta-analysis in clinical trials. *Controlled clinical trials*, 7(3): 177-188.
- Dhanachandra, N., Manglem, K. and Chanu, Y.J., 2015. Image segmentation using K- means clustering algorithm and subtractive clustering algorithm. *Procedia Computer Science*, 54: 764-771.
- Dhillon, I.S., Guan, Y. and Kulis, B., 2007. Weighted graph cuts without eigenvectors a multilevel approach. *IEEE Transactions on Pattern Analysis and Machine*, 29(11): 1944-1957.
- Dollár, P. and Zitnick, C.L., 2014. Fast edge detection using structured forests. *IEEE Transactions on Pattern Analysis and Machine Intelligence*, 37(8): 1558-1570.
- Dolz, J., Ayed, I.B. and Desrosiers, C., 2017, September. Unbiased shape compactness for segmentation. In International Conference on Medical Image Computing and Computer-Assisted Intervention (pp. 755-763). Springer, Cham.
- Du, M., Wu, X., Chen, W. and Li, Z., 2017. Supervised training and contextually guided salient object detection. *Digital Signal Processing*, 63: 44-55.
- Elen, A. and Avuçlu, E., 2021. Standardized Variable Distances: A distance-based machine learning method. *Applied Soft Computing*, 98, p.106855.
- Faisal, M. and Zamzami, E.M., 2020, June. Comparative Analysis of Inter-Centroid K- Means Performance using Euclidean Distance, Canberra Distance and Manhattan Distance. In *Journal of Physics: Conference Series* (Vol. 1566, No. 1, p. 012112). IOP Publishing.
- Felipe, J.C., Traina, C. and Traina, A.J.M., 2009. A new family of distance functions for perceptual similarity retrieval of medical images. *Journal of Digital Imaging*, 22(2): 183.
- Felzenszwalb, P.F. and Huttenlocher, D.P., 2004. Efficient graph-based image segmentation. *International Journal of Computer Vision*, 59(2): 167-181.
- Forouzanfar, M., Forghani, N. and Teshnehlal, M., 2010. Parameter optimization of improved fuzzy c-means clustering algorithm for brain MR image segmentation. *Engineering Applications of Artificial Intelligence*, 23(2): 160-168.
- Ganesan, P., Rajini, V. and Rajkumar, R.I., 2010, December. Segmentation and edge detection of colour images using CIELAB colour space and edge detectors. In *INTERACT- 2010* (pp. 393-397). IEEE.
- Ganguly, D., Mukherjee, S., Mitra, K. and Mukherjee, P., 2009, March. A novel approach for edge detection of images. In *2009 International Conference on Computer and Automation Engineering* (pp. 49-53). IEEE.
- Ge, Q., Xiao, L., Zhang, J. and Wei, Z.H., 2012. An improved region-based model with local statistical features for image segmentation. *Pattern Recognition*, 45(4):1578- 1590.

- George, E.B. and Karnan, M., 2012. MR brain image segmentation using bacteria foraging optimization algorithm. *International Journal of Engineering and Technology*, 4(5): 295-301.
- Ghorbani, H., 2019. Mahalanobis distance and its application for detecting multivariate outliers. *Facta Univ Ser Math Inform*, 34(3): 583-95.
- Ghosh, P., Mali, K. and Das, S.K., 2018. Use of Spectral Clustering Combined with Normalized Cuts (N-Cuts) in an Iterative k-Means Clustering Framework (NKSC) for Superpixel Segmentation with Contour Adherence. *Pattern Recognition and Image Analysis*, 28(3): 400-409.
- Giordano, D., Murabito, F., Palazzo, S. and Spampinato, C., 2015. Superpixel-based video object segmentation using perceptual organization and location prior. In Proceedings of the IEEE conference on computer vision and pattern recognition (pp. 4814-4822).
- Girshick, R., Donahue, J., Darrell, T. and Malik, J., 2015. Region-based convolutional networks for accurate object detection and segmentation. *IEEE Transactions on Pattern Analysis and Machine Intelligence*, 38(1): 142-158.
- Goferman, S., Zelnik-Manor, L. and Tal, A. 2012. Context-aware saliency detection. *IEEE Transactions on Pattern Analysis and Machine Intelligence*, 34(10): 1915-1926.
- Gong, Y.J. and Zhou, Y., 2017. Differential evolutionary superpixel segmentation. *IEEE Transactions on Image Processing*, 27(3): 1390-1404.
- Gu, X., 2017. *Image segmentation using superpixel ensembles* (Doctoral dissertation, University of Otago).
- Gueorguieva, N., Valova, I. and Georgiev, G., 2017. M&MFCM: fuzzy c-means clustering with Mahalanobis and Minkowski distance metrics. *Procedia Computer Science*, 114: 224-233.
- Gultom, S., Sriadhi, S., Martiano, M. and Simarmata, J., 2018, September. Comparison analysis of K-means and K-medoid with Ecludience distance algorithm, Canberra distance, and Chebyshev distance for big data clustering. In IOP Conference Series: Materials Science and Engineering (Vol. 420, No. 1, p. 012092). IOP Publishing
- Gupta, D. and Anand, R.S., 2017. A hybrid edge-based segmentation approach for ultrasound medical images. *Biomedical Signal Processing and Control*, 31: 116-126.
- Gupta, R.K., Chia, A.Y.S., Rajan, D., Ng, E.S. and Zhiyong, H., 2012, October. Image colourization using similar images. In *Proceedings of the 20th ACM international conference on Multimedia* (pp. 369-378).
- Hahm, G.-J. and Cho, K. 2016. Event-based sports video segmentation using multimodal analysis. In: *Proceedings of Information and Communication Technology Convergence (ICTC), 2016 International Conference on*. IEEE, 1119-1121.

- Hanoun, T.M. and Hashim, K.M., 2019. Modify Manhattan Distance For Image Similarity. *Open Journal of Science and Technology*, 2(4): 12-16.
- Haralick, R.M. and Shapiro, L.G., 1985. Image segmentation techniques. *Computer Vision, Graphics, and Image Processing*, 29(1): 100-132.
- Haralick, R.M. and Shapiro, L.G., 1988. Segmentation and Its Place in Machine Vision. (Retroactive Coverage). *Scanning Microscopy*.
- Higgins, J.P. and Thompson, S.G., 2002. Quantifying heterogeneity in a meta-analysis. *Statistics in Medicine*, 21(11): 1539-1558.
- Hojjatolleslami, S.A. and Kittler, J., 1998. Region growing: a new approach. *IEEE Transactions on Image processing*, 7(7): 1079-1084.
- Hutton, B., Catala-Lopez, F. and Moher, D., 2016. The PRISMA statement extension for systematic reviews incorporating network meta-analysis: PRISMA-NMA. *Med Clin (Barc)*, 147(6): 262-266.
- Ibraheem, N.A., Hasan, M.M., Khan, R.Z. and Mishra, P.K., 2012. Understanding colour models: a review. *ARPJ Journal of Science and Technology*, 2(3): 265-275.
- Isa, N.A.M., Salamah, S.A. and Ngah, U.K., 2009. Adaptive fuzzy moving K-means clustering algorithm for image segmentation. *IEEE Transactions on Consumer Electronics*, 55(4): 2145-2153.
- Jiang, H. and Learned-Miller, E., 2017, May. Face detection with the faster R-CNN. In *2017 12th IEEE International Conference on Automatic Face & Gesture Recognition (FG 2017)* (pp. 650-657). IEEE.
- Kaiser, M. S., Lwin, K. T., Mahmud, M., Hajializadeh, D., Chaipimonplin, T., Sarhan, A. and Hossain, M. A. 2017. Advances in crowd analysis for urban applications through urban event detection. *IEEE Transactions on Intelligent Transportation Systems*.
- Kakhani, N., Mokhtarzade, M. and Zouj, M.J.V., 2019. Classification of very high- resolution remote sensing images by applying a new edge-based marker-controlled watershed segmentation method. *Signal, Image and Video Processing*, 13(7): 1319- 1327.
- Kamalakannan, S., Gururajan, A., Sari-Sarraf, H., Long, R. and Antani, S., 2010. Double- edge detection of radiographic lumbar vertebrae images using pressurized open DGVF snakes. *IEEE Transactions on Biomedical Engineering*, 57(6): 1325-1334.
- Kang, C.C. and Wang, W.J., 2009, June. Fuzzy based seeded region growing for image segmentation. In *NAFIPS 2009-2009 Annual Meeting of the North American Fuzzy Information Processing Society* (pp. 1-5). IEEE.
- Kanwal, K., Liaquat, A., Mughal, M., Abbasi, A.R. and Aamir, M., 2017. Towards development of a low cost early fire detection system using wireless sensor network and machine vision. *Wireless Personal Communications*, 95(2): 475-489.

- Kaur, A. and Kranthi, B.V., 2012. Comparison between YCbCr colour space and CIELab colour space for skin colour segmentation. *International Journal of Applied Information Systems*, 3(4): 30-33.
- Kaur, B. and Garg, A., 2011. Comparative study of different edge detection techniques. *International Journal of Engineering Science and Technology*, 3(3): 1927- 1935.
- Kaur, M. and Goyal, P., 2015. A review on Region-based segmentation. *International Journal of Science and Research (IJSR)*, 4(4): 3194-3197.
- Kaur, R., Juneja, M. and Mandal, A.K., 2019. A hybrid edge-based technique for segmentation of renal lesions in CT images. *Multimedia Tools and Applications*, 78(10): 12917-12937.
- Kavitha, K. and Rao, B.T., 2019. Evaluation of distance measures for feature based image registration using alexnet. *arXiv preprint arXiv:1907.12921*.
- Kavzoglu, T. and Tonbul, H., 2017, June. A comparative study of segmentation quality for multi-resolution segmentation and watershed transform. In *2017 8th International Conference on Recent Advances in Space Technologies (RAST)* (pp. 113-117). IEEE.
- Khadidos, A., Sanchez, V. and Li, C.T., 2017. Weighted level set evolution based on local edge features for medical image segmentation. *IEEE Transactions on Image Processing*, 26(4): 1979-1991.
- Khattab, D., Ebied, H.M., Hussein, A.S. and Tolba, M.F., 2014. Colour image segmentation based on different colour space models using automatic GrabCut. *The Scientific World Journal*, 2014.
- Khattab, D., Ebeid, H.M., Tolba, M.F. and Hussein, A.S., 2016. Clustering-based image segmentation using automatic grabcut. In *Proceedings of the 10th International Conference on Informatics and Systems* (pp. 95-100).
- Kokare, M., Chatterji, B.N. and Biswas, P.K., 2003, October. Comparison of similarity metrics for texture image retrieval. In *TENCON 2003. Conference on convergent technologies for Asia-Pacific region* (Vol. 2, pp. 571-575). IEEE.
- Krishna Prasad, K. and Aithal, P. 2017. Fingerprint Image Segmentation: A Review of State of the Art Techniques.
- Lala, A., Gupta, J.K. and Shringirishi, M., 2013. Implementation on K-means Clustering and Fuzzy C-means Algorithm For Brain Tumor Segmentation. *International Journal of Computer Engineering & Science*, 3(1): 27-33.
- Lalaoui, L. and Mohammadi, T., 2013. A comparative study of image region-based segmentation algorithms. *International Journal of Advanced Computer Science and Applications*, 4(6).
- Lavanya, M. and Kannan, P. M. 2017. Lung Lesion Detection in CT Scan Images Using the Fuzzy Local Information Cluster Means (FLICM) Automatic Segmentation Algorithm and Back Propagation Network Classification. *Asian Pacific Journal of Cancer Prevention*, 18(12): 3395-3399.

- Lei, T., Jia, X., Zhang, Y., Liu, S., Meng, H. and Nandi, A.K., 2018. Superpixel-based fast fuzzy C-means clustering for colour image segmentation. *IEEE Transactions on Fuzzy Systems*, 27(9): 1753-1766.
- Leung, T. and Malik, J., 1998, June. Contour continuity in Region-based image segmentation. In *European Conference on Computer Vision* (pp. 544-559). Springer, Berlin, Heidelberg.
- Levinshtein, A., Stere, A., Kutulakos, K.N., Fleet, D.J., Dickinson, S.J. and Siddiqi, K., 2009. Turbopixels: Fast superpixels using geometric flows. *IEEE Transactions on Pattern Analysis and Machine Intelligence*, 31(12): 2290-2297.
- Leys, C., Klein, O., Dominicy, Y. and Ley, C., 2018. Detecting multivariate outliers: Use a robust variant of the Mahalanobis distance. *Journal of Experimental Social Psychology*, 74: 150-156.
- Li, C., Guo, B., Liao, N., Gong, J., Han, X., Hou, S., Chen, Z. and He, W., 2021. CONIC: Contour Optimized Non-Iterative Clustering Superpixel Segmentation. *Remote Sensing*, 13(6): 1061.
- Li, Z. and Chen, J., 2015. Superpixel segmentation using linear spectral clustering. In *Proceedings of the IEEE Conference on Computer Vision and Pattern Recognition* (pp. 1356-1363).
- Li, Y., Fu, K., Liu, Z. and Yang, J. 2015. Efficient saliency-model-guided visual co- saliency detection. *IEEE Signal Processing Letters*, 22(5): 588-592.
- Li, Y.H., Huang, P.J. and Juan, Y., 2019. An efficient and robust iris segmentation algorithm using deep learning. *Mobile Information Systems*, 2019.
- Lim, J. and Han, B., 2014, September. Generalized background subtraction using superpixels with label integrated motion estimation. In *European Conference on Computer Vision* (pp. 173-187). Springer, Cham.
- Liu, J. and Yang, Y.H., 1994. Multiresolution colour image segmentation. *IEEE Transactions on Pattern Analysis and Machine Intelligence*, 16(7): 689-700.
- Liu, M.Y., Tuzel, O., Ramalingam, S. and Chellappa, R., 2011, June. Entropy rate superpixel segmentation. In *CVPR 2011* (pp. 2097-2104). IEEE.
- Liu, Z., Meur, L. and Luo, S., 2013, July. Superpixel-based saliency detection. In *2013 14th International Workshop on Image Analysis for Multimedia Interactive Services (WIAMIS)* (pp. 1-4). IEEE.
- Liu, X. and Tang, J., 2013. Mass classification in mammograms using selected geometry and texture features, and a new SVM-based feature selection method. *IEEE Systems Journal*, 8(3): 910-920.
- Liu, Y.J., Yu, C.C., Yu, M.J. and He, Y., 2016. Manifold SLIC: A fast method to compute content-sensitive superpixels. In *Proceedings of the IEEE Conference on Computer Vision and Pattern Recognition* (pp. 651-659).

- Lou, J., Qi, L., Dong, J., Yu, H. and Zhong, G., 2016, July. Learning perceptual texture similarity and relative attributes from computational features. In *2016 International Joint Conference on Neural Networks (IJCNN)* (pp. 2540-2546). IEEE.
- Lu, H., Feng, X., Li, X. and Zhang, L., 2013. Superpixel level object recognition under local learning framework. *Neurocomputing*, 120:203-213.
- Lucas, L.F., Rodrigues, N.M., de Faria, S.M., da Silva, E.A., de Carvalho, M.B. and da Silva, V.M., 2010, September. Intra-prediction for colour image coding using YUV correlation. In *2010 IEEE International Conference on Image Processing* (pp. 1329- 1332). IEEE.
- Ma, W.Y. and Manjunath, B.S., 1997, June. Edge flow: a framework of boundary detection and image segmentation. In *Proceedings of IEEE Computer Society Conference on Computer Vision and Pattern Recognition* (pp. 744-749). IEEE.
- Machairas, V., Decencière, E. and Walter, T., 2014, October. Waterpixels: Superpixels based on the watershed transformation. In *2014 IEEE International Conference on Image Processing (ICIP)* (pp. 4343-4347). IEEE.
- Machairas, V., Faessel, M., Cárdenas-Peña, D., Chabardes, T., Walter, T. and Decencière, E., 2015. Waterpixels. *IEEE Transactions on Image Processing*, 24(11): 3707-3716.
- Madhulatha, T.S., 2012. An overview of clustering methods. arXiv preprint arXiv:1205.1117.
- Margolin, R., Tal, A. and Zelnik-Manor, L. 2013. What makes a patch distinct? In: *Proceedings of Computer Vision and Pattern Recognition (CVPR)*, 2013 IEEE Conference on. IEEE, 1139-1146.
- Martin, P., Réfrégier, P., Goudail, F. and Guérault, F., 2004. Influence of the noise model on level set active contour segmentation. *IEEE Transactions on Pattern Analysis and Machine Intelligence*, 26(6): 799-803.
- Meher, B., Agrawal, S., Panda, R. and Abraham, A., 2019. A survey on Region-based image fusion methods. *Information Fusion*, 48: 119-132.
- Mercioni, M.A. and Holban, S., 2019, June. A survey of distance metrics in clustering data mining techniques. In *Proceedings of the 2019 3rd International Conference on Graphics and Signal Processing* (pp. 44-47).
- Mi, L. and Chen, Z., 2020. Superpixel-enhanced deep neural forest for remote sensing image semantic segmentation. *ISPRS Journal of Photogrammetry and Remote Sensing*, 159, pp.140-152.
- Minaee, S., Boykov, Y.Y., Porikli, F., Plaza, A.J., Kehtarnavaz, N. and Terzopoulos, D., 2021. Image segmentation using deep learning: A survey. *IEEE Transactions on Pattern Analysis and Machine Intelligence*.

- Möller, M., Lymburner, L. and Volk, M., 2007. The comparison index: A tool for assessing the accuracy of image segmentation. *International Journal of Applied Earth Observation and Geoinformation*, 9(3): 311-321.
- Moore, A.P., Prince, S.J., Warrell, J., Mohammed, U. and Jones, G., 2008, June. Superpixel lattices. In *2008 IEEE conference on computer vision and pattern recognition* (pp. 1-8). IEEE.
- Motwani, P. and Sharma, R., 2020. Comparative study of pothole dimension using machine learning, manhattan and euclidean algorithm. *International Journal of Innovative Science and Research Technology*, 5(2):165-170.
- Na, S., Xumin, L. and Yong, G., 2010, April. Research on k-means clustering algorithm: An improved k-means clustering algorithm. In *2010 Third International Symposium on intelligent information technology and security informatics* (pp. 63-67). IEEE.
- Napoleon, D. and Lakshmi, P.G., 2010. An enhanced K-means algorithm to improve the efficiency using normal distribution data points. *International Journal on Computer Science and Engineering*, 2(7): 2409-2413.
- Nazeer, K.A. and Sebastian, M.P., 2009, July. Improving the Accuracy and Efficiency of the k-means Clustering Algorithm. In *Proceedings of the world congress on engineering* (Vol. 1, pp. 1-3). London: Association of Engineers.
- Neubert, P. and Protzel, P., 2013, September. Evaluating Superpixels in Video: Metrics Beyond Figure-Ground Segmentation. In *BMVC*.
- Niu, S., Chen, Q., De Sisternes, L., Ji, Z., Zhou, Z. and Rubin, D.L., 2017. Robust noise region-based active contour model via local similarity factor for image segmentation. *Pattern Recognition*, 61: 104-119.
- Okuboyejo, D., Olugbara, O. O. and Odunaike, S. 2014. Unsupervised Restoration of Hair-Occluded Lesion in Dermoscopic Images. In: *Proceedings of MIUA*. 91-96.
- Olugbara, O.O., Adetiba, E. and Oyewole, S.A., 2015. Pixel intensity clustering algorithm for multilevel image segmentation. *Mathematical Problems in Engineering*, 2015.
- Pandit, S. and Gupta, S., 2011. A comparative study on distance measuring approaches for clustering. *International Journal of Research in Computer Science*, 2(1): 29-31.
- Panic, N., Leoncini, E., De Belvis, G., Ricciardi, W. and Boccia, S., 2013. Evaluation of the endorsement of the preferred reporting items for systematic reviews and meta-analysis (PRISMA) statement on the quality of published systematic review and meta-analyses. *PloS One*, 8(12): e83138.
- Papazoglou, A. and Ferrari, V., 2013. Fast object segmentation in unconstrained video. In *Proceedings of the IEEE International Conference on Computer Vision* (pp. 1777-1784).

- Patel, B. and Ghosh, D., 2020, December. State-of-Art: Similarity Assessment for Content Based Image Retrieval System. In *2020 IEEE International Symposium on Sustainable Energy, Signal Processing and Cyber Security (iSSSC)* (pp. 1-6). IEEE.
- Patel, S.P. and Upadhyay, S.H., 2020. Euclidean distance based feature ranking and subset selection for bearing fault diagnosis. *Expert Systems with Applications*, 154: 113400.
- Pathegama, M. and Göl, Ö., 2004. Edge-end pixel extraction for edge-based image segmentation. ICSP.
- Peng, B. and Zhang, L., 2012, October. Evaluation of image segmentation quality by adaptive ground truth composition. In *European Conference on Computer Vision* (pp. 287-300). Springer, Berlin, Heidelberg.
- Perbet, F. and Maki, A., 2011, June. Homogeneous Superpixels from Random Walks. In MVA (pp. 26-30).
- Pham, D.L., Xu, C. and Prince, J.L., 2000. Current methods in medical image segmentation. *Annual Review of Biomedical Engineering*, 2(1): 315-337.
- Popovic, A., De la Fuente, M., Engelhardt, M. and Radermacher, K., 2007. Statistical validation metric for accuracy assessment in medical image segmentation. *International Journal of Computer Assisted Radiology and Surgery*, 2(3-4): 169-181.
- Pratondo, A., Chui, C.K. and Ong, S.H., 2015. Robust edge-stop functions for edge-based active contour models in medical image segmentation. *IEEE Signal Processing Letters*, 23(2): 222-226.
- Pratondo, A., Chui, C.K. and Ong, S.H., 2017. Integrating machine learning with region-based active contour models in medical image segmentation. *Journal of Visual Communication and Image Representation*, 43, pp.1-9.
- Rad, A.E., Rahim, M.S.M., Kolivand, H. and Amin, I.B.M., 2017. Morphological region-based initial contour algorithm for level set methods in image segmentation. *Multimedia Tools and Applications*, 76(2): 2185-2201.
- Ranjan, R., Patel, V. M. and Chellappa, R. 2017. Hyperface: A deep multi-task learning framework for face detection, landmark localization, pose estimation, and gender
- Rauf, A., Sheeba, S.M., Khusro, S. and Javed, H., 2012. Enhanced k-mean clustering algorithm to reduce number of iterations and time complexity. *Middle-East Journal of Scientific Research*, 12(7): 959-963.
- Ray, S. and Turi, R.H., 1999, December. Determination of number of clusters in k- means clustering and application in colour image segmentation. In *Proceedings of the 4th international conference on advances in pattern recognition and digital techniques* (pp. 137-143).
- recognition. IEEE Transactions on Pattern Analysis and Machine Intelligence, Jiang and Learned-Miller, 2017.

- Reddy, N.S., 2016. Image segmentation by using linear spectral clustering. *Journal of Telecommunication System and Management*, 5(03): 1-5.
- Ren, C.Y. and Reid, I., 2011. gSLIC: a real-time implementation of SLIC superpixel segmentation. *University of Oxford, Department of Engineering, Technical Report*, pp.1- 6.
- Ren, X. and Malik, J., 2003, October. Learning a classification model for segmentation. In *Computer Vision, IEEE International Conference on* (Vol. 2, pp. 10-10). IEEE Computer Society.
- Ricotta, C., 2021. From the euclidean distance to compositional dissimilarity: What is gained and what is lost. *Acta Oecologica*, 111: 103732.
- Roopaei, M., Rad, P. and Choo, K.-K. R. 2017. Cloud of things in smart agriculture: Intelligent irrigation monitoring by thermal imaging. *IEEE Cloud Computing*, 4 (1): 10- 15.
- Safdar, M., Cui, G., Kim, Y.J. and Luo, M.R., 2017. Perceptually uniform colour space for image signals including high dynamic range and wide gamut. *Optics Express*, 25(13): 15131-15151.
- Saini, S. and Arora, K., 2014. A study analysis on the different image segmentation techniques. *International Journal of Information & Computation Technology*, 4(14): 1445-1452.
- Saki, F., Tahmasbi, A., Soltanian-Zadeh, H. and Shokouhi, S.B., 2013. Fast opposite weight learning rules with application in breast cancer diagnosis. *Computers in Biology and Medicine*, 43(1): 32-41.
- Salmin, M., Tempola, F., Fuad, A. and Papuangan, M., 2020, July. Case-based reasoning for the diagnosis of acute respiratory infections using Minkowski Distance. *Journal of Physics*:1569(2): 022033.
- Sarmadi, H., Entezami, A., Saeedi Razavi, B. and Yuen, K.V., 2021. Ensemble learning-based structural health monitoring by Mahalanobis distance metrics. *Structural Control and Health Monitoring*, 28(2): e2663.
- Schick, A., Fischer, M. and Stiefelhagen, R., 2012, November. Measuring and evaluating the compactness of superpixels. In *Proceedings of the 21st International Conference on Pattern Recognition (ICPR2012)* (pp. 930-934). IEEE.
- Schick, A., Fischer, M. and Stiefelhagen, R., 2014. An evaluation of the compactness of superpixels. *Pattern Recognition Letters*, 43: 71-80.
- Shapero, M., Dronova, I. and Macaulay, L. 2017. Implications of changing spatial dynamics of irrigated pasture, California's third largest agricultural water use. *Science of the Total Environment*, 605: 445-453.
- Sharma, K.K. and Seal, A., 2020. Clustering analysis using an adaptive fused distance. *Engineering Applications of Artificial Intelligence*, 96: 103928.
- Shen, J., Du, Y., Wang, W. and Li, X., 2014. Lazy random walks for superpixel segmentation. *IEEE Transactions on Image Processing*, 23(4): 1451-1462.

- Shen, J., Hao, X., Liang, Z., Liu, Y., Wang, W. and Shao, L., 2016. Real-time superpixel segmentation by DBSCAN clustering algorithm. *IEEE Transactions on Image Processing*, 25(12): 5933-5942.
- Shi, J. and Malik, J., 2000. Normalized cuts and image segmentation. *IEEE Transactions on Pattern Analysis and Machine Intelligence*, 22(8): 888-905.
- Shih, F.Y. and Cheng, S., 2005. Automatic seeded region growing for colour image segmentation. *Image and Vision Computing*, 23(10): 877-886.
- Simu, S., Lal, S., Nagarsekar, P. and Naik, A., 2017. Fully automatic ROI extraction and edge-based segmentation of radius and ulna bones from hand. *Biocybernetics and Biomedical Engineering*, 37(4): 718-732.
- Siva, P. and Wong, A., 2014, May. Grid seams: A fast superpixel algorithm for real-time applications. In *2014 Canadian Conference on Computer and Robot Vision* (pp. 127-134). IEEE.
- Soufi, M., Kamali-Asl, A., Geramifar, P. and Rahmim, A. 2017. A novel framework for automated segmentation and labeling of homogeneous versus heterogeneous lung tumors in [18 F] FDG-PET Imaging. *Molecular Imaging and Biology*, 19 (3): 456-468.
- Sowmya, B. and Rani, B.S., 2011. Colour image segmentation using fuzzy clustering techniques and competitive neural network. *Applied Soft Computing*, 11(3): 3170- 3178.
- Stella, X.Y. and Shi, J., 2003, October. Multiclass spectral clustering. In *null* (p. 313). IEEE.
- Stokman, H. and Gevers, T., 2007. Selection and fusion of colour models for image feature detection. *IEEE Transactions on Pattern Analysis and Machine Intelligence*, 29(3): 371-381.
- Sultana, F., Sufian, A. and Dutta, P., 2020. Evolution of image segmentation using deep convolutional neural network: a survey. *Knowledge-Based Systems*, 201, 106062.
- Sural, S., Qian, G. and Pramanik, S., 2002. Segmentation and histogram generation using the HSV colour space for image retrieval. In *Proceedings. International Conference on Image Processing* (Vol. 2, pp. II-II). IEEE.
- Suwanda, R., Syahputra, Z. and Zamzami, E.M., 2020, June. Analysis of Euclidean Distance and Manhattan Distance in the K-Means algorithm for variations number of Centroid K. *Journal of Physics*, 1566(1): 012058).
- Taha, A.A. and Hanbury, A., 2015. Metrics for evaluating 3D medical image segmentation: analysis, selection, and tool. *BMC Medical Imaging*, 15(1): 29.
- Taha, A.A., Hanbury, A. and del Toro, O.A.J., 2014, October. A formal method for selecting evaluation metrics for image segmentation. In *2014 IEEE international conference on image processing (ICIP)* (pp. 932-936). IEEE.

- Tahmasbi, A., Saki, F. and Shokouhi, S.B., 2011. Classification of benign and malignant masses based on Zernike moments. *Computers in Biology and Medicine*, 41(8): 726-735.
- Tang, D., Fu, H. and Cao, X., 2012, July. Topology preserved regular superpixel. In 2012 IEEE International Conference on Multimedia and Expo (pp. 765-768). IEEE.
- Thanammal, K.K. and Sudha, J.J., 2014. Comparative Study Of Edge Detection Algorithms on Medical Images.
- Thant, A.A., Aye, S.M. and Mandalay, M., 2020. Euclidean, Manhattan and Minkowski Distance Methods For Clustering Algorithms.
- Tian, X., Jiao, L., Yi, L., Guo, K. and Zhang, X., 2015. The image segmentation based on optimized spatial feature of superpixel. *Journal of Visual Communication and Image Representation*, 26: 146-160.
- Tiburzi, F., Escudero, M., Bescós, J. and Martínez, J. M. 2008. A ground truth for motion-based video-object segmentation. In: Proceedings of 2008 15th IEEE International Conference on Image Processing. IEEE, 17-20.
- Toews, L.C., 2017. Compliance of systematic reviews in veterinary journals with Preferred Reporting Items for Systematic Reviews and Meta-Analysis (PRISMA) literature search reporting guidelines. *Journal of the Medical Library Association: JMLA*, 105(3): 233.
- Tolentino, J.A. and Gerardo, B.D., 2019. Enhanced Manhattan-based clustering using fuzzy c-means algorithm for high dimensional datasets. *International Journal on Advanced Science Engineering Information Technology*, 9: 766-771.
- Van den Bergh, M., Boix, X., Roig, G., de Capitani, B. and Van Gool, L., 2012, October. Seeds: Superpixels extracted via energy-driven sampling. In *European conference on computer vision* (pp. 13-26). Springer, Berlin, Heidelberg.
- Varma, N.M. and Choudhary, A., 2019, June. Evaluation of Distance Measures in Content Based Image Retrieval. In *2019 3rd International Conference on Electronics, Communication and Aerospace Technology (ICECA)* (pp. 696-701). IEEE.
- Vedaldi, A. and Soatto, S., 2008, October. Quick shift and kernel methods for mode seeking. In *European Conference on Computer Vision* (pp. 705-718). Springer, Berlin, Heidelberg.
- Veksler, O., Boykov, Y. and Mehrani, P., 2010, September. Superpixels and supervoxels in an energy optimization framework. In *European conference on Computer vision* (pp. 211-224). Springer, Berlin, Heidelberg.
- Vélez-Falconí, M., Marín, J., Jiménez, S. and Guachi-Guachi, L., 2020. Comparative Study of Distance Measures for the Fuzzy C-means and K-means Non-Supervised Methods Applied to Image Segmentation. In *ICAI Workshops* (pp. 1-14).

- Vidal, M. and Amigo, J.M., 2012. Pre-processing of hyperspectral images. Essential steps before image analysis. *Chemometrics and Intelligent Laboratory Systems*, 117: 138-148.
- Wady, S.H. and Ahmed, H.O., Effects of Different Distance Measures on Ethnicity Identification. *The Scientific Journal of Cihan University–Slemani PP*, 45: 56.
- Wan, M., Gu, G., Sun, J., Qian, W., Ren, K., Chen, Q. and Maldague, X., 2018. A level set method for infrared image segmentation using global and local information. *Remote Sensing*, 10(7): 1039.
- Wang, G., Zhang, Y. and Li, J. 2017. High-level background prior based salient object detection. *Journal of Visual Communication and Image Representation*, 48: 432-441.
- Wang, J. and Wang, X., 2012. VCells: Simple and efficient superpixels using edge-weighted centroidal Voronoi tessellations. *IEEE Transactions on Pattern Analysis and Machine Intelligence*, 34(6): 1241-1247.
- Wang, L., Zhang, Y. and Feng, J., 2005. On the Euclidean distance of images. *IEEE Transactions on Pattern Analysis and Machine Intelligence*, 27(8): 1334-1339.
- Wang, M., Liu, X., Gao, Y., Ma, X. and Soomro, N.Q., 2017. Superpixel segmentation: A benchmark. *Signal Processing: Image Communication*, 56: 28-39.
- Wang, S.J., Yan, W.J., Li, X., Zhao, G., Zhou, C.G., Fu, X., Yang, M. and Tao, J., 2015. Micro-expression recognition using colour spaces. *IEEE Transactions on Image Processing*, 24(12): 6034-6047.
- Wang, X., Li, H., Bichot, C.E., Masnou, S. and Chen, L., 2013, September. A graph-cut approach to image segmentation using an affinity graph based on ℓ_0 -sparse representation of features. In *2013 IEEE International Conference on Image*
- Wang, X., Yang, S., Zhao, Y. and Wang, Y., 2018. Lithology identification using an optimized KNN clustering method based on entropy-weighted cosine distance in Mesozoic strata of Gaoqing field, Jiyang depression. *Journal of Petroleum Science and Engineering*, 166: 157-174.
- Wang, Z., Jensen, J.R. and Im, J., 2010. An automatic region-based image segmentation algorithm for remote sensing applications. *Environmental Modelling & Software*, 25(10): 1149-1165.
- Wang, Z., Wang, E. and Zhu, Y., 2020. Image segmentation evaluation: a survey of methods. *Artificial Intelligence Review*, 53(8): 5637-5674.
- Weatherall, I.L. and Coombs, B.D., 1992. Skin colour measurements in terms of CIELAB colour space values. *Journal of Investigative Dermatology*, 99(4): 468-473.
- Wei, X., Yang, Q., Gong, Y., Ahuja, N. and Yang, M.H., 2018. Superpixel hierarchy. *IEEE Transactions on Image Processing*, 27(10): 4838-4849.
- Wesolkowski, S., 1999. *Colour image edge detection and segmentation: A comparison of the vector angle and the euclidean distance colour similarity measures* (Master's thesis, University of Waterloo).

- Wirth, M., Frascini, M., Masek, M. and Bruynooghe, M., 2006. Performance evaluation in image processing.
- Wu, M.N., Lin, C.C. and Chang, C.C., 2007, November. Brain tumor detection using colour-based k-means clustering segmentation. In *Third International Conference on Intelligent Information Hiding and Multimedia Signal Processing (IIH-MSP 2007)* (Vol. 2, pp. 245-250). IEEE.
- Wu, P., Hoi, S.C., Xia, H., Zhao, P., Wang, D. and Miao, C., 2013, October. Online multimodal deep similarity learning with application to image retrieval. In *Proceedings of the 21st ACM international conference on Multimedia* (pp. 153-162). ACM.
- Wu, W., Chen, A.Y., Zhao, L. and Corso, J.J., 2014. Brain tumor detection and segmentation in a CRF (conditional random fields) framework with pixel-pairwise affinity and superpixel-level features. *International journal of computer assisted radiology and surgery*, 9(2): 241-253.
- Wu, Y., Lim, J. and Yang, M.H., 2013. Online object tracking: A benchmark. In *Proceedings of the IEEE conference on computer vision and pattern recognition* (pp. 2411-2418).
- Xia, Y., Wang, T., Zhao, R. and Zhang, Y., 2007. Image segmentation by clustering of spatial patterns. *Pattern Recognition Letters*, 28(12): 1548-1555.
- Xiang, D., Tang, T., Zhao, L. and Su, Y., 2013. Superpixel generating algorithm based on pixel intensity and location similarity for SAR image classification. *IEEE Geoscience and Remote Sensing Letters*, 10(6): 1414-1418.
- Xiao, X., Zhou, Y. and Gong, Y.J., 2018. Content-adaptive superpixel segmentation. *IEEE Transactions on Image Processing*, 27(6): 2883-2896.
- Xie, X., Xie, G., Xu, X., Cui, L. and Ren, J., 2019. Automatic image segmentation with superpixels and image-level labels. *IEEE Access*, 7: 10999-11009.
- Yan, J., Yu, Y., Zhu, X., Lei, Z. and Li, S.Z., 2015. Object detection by labeling superpixels. In *Proceedings of the IEEE Conference on Computer Vision and Pattern Recognition* (pp. 5107-5116).
- Yang, F., Sun, Q., Jin, H. and Zhou, Z., 2020. Superpixel segmentation with fully convolutional networks. In *Proceedings of the IEEE/CVF Conference on Computer Vision and Pattern Recognition* (pp. 13964-13973).
- Yang, F., Sun, Q., Jin, H. and Zhou, Z., 2020. Superpixel segmentation with fully convolutional networks. In *Proceedings of the IEEE/CVF Conference on Computer Vision and Pattern Recognition* (pp. 13964-13973).
- Yang, H.Y., Wang, X.Y., Wang, Q.Y. and Zhang, X.J., 2012. LS-SVM based image segmentation using colour and texture information. *Journal of Visual Communication and Image Representation*, 23(7): 1095-1112.

- Yang, H.Y., Wang, X.Y., Wang, Q.Y. and Zhang, X.J., 2012. LS-SVM based image segmentation using colour and texture information. *Journal of Visual Communication and Image Representation*, 23(7): 1095-1112.
- Yang, L., Yang, G., Zhou, L. and Yin, Y., 2015. Superpixel based finger vein roi extraction with sensor interoperability. In *2015 International Conference on Biometrics (ICB)* (pp. 444-451). IEEE.
- Yao, J., Boben, M., Fidler, S. and Urtasun, R., 2015. Real-time coarse-to-fine topologically preserving segmentation. In *Proceedings of the IEEE Conference on Computer Vision and Pattern Recognition* (pp. 2947-2955).
- Yao, J., Boben, M., Fidler, S. and Urtasun, R., 2015. Real-time coarse-to-fine topologically preserving segmentation. In *Proceedings of the IEEE Conference on Computer Vision And Pattern Recognition* (pp. 2947-2955).
- Yasmin, J. J. 2017. Accurate Border Detection of Skin Lesions in Skin Cancer Images using Log Edge Detector. *International Journal of Applied Engineering Research*, 12 (9): 1860-1866.
- Yogamangalam, R. and Karthikeyan, B., 2013. Segmentation techniques comparison in image processing. *International Journal of Engineering and Technology (IJET)*, 5(1): 307-313.
- ..
- Zhang, C., Xiao, X., Li, X., Chen, Y.J., Zhen, W., Chang, J., Zheng, C. and Liu, Z., 2014. White blood cell segmentation by colour-space-based k-means. *Sensors*, 14(9): 16128-16147.
- Zhang, Q., Lin, J., Li, W., Shi, Y. and Cao, G., 2018a. Salient object detection via compactness and objectness cues. *The Visual Computer*, 34(4), pp.473-489.
- Zhang, Q.X., Lin, G.H., Zhang, Y.M., Xu, G. and Wang, J.J., 2018b. Wildland forest fire smoke detection based on faster R-CNN using synthetic smoke images. *Procedia Engineering*, 211: 441-446.
- Zhang, X. and Wandell, B.A., 1996. A spatial extension of CIELAB for digital colour image reproduction. In *SID International Symposium Digest of Technical Papers*, 27: 731-734.
- Zhang, Y., Hartley, R., Mashford, J. and Burn, S., 2011. Superpixels via pseudo-boolean optimization. In *2011 International Conference on Computer Vision* (pp. 1387-1394). IEEE.
- Zhang, Y., Li, X., Gao, X. and Zhang, C., 2016. A simple algorithm of superpixel segmentation with boundary constraint. *IEEE Transactions on Circuits and Systems for Video Technology*, 27(7): 1502-1514.
- Zhang, Y., Ma, L., Zhou, Y. and Zhang, C., 2017. Automatic superpixel generation algorithm based on a quadric error metric in 3D space. *Signal, Image and Video Processing*, 11(3): 471-478.
- Zhang, Z., Zhang, J. and Xue, H., 2008a. Improved K-means clustering algorithm. In *2008 Congress on Image and Signal Processing*, 5: 169-172, IEEE.

Zhang, Z., Gunes, H. and Piccardi, M., 2008b. An accurate algorithm for head detection based on XYZ and HSV hair and skin colour models. In *2008 15th IEEE International Conference on Image Processing* (pp. 1644-1647). IEEE.

Zhang, Z., Zhu, Q. and Xie, Y., 2012. Learning based alpha matting using support vector regression. In *2012 19th IEEE International Conference on Image Processing* (pp. 2109-2112). IEEE.

Zheng, X., Lei, Q., Yao, R., Gong, Y. and Yin, Q., 2018. Image segmentation based on adaptive K-means algorithm. *EURASIP Journal on Image and Video Processing*, 2018(1): 1-10.

Zuva, T., Olugbara, O.O., Ojo, S.O. and Ngwira, S.M., 2011. Image segmentation, available techniques, developments and open issues. *Canadian Journal on Image Processing and Computer Vision*, 2(3): 20-29.